QUATERNARY MURID RODENTS OF TIMOR PART I: NEW MATERIAL OF *CORYPHOMYS BUEHLERI* SCHAUB, 1937, AND DESCRIPTION OF A SECOND SPECIES OF THE GENUS

K. P. APLIN

Australian National Wildlife Collection, CSIRO
Division of Sustainable Ecosystems, Canberra
and Division of Vertebrate Zoology
(Mammalogy)
American Museum of Natural History
(ken.aplin@csiro.au)

K. M. HELGEN

Department of Vertebrate Zoology
National Museum of Natural History
Smithsonian Institution, Washington and
Division of Vertebrate Zoology (Mammalogy)
American Museum of Natural History
(HELGENK@si.edu)

BULLETIN OF THE AMERICAN MUSEUM OF NATURAL HISTORY
Number 341, 80 pp., 21 figures, 4 tables
Issued July 21, 2010

Copyright © American Museum of Natural History 2010 ISSN 0003-0090

CONTENTS

Abstract 3
Introduction 3
The environmental context 5
Materials and methods 7
Systematics 11
Coryphomys Schaub, 1937 11
Coryphomys buehleri Schaub, 1937 12
Extended description of *Coryphomys buehleri* 12
Coryphomys musseri, sp. nov. 25
Description 26
Coryphomys, sp. indet. 34
Discussion 40
Species diversity in *Coryphomys* 41
Phylogenetic affinities of *Coryphomys* 43
Paleoecology of *Coryphomys* 63
Conclusions 68
Acknowledgments 69
References 69

ABSTRACT

Large collections of fragmentary animal bones excavated from archaeological contexts in East Timor between 1968 and 2002 provide new material referable to the recently extinct, gigantic murine genus *Coryphomys*. We document the upper and lower dentition and palatal anatomy of *C. buehleri* Schaub, 1937, and identify and name a second species of *Coryphomys*, based on differences in molar size and morphology and skeletal robusticity. Alternative interpretations of the observed morphological and metric variability (sexual dimorphism, resource-based polymorphism, sample heterochroneity) are each carefully assessed and rejected, and we conclude that the genus comprised two species of approximately similar body size. Preserved cranial elements of both species of *Coryphomys* feature a high degree of anatomical specialization, including an unusual elaboration of the maxillary sinus complex. Though the specialized anatomy of *Coryphomys* invites consideration of its phylogenetic relationships, this exercise is hindered by a demonstrable high level of homoplasy (i.e., multiple, independent evolutionary losses and gains) in many of the key craniodental features traditionally surveyed within Murinae, while other features are insufficiently well surveyed for broad-scale analysis. Nevertheless, our comparisons highlight two potentially related lineages among the geographically proximate Murinae—the Philippine Phloeomyini and the Australo-Papuan Hydromyini. The remains of *Coryphomys* are relatively scarce in all the archaeological samples, but distributional evidence suggests that both species of *Coryphomys* were found primarily in upland habitats. Late Pleistocene samples document their former presence at lower elevations, possibly reflecting cooler climatic conditions at that time.

INTRODUCTION

Timor is located near the eastern end of the Indonesian archipelago and is the largest and highest of the Lesser Sunda Islands (fig. 1). The surrounding region is geologically young and tectonically active, the product of late Tertiary collision between three major earth units—the Asian and Australian continental plates, and the Pacific oceanic plate. Plants and animals of Asian and Australian affinities intermingle across the region and it was this melding of two such different biotas that inspired the nascent biogeographer Alfred Russel Wallace, and continues to excite the imagination of students of historical biogeography today.

Timor was one of the first of the Lesser Sunda Islands to be explored biologically, with collections made during the Baudin expeditions of 1801 and 1803, and subsequently by Müller, Wallace, and others (see Hellmayr, 1914, and Mayr, 1944, for the history of ornithological collecting). These expeditions encountered a distinctive avifauna, including a significant number of endemic species and subspecies. In contrast, the early expeditions encountered a fairly impoverished mammal fauna made up of the familiar suite of domesticates and commensals, and a moderate number of bat species, the majority of which were subsequently found elsewhere within the Indonesian archipelago and beyond (see Goodwin, 1979, for a summary). Indeed, prior to the 1990s, the only potentially endemic Timorese mammals were two shrews (*Crocidura tenuis*: treated as a synonym of *C. fuliginosa* [Blyth, 1835] by Jenkins [1982] but maintained by Corbet and Hill, 1992: 42; and *C. macklotti*: included within *C. fuliginosa* by Jenkins [1982] but considered a synonym of *C. tenuis* by Corbet and Hill, 1992) and one bat, the enigmatic *Nyctophilus timorensis* (see Goodwin, 1979; Kitchener et al., 1991d, for discussion of this taxon). The impoverished nature of the Timorese mammal fauna was further highlighted by subsequent discovery through the course of the 1900s of endemic nonvolant mammals on Seram and several other Moluccan islands (summarized by Helgen, 2003) and Flores (e.g., Sody, 1941; Kock, 1974). More recent surveys of the Lesser Sunda Islands, particularly by staff of the Museum Zoologicum Bogoriense and the Western Australian Museum (Kitchener and Maryanto, 1993, 1995; Kitchener and Suyanto, 1996; Kitchener et al., 1991a, 1991b, 1991c, 1991d, 1994), also resulted in discovery of several additional endemic mammals including one native rodent extant on Timor, *Rattus timorensis* (Kitchener et al., 1991a).

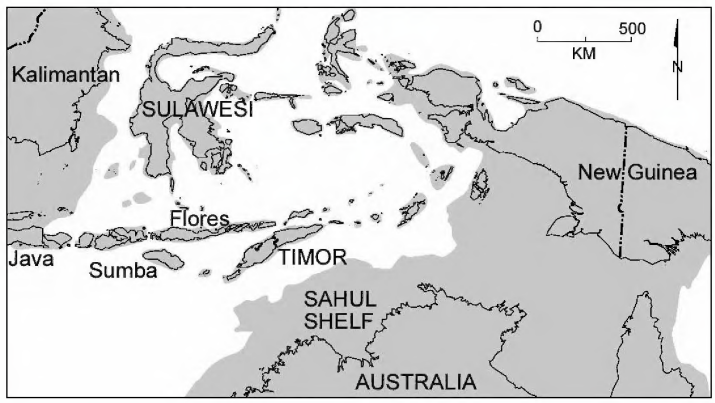

Fig. 1. Regional map showing the location of Timor and other significant islands and continental landmasses of Wallacea. The grey shading indicates the approximate extent of land that is exposed with a sea level depression of 100–120 m below present level. Note that Timor remains isolated from other major islands and continental landmasses during episodes of lowered sea level.

The first hint of a much higher endemic mammalian diversity on Timor came to light during excavations by Alfred Bühler (see Sarasin, 1936) in a limestone cave near Nikiniki in southwest Timor. A damaged mandible and an incomplete femur of a very large rodent were forwarded to Schaub (1937), who described them as a new fossil murid, *Coryphomys buehleri.* The dental morphology of *C. buehleri* was later revisited by Stehlin and Schaub (1951: 348) who regarded the morphology of the anterior portion of m1 to be unparalleled among murines. Not long after, additional Timorese rodent material was recovered by Th. L. Verhoeven from archaeological contexts at Lian Leluat on the Maubesi River, southern Timor (Verhoeven, 1959). Hooijer (1965) described and figured a total of three dentaries and though he noted considerable morphological variation, especially in the form of the anterior moiety of m1, he concluded that a single species was represented.

Large samples of prehistoric mammal remains from Timor first came available through archaeological excavations by Ian Glover (1986) over the period 1966–1967. Glover excavated a total of five sites using systematic methods and retrieved animal remains from contexts dated back as far as the terminal Pleistocene. The enormously abundant and surprisingly diverse rodent specimens were turned over to Jack Mahoney for detailed study. Mahoney distinguished a total of four large murids including *C. buehleri*, four smaller native murids, and two commensal murids, the latter found in association with remains of other introduced mammals including domesticates, and he figured each of the four "giant" rats (Mahoney, appendix 3 in Glover, 1986). Musser (1981b) examined some of this new material and commented briefly on the possible affinities of the Timorese rodents, pending publication of Mahoney's full account. Sadly, Mahoney did not complete his studies of the Timor rats before his death in 1985. Since that time the Glover material has passed through several sets of hands with the intention of completing his work, but so far this goal remains unfulfilled.

Additional impetus to document the prehistoric Timorese rodents arose after recommencement of archaeological research in East Timor in 2000 by archaeologists from the Australian National University, Canberra. Excavations in five cave sites, one of them studied previously by the Portuguese archaeologist Antonio de Almeida, again produced abundant vertebrate remains from contexts ranging from near contemporary back to more than 38,000 BP (O'Connor et al., 2002; O'Connor and Aplin, 2007; Veth et al., 2005). Our studies of the combined Glover and newly excavated collections inspired a new interpretation of taxic diversity within this fascinating prehistoric fauna. Like Mahoney

and Musser, we recognize a total of four genera of large to gigantic murine rodents, and a total of five native smaller murines. However, we depart from previous assessments in distinguishing a higher diversity among the large-bodied rats, with a minimum of eight species in the four genera. The total prehistoric murine fauna of Timor thus comprised at least 13 species, some with clear affinities with the murine fauna of Melanesia, others linked to the contemporary murine fauna of Southeast Asia, and others again of obscure affinities and potentially more ancient origin.

The scale of the descriptive and comparative effort needed to document the prehistoric Timorese murine fauna requires that it be divided among a number of contributions. This first paper sets the scene by describing the physical, biological, and archaeological context of the prehistoric Timorese rodents, and presents our conclusions on the taxonomy of the genus *Coryphomys*, with two species recognized. We also present our preliminary observations on the phylogenetic relationships and paleoecology of this fascinating genus of murine rodent.

The Environmental Context

GEOGRAPHY: Timor is an impressive island even by global standards, with an area of 28,418 km^2 and a maximum elevation of 2962 m. It is the largest and highest of the Lesser Sunda Islands, and one of the more varied in terms of climatic regimes and vegetation. It is also one of the more isolated, with a deep oceanic trench along the northern side of the island separating it from the Inner Banda Arc, a chain of volcanic islands that runs east from Flores and includes Lembata, Pantar, Alor, and Wetar. Further to the west, and again separated by very deep water, lie Savu and Sumba islands, while to the south, more than 450 km across the Timor Sea, extends the northwestern coastline of Australia. Timor has a significant satellite island at its southwestern end—Roti, with an area of 1227 km^2 and an elevation of 430 m. The two islands are separated by a 10 km wide strait with a sill depth of ca. 100 m.

A high central massif running the full length of Timor includes several peaks rising to over 2000 m. The northern side of the massif rises abruptly from the coast, whereas in the south and southwest the ranges are fringed by broad alluvial and coastal plains. Rugged relief with steep slopes, often in excess of 40% inclination, thus typifies much of the habitat on Timor, broken locally by valleys, uplifted sedimentary basins and uneven limestone plateaux.

Timor Island is divided politically in two roughly equal parts—an Indonesian portion in the west (forming part of the province of Nusa Tenggara Timur) and the independent nation of Timor Lorosa'e (East Timor) in the east.

GEOLOGY: Timor is located in the Neogene collision zone between the northwest continental margin of Australia and the Banda Island arc system and has a complex geology that has been subject to contrasting tectonic interpretations (Price and Audley-Charles, 1987; Charlton, 1991). A paleogeographic framework for Eastern Indonesia based on tectonic and geological evidence is provided by Hall (2002).

Rocks belonging to four major tectonostratigraphic units are exposed on Timor, namely: (1) basal, unmetamorphosed sedimentary rocks of the Australian continental shelf, ranging in age from Permian to Paleocene; (2) metamorphic rocks of variable age, extruded along the subduction zone; (3) volcanic fore-arc ophiolites of late Tertiary age; and (4) Neogene to Quaternary sedimentary formations, including postorogenic molasse sediments and uplifted coral reefs, the latter present locally to 1400 m and often highly karstic (Audley-Charles, 1968; Middleton et al., 2006).

For biogeographers, the key points of interest are the age of subaerial emergence and of subsequent uplift of Timor. These are not known with any precision but are constrained by stratigraphic and radiometric data. Berry and Grady (1981) dated the main phase of deformation in the metamorphic Aileu Complex to between ca. 8 mya and 5.5 mya, and interpreted this phase as marking the main arc-continent collision. Kaneko et al. (1987) suggested that exhumation of the metamorphic belt doming commenced in the late Miocene in West Timor but attributed major uplift to doming and

high-angle faulting of the welded sedimentary stack during the Quaternary, as a response to slab break-off of subducting Australian continental crust. Evidence of rapid uplift of Timor through the Quaternary comes from dated flights of coral terraces, with the uplift rate during the late Quaternary estimated at 0.5 m per 1000 yrs for northeastern Timor (Chappell and Veeh, 1978). Even higher local rates are implied by de Smet et al.'s (1989) suggestion of more than 2 km of uplift since ca. 5 mya in central West Timor.

CLIMATE: Timor enjoys a tropical oceanic climate but the pattern of rainfall is highly variable, due to the complex interaction of two monsoonal systems and local topography (Monk et al., 1997). From November to May, monsoonal winds blow from the north and bring thunderstorms and rain to most of the island but especially over the central ranges. From June to October, offshore winds from northern Australia cross the Timor Sea to bring rain to the southern side of the central ranges. Mean annual rainfall ranges from less than 600 mm on the north coast to over 3000 mm in mountainous areas along the south coast. Mean daily temperatures range from 23°–31° C in the lowlands to 15°–24° C at 1000 m. November is the hottest month, and July the coldest. Precipitation generally exceeds evaporation between December and April, but there is a deficit between May and November (Monk et al., 1997).

VEGETATION: Less than 15% of the primary forest cover of Timor survives today and even this is highly fragmented, with the largest remnants mainly confined to the mountains and pockets along the south coast. Monk et al. (1997) reconstructed the original cover as a mosaic of evergreen and semievergreen rainforests, principally located along the southern side of the central ranges, and deciduous forests, with a largely complementary northern distribution but also found on the southern coastal strip. Small pockets of mesophyll vine forest occurred in the southeast of the island. All forest communities above 600–1000 m were evergreen, with broadleaf communities probably dominant. Drier sites probably supported sclerophyllous vegetation featuring endemic Myrtaceae including *Eucalyptus urophylla* (Whitmore et al., 1989; Martin and Cossalter, 1977, 1979). Above 1500 m, all forests support a heavy mantle of mosses, lichens, and epiphytes, giving way to mosses alone above 1800 m. At the highest elevations, high wind shear creates stunted (elfin) tree communities and patches of low heath dominated by plants of "Himalayan" affinity (e.g., *Rubus rosifolins*, *Ranunculus* spp.). Mangrove and beach communities occupy suitably sheltered sites around the coastal margin.

Today, most of the land below 1000 m supports savannah woodland of casuarinas and eucalypts (mainly *Eucalyptus alba*), usually with a weedy understory heavily grazed by goats, cattle (mainly banteng or Balinese cattle), and horses (Metzner, 1977). This community presumably developed over millennia through the practice of traditional shifting agriculture, which involves widespread burning at the end of the dry season. Soil loss from steep slopes following initial forest destruction has also contributed to a radical change in the nature of the Timorese environment and there is little evidence of regeneration to original forest types. In the mountainous regions, the creation of open pasture by repeated burning has converted much of the adjoining forest to sclerophyll communities dominated by *E. urophylla*. Commercial extraction of sandalwood (*Santalum album*) over many centuries has also affected forest communities (WCMC, 1995) and there has been a recent sharp increase over the last few decades in the rate of deforestation, in response to both population growth and commercial plantations and broad-acre agriculture (Bouma and Kobryn, 2004).

HUMAN PREHISTORY: The earliest evidence for human occupation of Timor dates to around 40,000 years ago (O'Connor and Aplin, 2007), and there is growing evidence for continuous occupation after that time, at least in the coastal regions. The earliest populations presumably lived by hunting and gathering, possibly combined with basic arboriculture, with little archaeological evidence for cultural or economic change prior to the appearance of various "Neolithic" markers (pottery, remains of various domesticates) in the late Holocene, dated to ~3500 BP (Glover, 1986; O'Connor and Aplin,

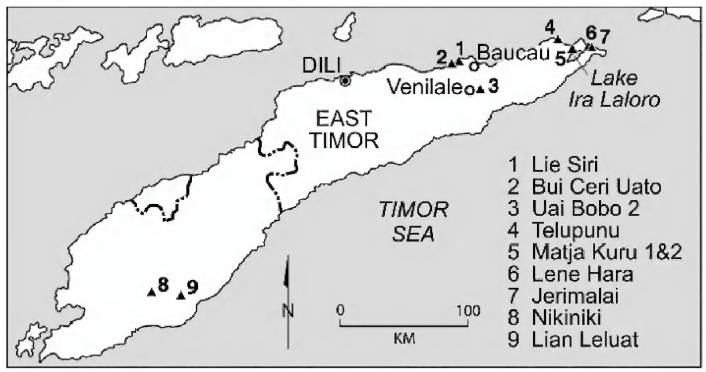

Fig. 2. Map of Timor showing the location of major towns and the various archaeological sites that have produced fossil murine remains.

2007). A notable exception is the sudden appearance during the early Holocene of a New Guinean marsupial, *Phalanger orientalis*, presumably as a consequence of increasing human interaction between the Lesser Sunda Islands and Melanesia. The remains of now-extinct rodents occur in all the excavated sites, often co-occurring with Neolithic artifacts and the bones of domesticates. The same layers also contain the bones of two commensal murines (*Rattus exulans* and *R. rattus*) that probably accompanied early agriculturalists into Eastern Indonesia some 3500 years ago (Bellwood, 1997). Whether these co-occurrences faithfully reflect the survival of the "giant" rats into recent millennia cannot be answered until such time as direct radiocarbon dating is undertaken on relevant bones and teeth.

The archaeological record of Flores Island to the west features a much longer record of human occupation, with strong evidence for initial colonization prior to 780,000 years ago (Morwood et al., 1998, 1999) and still controversial evidence for local evolution of a now extinct hominin species (Brown et al., 2004; Morwood et al., 2004; Jacob et al., 2006). To date, Timor has not produced any evidence for a long history of human occupation. However, it should be noted that poorly dated Quaternary sediments (Ainaro Formation of Audley-Charles, 1968) on Timor have produced fossil remains of three large vertebrates (a pygmy proboscidean *Stegodon* sp., a "giant" turtle, and a "giant" varanid lizard [Verhoeven, 1964; Hooijer, 1969a, 1969b]), none of which have yet turned up in any of the archaeological assemblages. Exactly when and why these "megafaunal" species became extinct on Timor is not known. However, if the extinctions on Timor are linked to human activities, as they so often seem to be (Burney and Flannery, 2005), we might reasonably postulate a longer history of human occupation of Timor.

Material and Methods

The Archaeological Sites: The collections we studied come from excavations in nine archaeological sites, all located in East Timor (fig. 2). All the sites are shallow caverns or shelters developed in uplifted coralline limestones. The sites are clustered in five regions, as follows:

1. Northern flank of the Baucau Plateau, west of Baucau township on the north coast of East Timor. The plateau is approximately 400 km^2 in area and comprises a series of Quaternary coral limestone terraces that rise from sea level to 500 m. Two sites were excavated by Ian Glover and his team.
   Lie Siri (TL): a large, open cavern located just over 1 km from the coast, at an elevation of 240 m, and at approximately 8°26′S, 126°22′E. The cave deposit was excavated to a maximum depth of 2.05 m and produced a maximum carbon 14 (^{14}C) determination of 7270 ± 160 BP (ANU-236) from scattered charcoal fragments. Glover (1986) inferred a basal age of ca. 10,000 BP for the deposit and recognized a total of seven "horizons" (number from deepest to most surficial; corresponding to sedimentological and cul-

tural subdivisions of the stratigraphic column). Horizons Vc to VII contained pottery and the remains of domesticates. Jaws and teeth of large murids were obtained from horizons II to Vc.

Bui Ceri Uato (TB): a large, open cavern located around 2 km inland, 175 m and at approximately 8°27′S, 126°22′E. The deposit was excavated to a maximum depth of 1.45 m, with a total of 10 horizons identified. Pottery and bones of domesticates were found in horizons V to X and bones of large murids from horizons I to VI or VII. Glover encountered problems with radiocarbon dating of this site but more recent ^{14}C determinations place the basal layers of Bui Ceri Uato in the terminal Pleistocene (Selimiotis, unpublished data cited by Oliveira, 2006: 95).

2. Central highlands of East Timor at about 600 m and just over 20 km from the nearest coast. Two sites located east of the township of Venilale, on the eastern side of Hatu Ariana, were excavated by Glover.

Uai Bobo 1 (TO1): a small, enclosed cave at approximately 8°38′S, 126°23′E. Excavation reached a maximum depth of 1.4 m, with a total of eight horizons recognized. The lowest ^{14}C date obtained is 3470 ± 90 BP (ANU-414), but Glover (1986: table 65) inferred a basal age of around 9000 BP. Pottery and the bones of domesticates was found in horizons III to VIII, and bones of large murids from horizons I to V. Very large numbers of bones of small murids and bats were found in horizons I to IV; Glover attributed the accumulation of these remains to a nonhuman predator. We agree and suggest an owl as the most likely agent.

Uai Bobo 2 (TO2): a small, enclosed cave located adjacent to Uai Bobo 1. Excavation reached a maximum depth of 4.9 m in a loose, dry deposit. Thirteen horizons were distinguished, with a ^{14}C determination for Horizon I of 13,400 ± 520 BP (ANU-238). Pottery and bones of domesticates were found in horizons VII or VIII to XIIII. Large murids were recovered from horizons I to X. A large quantity of small mammal bones was also recovered from this site.

3. Coastal scarp at the eastern end of East Timor, in the vicinity of Tutualu village.

Lene Hara (LH): a large, open cavern located about 5 km east of the village of Tutuala, 100 m and at approximately 8°24′S, 127°16′E. The site was excavated in 1963 by Antonio de Almeida (Almeida and Zbyszweski, 1967), reinvestigated by Glover in 1966 (Glover, 1986: 17) and then re-excavated by the ANU team in 2000–2002. The deposit has a complex stratigraphy and excavations in different parts of the site produced cultural and faunal assemblages that span three periods: from 30,000–35,000 BP; from 18,000–25,000 BP; and from ca.10,000 to recent (O'Connor et al., 2002; O'Connor and Aplin, 2007). Small samples of large murid remains were obtained from each stratigraphic context.

Jerimalai (JM): This site is located close to Lene Hara but is at slightly higher elevation and somewhat further inland. Excavated by O'Connor (2007) in 2005 to a maximum depth of 1.5 m. Basal ^{14}C dates in each of two excavated pits fall in the range 37,000–39,000 BP, but most of the stratigraphic profile spans the terminal Pleistocene and Holocene. Small samples of large murid remains were obtained from each stratigraphic context.

4. Adjacent to Lake Ira Laloro, the largest freshwater lake in Timor, located at ca. 334 m in Lautém Province, central to the eastern peninsula of East Timor. Two sites were excavated by the ANU team in 2001. Both caves are in a cliffline located a few hundreds of meters from the northern margin of the lake floodplain.

Matja Kuru 1 (MK1): a large, open cavern, at approximately 8°26′S, 127°08′E. Excavation reached a maximum depth of 1.55 m. The basal part of the deposit is terminal Pleistocene, but the bulk of the sediments accumulated during the period 5600–4600 BP (Veth et al., 2005). Large samples of murid remains were obtained from these levels.

Matja Kuru 2 (MK2): a large, open cavern located a few hundreds of meters to the east of Matja Kuru 1. Excavation by the ANU team reached a maximum depth of 2 m. The sequence produced a basal date around 32,000 BP but features an apparent hiatus in deposition over the period 30,000–15,000 BP. Large samples of "giant" rat remains were obtained from this site.

5. The Com area, on the north coast of the eastern peninsula.

Telupunu cave: a moderately large, open cavern located approximately 5 km inland from the coast, at 260 m, and at approximately 8°22′S, 127°02′E. Excavation by Spriggs in 2002 reached a depth of 1.5 m. The greater part of the sequence is preceramic and contains sparse cultural and faunal

remains, with a basal age of around 13,500 BP (Veth et al., 2005). Preservation of organic remains including bone in this deposit is superior to that of all others.

ASSOCIATION OF UPPER AND LOWER DENTITIONS: As reported previously by both Mahoney (appendix 3 in Glover, 1986) and Musser (1981b), the Timorese "giant" murids fall into three major groups based on their dental morphology: (1) specimens with highly cuspidate, complex molars (*Coryphomys* and Mahoney's genus A); (2) specimens with high-crowned, transversely laminate molars (Mahoney's genus B); and (3) specimens with low-crowned molars with cusps fused into transverse laminae (Mahoney's genus C). Upper and lower dentitions of each general group are easily paired. However, *Coryphomys* and Mahoney's genus A are similar in general size and morphology and greater care is needed to correctly associate upper and lower molars. To do so, we paid attention to the following attributes of the specimens: (1) relative upper and lower molar row lengths (in murines length of the upper molar row usually exceeds that of the lower molar row, usually by 4%–6%); (2) the morphology and dimensions of the upper and lower incisors (in murines width of the upper incisors almost always exceeds that of the lowers; one exception is *Nesokia indica*); and (3) the relative abundances of the various morphological forms recognized within the complex-toothed group. Using these criteria, it is possible to confidently associate upper and lower dentitions with each of the individual species.

ALLOCATION OF DISSOCIATED CRANIAL ELEMENTS: As is commonly the case with archaeological assemblages, almost all the cranial specimens of the Timorese murines consist of individual dissociated elements, the majority with some damage. In the present collection, two partial crania are available, each referable to a different genus, and these provide the key to allocation of other less complete specimens. One of the two partial crania is thoroughly burnt and fragmented but could be reconstructed to provide an almost complete cranium belonging to Mahoney's Genus A. This specimen is critically important as it allows for direct association of an upper molar morphology with various other craniodental elements including the premaxilla and upper incisor, and the frontal, petrosal, and ectotympanic bones. The second specimen consists of a palate with associated interorbital portions of the neurocranium, referable to a species of Mahoney's Genus B. Both specimens will be described in a later contribution of this series. Judging from the relative abundance of the tooth-bearing elements, these two genera are the most abundant taxa overall in the collection. With these specimens as a reference point, the large number of dissociated specimens of other bones could be assessed as to their probable affinity. As a result, it is possible to generically assign the majority of isolated upper incisors and premaxillae, frontal bones, and petrosal bones, and to assign some specimens to species level.

The isolated petrosal bones from large murines showed striking morphological variation and particular effort was made to allocate these elements. An initial analysis produced four morphological groups. One well-defined group, represented by five examples, includes the petrosal associated with the burnt cranium of Mahoney's Genus A. A second distinctive group, including several dozens of specimens, consists of petrosals that are morphologically very similar to the petrosal of *Rattus norvegicus*, albeit of much larger size. This group is referred with confidence to Mahoney's genus B, for two reasons: (1) this genus is also most abundantly represented among the jaws and teeth; and (2) its dental morphology also suggests an affinity with *Rattus* and its close allies (members of the *Rattus* Division, sensu Musser and Carleton, 2005). The third and fourth groups are represented by three and two petrosals, respectively. These groups presumably represent *Coryphomys* and Mahoney's Genus C, the latter of which shows strong dental similarities with various Australo-Papuan murines including *Uromys*, *Solomys*, and *Melomys*. Petrosals of the third group are referred with confidence to Mahoney's Genus C, for three reasons: (1) they are consistently smaller than petrosals of the fourth group (judging from mandible dimensions, Genus C is a smaller murine than *Coryphomys*); (2) they do not show any significant variation in size or morphology

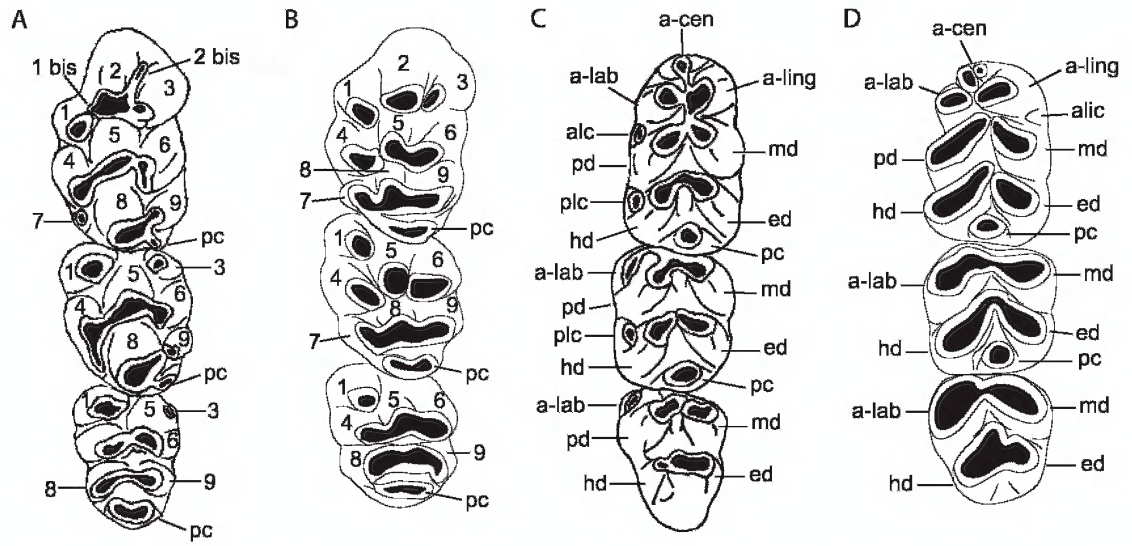

Fig. 3. Nomenclature of upper and lower molar crown structures in each of *Lenothrix canus* (after Musser, 1981) and *Coryphomys buehleri*. **A,** upper molars of *Lenothrix canus*; **B,** upper molars of *Coryphomys buehleri*; **C,** upper molars of *Lenothrix canus*; **D,** upper molars of *Coryphomys buehleri*. For upper molars principal cusps are numbered according to Miller's (1912) system; these are identified in the text with the prefix "t." *Abbreviation*: **pc**, posterior cingulum. Lower molar cusps are labelled according to the system of Weerd (1976). *Abbreviations*: **a-cen**, anterocentral cuspid; **a-lab**, anterolabial cuspid; **a-lin**, anterolingual cuspid; **alc**, anterolabial cusplet; **alic**, anterolingual cusplet; **ed**, entoconid; **hd**, hypoconid, **md**, metaconid, **pc**, posterior cingulid; **pd**, protoconid; **plc**, posterolabial cusplet.

(consistent with the lack of significant size variation in the dental sample of this taxon); and (3) they are consistent in general morphology with petrosals of *Uromys* and *Melomys*. In contrast, the two petrosals of the fourth group are larger, differ markedly in morphology from those of *Uromys* and *Melomys*, and differ considerably in size, consistent with our identification of two species within the *Coryphomys* sample.

None of the abundant postcranial remains from the various sites are associated with other skeletal elements, either postcranial or cranial. Though great morphological diversity is present in nearly every skeletal element, the task of allocating all of this dissociated postcranial material to particular taxa is one for the future.

TERMINOLOGY AND MEASUREMENTS: For naming the principal cusps and crests of the molar teeth of *Coryphomys* spp. we have followed the descriptive terminology employed by Musser in his numerous works (e.g., Musser, 1981a; Musser and Heaney, 1992), based for the upper molars on the system introduced by Miller (1912) and modified by Misonne (1969) and for the lower molars on the terminology of Weerd (1976: 44). This terminology is illustrated here (see fig. 3) for each of *Coryphomys buehleri* and *Lenothrix canus*, the latter to identify structures that are not represented in the dentition of *Coryphomys*. Where appropriate, we identify the equivalent structures in alternative terminologies as used by others.

We use the term "lamina" to refer to the more or less transverse rows of cusps that typify both the upper and lower molars of murine rodents. The first upper molar has three such laminae (anterior, middle, and posterior) while each of the second and third upper molars has two laminae each. In the lower molars, each tooth has two primary laminae that are also called "chevrons" in some contexts; this is supplemented in the case of the first lower molar by an additional structure—the anteroconid—that is attached to the front of the anterior lamina.

Osteological terminology of the mammalian skull remains highly multifarious, with many different terms often in use for what are undoubtedly homologous features in

different groups of mammals. Wahlert (e.g., 1974, 1985) has established a systematic terminology for cranial foramina across all major groups of rodents. For the most part here, we have followed his usage. However, for osteological features of the auditory region that relate to the passage of arteries and veins, we have adopted the terminology of Wible (e.g., Wible et al., 2001) as this better reflects both the embryology and phylogeny of the mammalian blood vascular systems.

There is a substantial body of work on the functional anatomy of the masticatory muscles of rodents, especially of *Rattus norvegicus* (e.g., Hiiemae, 1971; Hiiemae and Houston, 1971; Weijs and Dantuma, 1975), and a growing body of comparative work on other groups of muroids (Bekele, 1983; Satoh, 1997, 1999; Satoh and Iwaku, 2004, 2006, 2008). In contrast, osteological features that relate to the attachment of tendons and aponeuroses are generally given light treatment in standard anatomical sources. To more accurately describe these features, we have adapted the terminology of Satoh and Iwaku (2006) for subdivisions and aponeuroses of the primary masticatory muscles. For other elements of muscular anatomy, we have used the more conventional terminology of Greene (1968).

The internal osteology of the mammalian nasal cavity has attracted little general attention in the paleontological literature and virtually none in the case of fossil murines. Fortunately, for laboratory rats and mice, there is a rapidly growing literature on the anatomy, histology and embryology of the olfactory and glandular tissues of the nasal cavity (e.g., Jacob and Chole, 2006) and this provides both a basic terminology for major spaces and a basis for reconstruction of soft tissue relations in fossil murines. However, as this literature generally does not identify the osteological expression of soft tissues features, we have been obliged to introduce some new terminology for this region of the skull.

Craniodental measurements were taken with handheld digital calipers, to the nearest 0.01 millimeter (mm). Upper and lower molar lengths are maximal coronal dimensions taken along the approximate midline of the tooth, with the body of the caliper held parallel to the occlusal plane.

INSTITUTIONAL ABBREVIATIONS: The Timorese fossil samples are housed in three collections, identified by the following prefixes: Australian Museum, Sydney (Palaeontology): **AMF**; Australian National Wildlife Collection, CSIRO, Canberra (Palaeontology): **ANWCP**; American Museum of Natural History, New York (Modern mammals): **AMNH**. Comparative specimens in the modern mammal collection of the Australian National Wildlife Collection, CSIRO, Canberra (Mammals) are identified by the prefix **ANWCM**.

DENTAL ENUMERATION AND ABBREVIATIONS: Teeth of the upper and lower molar series are designated by superscript and subscript numbers, e.g., first upper molar is M1, second lower molar is m2. Symmetry of teeth is indicated by a prefixed R for right side and L for left side; e.g., right first lower molar is R m1.

ANATOMICAL ABBREVIATIONS: The abbreviations used for upper and lower molar cusps are shown in figure 3. Other abbreviations are listed beneath each figure in which they are used.

SYSTEMATICS

Family Muridae
Subfamily Murinae
Coryphomys Schaub, 1937

TYPE SPECIES: *Coryphomys buehleri* Schaub, 1937.

CONTENT: *Coryphomys buehleri* Schaub, 1937, *Coryphomys musseri*, sp. nov.

REVISED DIAGNOSIS: A genus of large-bodied, complex-toothed murines distinguished from all others by the combination of the following morphological features: molar crowns moderately hypsodont and weakly inclined; anterocentral cuspid prominent on m1; principal lingual cusps of upper molars (t1, t4) isolated from central cusps until molars attain advanced state of wear; a discrete cusp t7 united to cusp t8 on each of M1–2; posterior cingulum forming an elevated, transverse occlusal ridge behind cusps t8–t9 on each of M1–3, and barring contact between central row cusps on successive

molars; upper and lower third molars almost equal in area to the corresponding second molars; upper and lowers incisors large and with simple, D-shaped cross-sections; incisive foramen very short and narrow, penetrating only a short distance into palatal lamina of maxilla; zygomatic plate tall and narrow, with a straight anterior margin and shallow zygomatic notch; stem of stapedial artery extremely reduced such that promontorium lacks a conspicuous stapedial sulcus; rostrum shortened; and maxillary sinus complex enlarged and elaborate, causing a marked constriction of both the posterior nasopharynx and the infraorbital sulcus.

Presence of a large cusp t7 on each upper molar distinguishes *Coryphomys* from the majority of previously described murine genera. Among genera with large cusps t7, *Coryphomys* is distinguished from all except *Carpomys* and *Spelaeomys* (Hooijer, 1957; Musser, 1981b) by the presence of a substantial posterior cingulum on all three upper molars. It is distinguished from *Carpomys* by its highly cuspidate molar form (cusps are largely fused into transverse laminae in *Carpomys* spp.) and the absence of labial cusplets on m2–3. It differs from *Spelaeomys* in numerous details of molar morphology including the greater size of the posterior cinguli on all upper molars, the absence of cusp t3 on M2–3, and the absence of accessory labial cuspids and cusplets on all lower molars.

Remarks: Under Article 32.5.2.1 of the Fourth Edition of the International Code of Zoological Nomenclature (International Commission on Zoological Nomenclature, 2000: 40) the original specific epithet *bühleri* is adjusted to *buehleri*.

Coryphomys buehleri Schaub, 1937

Holotype: Naturhistorisches Museum Basel, NMB A.P.1. A right dentary with m1–3 and root of incisor; preserving condylar process but with damage to coronoid and angular processes. Figured by Schaub (1937: figs.1 and 2). Not examined for this study.

Referred Material: AMF 68831: Uai Bobo 1 (TO1/2), R Dentary with m1–3; AMF 68789: Bui Ceri Uato (TB/2), L Dentary with m1–2; AMF 68850: Lie Siri (TL/E 5C/C^3), R Dentary with m1–2; ANWCP1: Jerimalai (JM/B/19) L m2; ANWCP2: Matja Kuru 1 (MK1/A/17), L M3; ANWCP3: Matja Kuru 1 (MK1/AA/28), R M2; ANWCP4: Matja Kuru 1 (MK1/AA/25), L M3; AMF 68838: Lie Siri (TL/E/5C/C^3), L maxilla with M1; AMF 68751a: Uai Bobo 1 (TO1/3), L palatal fragment (partial maxilla and palatine) with M1–3; AMF 68751b: Uai Bobo 1 (TO1/3), R maxilla fragment with M1; AMF 68751c: Uai Bobo 1 (TO1/3), L zygomatic plate; ANWCP5: Matja Kuru 1 (MK1/AA/10), R M1; ANWCP6: Matja Kuru 2 (MK2/D/32), R m1; ANWCP7: Matja Kuru 2 (MK2/D/41), L M3; AMF 68824: Uai Bobo 1 (TO1/3), R M1; ANWCP8: Matja Kuru 1 (MK1/AA/10), L M2.

Remarks: Given the presence on Timor of various other equally large murines, it is possible that the murine femur referred by Schaub (1937: fig. 3) to *Coryphomys buehleri* may not belong to this taxon. Its identity will be reassessed following allocation of the abundant postcranial remains now available from the many excavated assemblages.

Only one of the three dentaries (no. 2) attributed to *C. buehleri* by Hooijer (1965) actually belongs to this species. Hooijer's specimen no. 1 is referable to Mahoney's Genus A, while his no. 3 belongs to the new species of *Coryphomys* described below. Ironically, *Coryphomys buehleri*, the only formally described member of the prehistoric Timorese murine fauna, is also one of the rarest of all the large-bodied taxa in the fossil samples.

Attribution of a maxillary dentition to this species is based on the recognition of a morphologically distinctive subset of *Coryphomys* specimens that are also slightly larger in all dental dimensions relative to those of the second species.

Extended Description of *Coryphomys buehleri*

Upper Molars (fig. 4; table 1): The upper molars are moderately hypsodont but comprised of variably discrete and partially united cusps arranged in more or less transverse series. The occlusal plane of the molar row is tilted outward (i.e., lingual

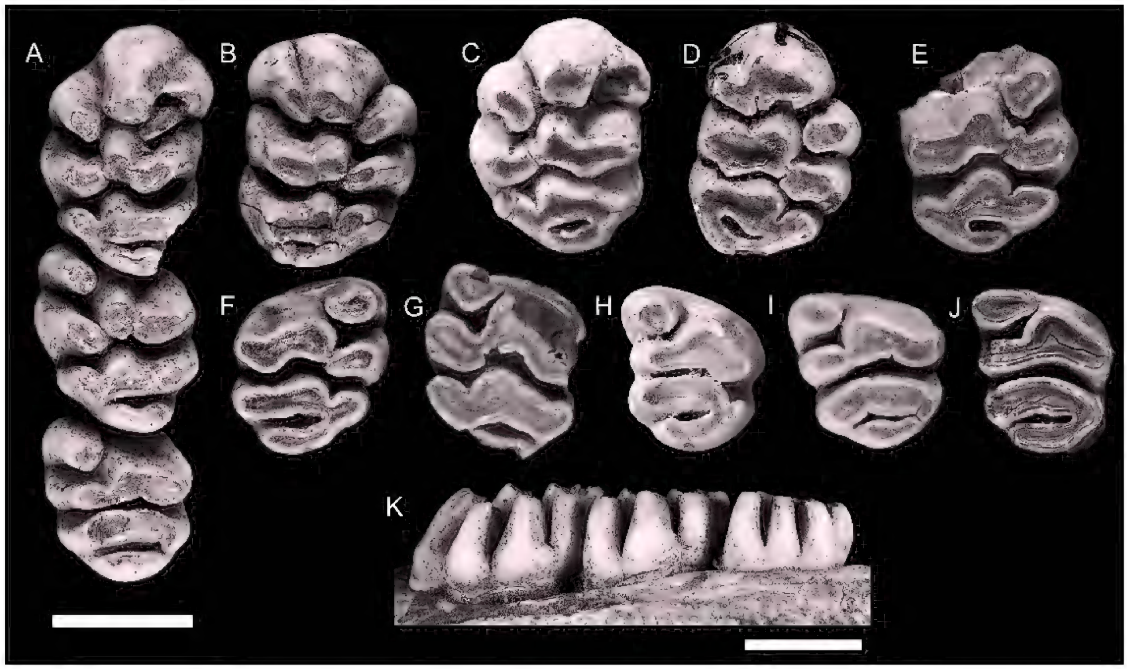

Fig. 4. Occlusal views and one lingual view of upper molars referred to *Coryphomys buehleri*. Occlusal views: **A,** AMF 68751a: associated left M1–3; **B,** AMF 68751b: a right M1 (same individual as AMF 68751a); **C,** AMF 68838: a left M1; **D,** AMF 68824: a right M1; **E,** ANWCP5: a right M1 (missing cusps t1–2); **F,** ANWCP3: a right M2; **G,** ANWCP8: a left M2; **H,** ANWCP7: a left M3; **I,** ANWCP4: a left M3; **J,** ANWCP2: a left M3. Lingual view: **K,** AMF 68751a: associated left M1–3. The lingual view illustrates the moderately hypsodont condition of the molars in *C. buehleri* and the slight posterior inclination of the cusps on M1, trending to vertical on M3. Scale bar beneath A also applies to B–J and represents 5 mm. A separate 5 mm scale bar is provided for K.

cusps are significantly lower than labial cusps) but there is little indication of helical torsion along the molar row.

No maxillae without molars are confidently assigned to this species. The M1 has four roots. The anterior root, supporting the anterior lamina, is broad and kidney shaped with the concavity facing the rear. Two small circular roots on the lingual side of the tooth support cusps t4 and t7. A posterolabial root, intermediate in size, supports cusps t8 and t9 and the associated posterior cingulum. The root pattern for M2 cannot be determined from available specimens. Two isolated M3 show a broad anterior root supporting cusps t1 and t4–6, a somewhat narrower root supporting cusps t7–8 and a small labial rootlet above cusp t9 and partially united to the front of the posterior root.

M1: This tooth is represented by a total of five specimens (fig. 4A–E). They are broadly ovate in occlusal outline but have a weakly concave labial margin.

The anterior lamina consists of three discrete, columnar cusps. The central cusp t2 curves forward and downward from a bulbous base, narrowing toward an occlusal surface that is rounded anteriorly but flattened on each of the labial, lingual, and posterior margins. The labial cusp t3 is positioned level with cusp t2. It is firmly adpressed to the labial surface of cusp t2 but is fully encircled by enamel for approximately one third of its total height. Above that level, the two cusps are united but with well-defined anterior and posterior grooves that extend to the crown base. Cusp t3 also has a bulbous base and narrower apical portion. The occlusal surface is ovate, with the long axis oriented at approximately 45° to the coronal major axis. Cusp t1 is isolated from the cusp t2–3 complex by a deep cleft that

TABLE 1

Measurements of Upper and Lower Dentition in Specimens Attributed to *Coryphomys buehleri*

Measurements are molar lengths (L) and widths (W) and the breadth (IB) and depth (ID) of the lower incisor. Sample sizes, means, standard deviations, and ranges are also shown.

Upper dentition	Symmetry	M1–3	M1 L	M1 W	M2 L	M2 W	M3 L	M3 W		
CP2	L						5.97	5.12		
CP3	R				5.69	5.51				
CP4	L						5.5	5.22		
AMF 68838	L		8.51	6.15						
CP7	L						5.59	5.53		
AMF 68824	R		8.5	6						
AMF 68751a	L	19.49	8.56	5.77	5.86	5.8	5.4	5.31		
AMF 68751b	R		8.6	5.66						
Mean		19.49	8.54	5.90	5.78	5.66	5.62	5.30		
s.d.			0.046	0.221	0.120	0.205	0.249	0.175		
Range			8.5–8.6	5.66–6.15	5.69–5.88	5.51–5.8	5.4–5.97	5.12–5.31		
N		1	4	4	2	2	4	4		
Lower dentition		**m1–3**	**m1 L**	**m1 W**	**m2 L**	**m2 W**	**m3 L**	**m3 W**	**IB**	**ID**
AMF 68831	R	18.84	7.75	5.14	5.36	5.56	5.50	5.39		
AMF 68789	L		7.62	5.14	5.4	5.48			3.15	4.88
AMF 68850	R		8.12	5.37	5.71	6.16			3.40	
CP1′	L				5.42	6.28				
CBP6	R		8.5	5						
Holotype	R	19.9	8.5	5.4	5.9	6.2	5.40	5.60		
Hooijer No. 2	L	20.1		5.2		5.7		5.80		
Mean		19.61	8.00	5.16	5.47	5.87	5.50	5.39	3.28	4.88
s.d.		0.677	0.410	0.152	0.236	0.356	0.071	0.205	0.177	
Range		18.84–20.1	7.62–8.12	5.14–5.37	5.36–5.71	5.48–6.28	5.4–5.5	5.39–5.8	3.15–3.40	
N		3	5	6	5	6	2	3	2	1

extends more than three quarters of the way to the crown base. The cusp is bulbous basally but narrows apically and folds against the anterolingual surface of cusp t5. A weak posterolingual groove on cusp t1 produces a kidney-shaped occlusal surface which is oriented at approximately 45° to the main coronal axis. The occlusal surface of cusp t1 lies in a plane slightly above that of cusps t1–2 and t5.

The middle lamina consists of a united but lobular cusp t5–6 complex and a discrete but adpressed cusp t4. Cusps t5 and t6 are approximately equal in bulk but differ in shape. The central cusp t5 is columnar and laterally compressed, and is smaller in occlusal area than cusp t2. Cusp t5 is firmly connected to cusp t6, but the cusp boundary is marked by strong posterior groove. Cusp t6 is an elongate, transversely oriented structure with a bulbous base, a rounded posterior surface, a flattened anterior surface and a well-developed posterolingually directed ridge. Cusp t4 is similar in basic shape and orientation to cusp t1, but differs in the presence of a well-developed anterolabial ridge that abuts against the corresponding ridge from cusp t4. As a result, the occlusal surface of cusp t4 is broadly arcuate (concave anteriorly) and continuous with the cusp t5–6 complex. The occlusal surface of cusp t4 lies in the same plane as cusp t1 and is thus slightly above that of cusps t5–6.

The posterior lamina consists of a transversely oriented t8–9 complex and a prominent t7 that is firmly connected to cusp t8. The central cusp t8 is similar in size and shape to cusp t5. The boundary between cusps t8 and t9 is well marked in relatively unworn specimens by an apical cleft but this is rapidly obliterated by wear. The lateral margin of cusp t9 supports a broad anterolabially directed ridge that ascends to the crown base. With progressive wear, this ridge produces an elongation of the occlusal surface of cusp t9. Cusp t7 is discrete apically from t8 but soon unites to this cusp with wear. In contrast, the fissure separating cusp t7 from cusp t4 extends almost to the crown base, thereby keeping the two cusps separate, even under advanced wear.

The posterior cingulum is an elevated transverse ridge that forms the posterior surface of the tooth. The cingulum shows a variable pattern of connections. On both sides of AMF 68751 (fig. 4A–B) it is firmly connected labially to the point of union of cusps t8 and t9, but remains well separated from the posterior surface of cusp t7 as it rises toward the crown base, creating a lingually open cingular shelf. On AMF 68838 (fig. 4C) the labial end of the cingulum is united high to the anterior surface of cusp t9, thereby enclosing a distinctive cingular fossette. AMF 68824 (fig. 4D), with more advanced wear, also has a fully enclosed fossette with broad cingular connection at both labial and lingual ends. Two small pimples on the elevated portion of the ridge create a weakly bicuspid occlusal outline on AMF 68751 (fig. 4A–B).

M2: Three specimens are available (fig. 4A, F–G), each at a different wear stage. The less worn example, part of the complete molar series in AMF 68751 (fig. 4A), is described first. In both size and cuspal arrangement the M2 closely resembles M1, save for the absence of elevated cusps t2–3. Cusp t1 is more vertically oriented than on M1 but is similarly folded against the anterolingual surface of cusp t5. Its posterior surface is rounded and the occlusal surface is correspondingly ovate rather than kidney shaped. The occlusal surface of cusp t1 lies in a plane slightly above that of cusp t5. Cusp t3 is represented by a small nubbin positioned near the crown base in the fold that marks union of cusps t5 and t6.

Cusps t5 and t6 of the middle lamina are firmly united but cuspal limits are marked by strong anterior and posterior grooves. The central cusp t5 is columnar and laterally compressed, and is slightly larger than the serial homolog on M1. Cusp t6 is larger in occlusal area than cusp t5. It is broader and more transversely oriented than the serial homolog on M1 but otherwise similar in form. Cusp t4 is similar in basic shape and orientation to cusp t1 but is larger in occlusal area. It lacks the anterolabial ridge seen on cusp t4 of M1 and this has a simpler, ovate occlusal outline. The occlusal surface of cusp t4 lies slightly above that of cusps t5–6, but the contrast is less marked than on M1.

The posterior lamina is an almost exact duplicate of this structure on M1 except that cusp t7 is slightly larger in occlusal area. The posterior cingulum is connected at its lingual end to the posterior surface of cusp t7. The labial end is deeply separated from cusp t9 by a cleft that ascends almost to the crown base.

ANWCP3 (fig. 4F) is in a more advanced state of wear. It shows comparable features save for a more elevated connection between the labial end of the posterior cingulum and the posterior surface of cusp t9. Cusps t7–t9 and the posterior cingulum are united by a common dentin pool in this specimen, while cusps t4 and t1 each remains discrete from cusp t5. ANWCP8 (fig. 4G) is even more heavily worn. Cusps on both laminae are united into common dentin pools but cusp t9 remains isolated from the labial end of the posterior cingulum.

M3: Four specimens are available (fig. 4A, H–J). The least worn examples of this tooth (AMF 68751, fig. 4A; ANWCP4, fig. 4I) are only slightly shorter and narrower than M2, but they differ in numerous morphological features. Cusp t1 is more conical in form but bears a short ridge on its labial surface, directed to the front of cusp t5. Cusps t5 and t6 are firmly united into a transversely oriented lamina with a common dentin pool. There is no delimiting anterior groove, and no cusp nubbin or fossette in the position of cusp t3. However, a posterior groove indicates the relative contribution of the two cusps, with cusp t6 being slightly the larger. Cusp t4 is smaller and more transversely oriented than it serial homologs on M1–2; the occlusal plane is only slightly above that of cusp t5 and the two cusps are united by a common dentin pool.

Cusps t7 and t8 are united into a broad, transversely oriented structure that is gently convex anteriorly. The boundary between the two equal-sized cusps is marked by a slight indentation of the anterior margin and a corresponding flexion of the occlusal surface. Cusp t9 is a smaller columnar cusp that is firmly applied to the labial surface of cusp t8 but projects posterior to this cusp.

The posterior cingulum forms a robust, transversely oriented lamina. It is united high on the crown to the posterior surfaces of cusps t7 and t9 and has a rounded and bulbous posterior surface. The occlusal surface consists of two facets, the lingual facet paralleling that on cusp t7.

The most heavily worn example of M3 (ANWCP2, fig. 4J) has the posterior cingulum joined by a common dentin pool to t9 but still discrete from cusp t7 at the lingual end.

Lower Incisor: The incisor is retained in AMF 68789 (fig. 9F) and lacks only the tip. The body of the tooth is approximately D-shaped in cross-section and has a width-to-depth ratio of 0.645 (table 1). A smoothly curved strip of enamel is present along the ventral and lower lateral surfaces of the tooth, extending just over half way up the lateral surface of the tooth and terminating at the widest point of the tooth. Enamel is absent from the medial surface, save for a 0.34 mm rim corresponding to the thickness of the enamel layer. Pale orange pigment is present medially in a 1.6 mm wide band. Otherwise the enamel is unpigmented. The enamel-free dorsal half of the incisor bears a weak dorsolateral groove. The medial surface is very slightly concave. The occlusal facet is incomplete but terminates posteriorly in a distinct step.

Lower Molars (fig. 5, table 1): The lower molars are also moderately hypsodont. The enamel is smooth on all surfaces, irrespective of intensity of wear. The occlusal plane of the molar row has a moderate degree of helical torsion, changing from transversely horizontal on m1 to lingually inclined (i.e., lingual cusps slightly lower than labial cusps) on m3.

No dentaries without molars are confidently assigned to this species; hence, information on molar root patterns is based on careful examination of teeth in situ. The m1 has two roots. The posterior root has similar dimensions on the labial and lingual sides and appears to bear a posterior groove; it probably occupies a symmetrical and possibly weakly bilobed alveolus. In contrast, the anterior root appears much broader labially than lingually, and the alveolus is presumably comma shaped with an anterior "head" and a posterolabial "tail." The m2 appears to have two broadly united, transverse roots, one supporting each of the two principal chevrons. The posterior root, as exposed on

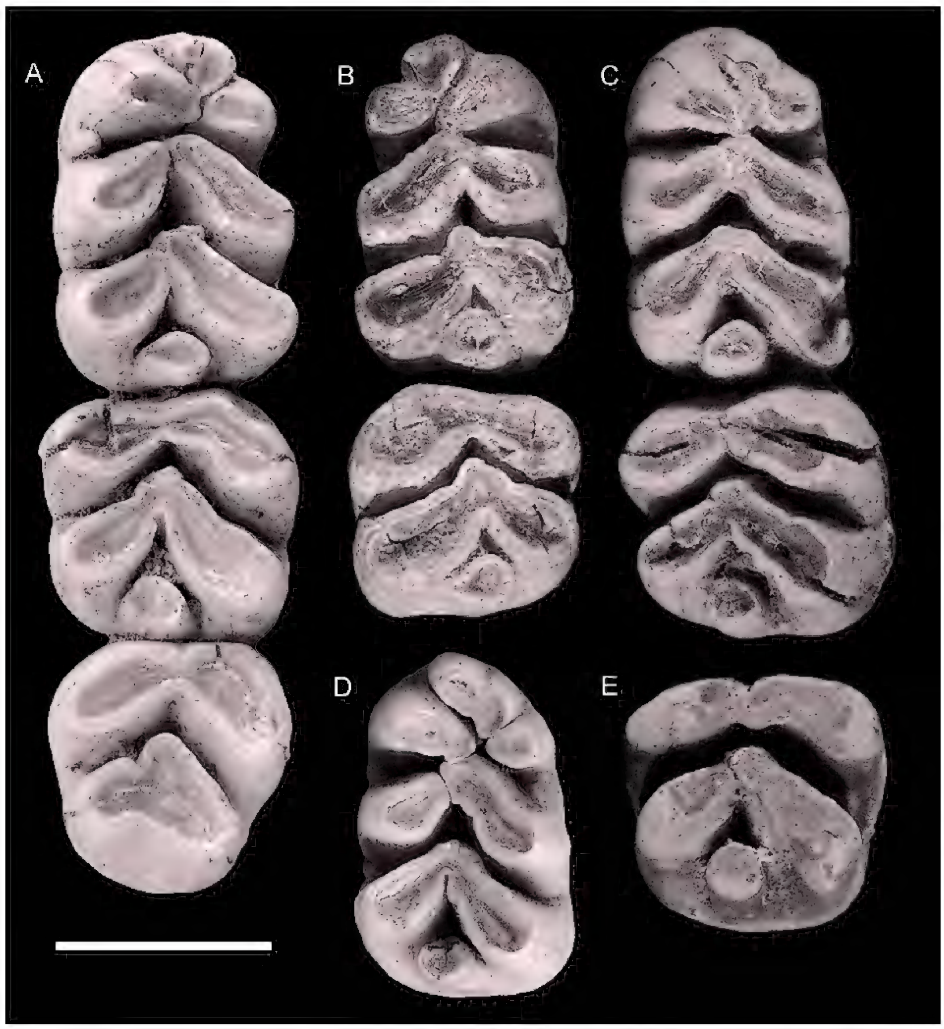

Fig. 5. Occlusal views of lower molars referred to *Coryphomys buehleri*. **A,** AMF 68831: associated right m1–3; **B,** AMF 68789: associated left m1–2; **C,** AMF 68850: associated right m1–2; **D,** ANWCP6: an isolated right m1; **E,** ANWCP1: an isolated right m2. Scale bar represents 5 mm and applies to all images.

AMF 68789, is solidly united to the root apices and shows an increase in width with depth. This firm anchoring of the molars presumably accounts for the high rate of retention of molars in preserved dentaries of this taxon. The alveoli of m3 are exposed on AMF 68850. The anterior alveolus is broad and contained a fused root that terminated in short separate nubbins. The posterior alveolus is narrower and more circular.

m1: This tooth is represented by four new examples (fig. 5A–D). They have a rectangular outline that is broadest across the posterior lamina and narrows slightly to the front. The anteroconid is relatively large and equals the two posterior lophids in occlusal area. The principal cuspids are weakly united, even in heavily worn examples. The occlusal surfaces of the labial and lingual rows of cuspids are elevated externally and slope down to a central occlusal valley. The external surfaces of the labial cuspids are vertical, whereas those of the lingual cuspids are slightly bowed in less heavily worn examples.

The anteroconid shows three principal cuspids arranged in a somewhat variable

pattern. The anterolingual cuspid is consistently the largest and most discrete of the three. It has an ovate occlusal outline, with the labial end adpressed against the front of the protoconid and a long axis that swings approximately 30° forward of transverse. The anterolabial cuspid is transversely aligned with the posterolabial end of the anterolingual cuspid but it is considerably smaller and has a more rounded occlusal outline. In all specimens the two cuspids are deeply separated almost to their bases. The anterocentral cuspid is more variable in size, morphology, and relations. In AMF 68850 (fig. 5C) it is a simple rounded cuspid that is broadly connected to the anterior surface of the anterolabial cuspid. All other examples show a bicuspid anterocentral cuspid. In ANWCP6 (fig. 5E) it is divided into two subequal components by an anterolabial groove; the posterolabial end is adpressed against the anterolabial cuspid. AMF 68831 (fig. 5a) shows a larger labial component and a smaller, pimplelike lingual component attached high on the anterolingual side; the combined anterocentral cuspid in this example is equally discrete from each of the anterolabial and anterolingual cuspids. AMF 68789 (fig. 5B) has the anterocentral cuspid divided into a larger lingual component and a smaller labial component, the combined cuspids having a specific attachment to the anterolabial cuspid. In all cases, the occlusal surface of the anterocentral cusp is elevated anteriorly and slopes down to the rear, thereby blocking the longitudinal occlusal valley of m1. The type specimen, as described and illustrated by Schaub (1937: fig. 2), has a divided anterocentral cuspid. Hooijer's (1965: pl. I) specimen no. 2, herein referred to *C. buehleri*, possesses an undivided cuspid.

Two specimens show small accessory cuspules attached to the anteroconid. AMF 68831 (fig. 5A) has a small cuspule attached to the posterolingual base of the anterolingual cuspid. The other (ANWCP2, fig. 5C) has a basal cuspule attached to the posterior surface of the anterolabial cuspid; a weak buttresslike ridge from the base of the protoconid joins this structure to produce a partial cingulum across the base of the anterolabial flexid. These cuspules appear to be absent from the holotype and Hooijer's specimen no. 2, judging from the respective illustration and figure.

The anterior lamina of m1 is made up of two elongate cuspids arranged in a forward-facing chevron. The labial protoconid is elongate and has an occlusal surface that is variably rectilinear or weakly dumbbell shaped, the latter condition produced by shallow concavities on both the anterolabial and the posterolingual surfaces. The lingual metaconid is D-shaped, flattened anteriorly, curved posteriorly, and smaller in occlusal area than the protoconid. In two specimens (AMF 68831, fig. 5A; AMF 68850, fig. 5C) the metaconid abuts the anterior end of the protoconid without overlap. In the other two (AMF 68789, fig. 5B; ANWCP6, fig. 5D), the protoconid overlaps the front of the metaconid, so that the latter abuts the lingual face of the protoconid. In both conditions the two cuspids remain narrowly separate almost to the crown base. Hooijer's (1965: pl. I) specimen no. 2, herein referred to *C. buehleri*, has the two cuspids abutting without overlap. The anterolophid chevron has an anterior angle of approximately 130° and a posterior angle of approximately 70°.

The posterior lamina of m1 repeats the basic structure of the anterior lamina but with minor differences in cusp size and orientation. The labial hypoconid is virtually identical in size and orientation to the protoconid, even to the presence of a low anterolabial buttress that partially encloses the posterolabial flexid. The lingual entoconid is slightly larger in occlusal area than the metaconid. Centrally, the hypoconid and entoconid are more firmly adpressed and the two cuspids show a transversely continuous dentin pool in more heavily worn examples. The hypoconid and entoconid abut without overlap on one specimen (ANWCP6, fig. 5D), but in the other three the hypoconid overlaps the front of the entoconid. They abut in Hooijer's (1965: pl. I) specimen no. 2, herein referred to *C. buehleri*. The posterior chevron has an anterior angle of approximately 115° and a posterior angle of approximately 90°. There is no contact between the anterior and posterior laminae above the level of the crown base.

The posterior cingulum is an isolated, round to oval-shaped cusp. It is positioned low and centrally at the rear of the tooth and, unlike the primary cusps, stands vertical rather than sloping forward.

m2: This tooth is represented by four new specimens (fig. 5A–C, E) one of which (ANWCP1, fig. 5E) is essentially unworn. All examples are slightly wider than long and the anterior lamina is slightly wider than the posterior lamina.

The anterior lamina is essentially transverse in orientation, with a broad and shallow anterior concavity and deeper and more broadly U-shaped posterior groove. In lightly worn specimens (ANWCP1, fig. 5E; AMF 68831, fig. 5A) the protoconid and metaconid contributions are defined by a short, vertical fissure located approximately two-thirds across from the labial margin. With additional wear the protoconid and metaconid rapidly merge into a common dentin pool. The metaconid is teardrop shaped in occlusal outline. The protoconid is more variable in shape. On three specimens it has a distinct anterolabial groove that may indicate the position of an incorporated anterolabial cuspid. One specimen lacks the anterolabial groove, as does Hooijer's (1965: pl. I) specimen no. 2, herein referred to *C. buehleri*. The posterior surface of the protoconid is gently rounded in two specimens and in Hooijer's (1965: pl. I) specimen no. 2, is narrowly grooved in one, and more deeply grooved in another.

The posterior lamina is a chevron-shaped structure that closely resembles the serial homolog on m1. The hypoconid and entoconid are more intimately united and share a common dentin pool after minimal wear. The posterior cingulum is erect and rounded on all specimens. In AMF 68789 (fig. 5B) it has a more elevated connection to the hypoconid than to the entoconid. The anterior and posterior laminae are unconnected above the level of the crown base.

m3: The m3 is represented by one new specimen (part of AMF 68831, fig. 5A) and is also present in Hooijer's (1965: pl. I) specimen no. 2, herein referred to *C. buehleri*. The m3 is subequal to the m2 in length and width as measured across the anterior lamina and is only slightly smaller than the m2 in occlusal area. The occlusal surface is weakly angled on the anterolophid but transversely flat on the posterior lamina.

The anterior lamina is a broadly open chevron, with a slightly concave anterior face and a posterior angle of approximately 95°. The protoconid is slightly larger than the metaconid in occlusal area. There is no anterolabial cuspid on AMF 68831, but the anterior margin of the protoconid is angular, suggestive of an amalgamated cuspid; this part of the tooth is more smoothly rounded in Hooijer's specimen no. 2.

The posterior lamina is considerably narrower than the anterior lamina on the m3 of AMF 68831, compared with slightly narrower on the holotype, as described and illustrated by Schaub (1937: fig. 2). It consists of a larger, obliquely oriented hypoconid and a smaller, adpressed conical entoconid that is defined by clear anterior and posterolingual grooves. On Hooijer's specimen no. 2 the two laminae are almost equal in width. A posterolingual groove alone marks the division between the hypoconid and entoconid on this more heavily worn tooth.

MAXILLA (figs. 6–8, 15): Information on the structure of the maxilla and palatine bones comes from associated left and right palatal fragments (AMF 68751, fig. 6). The left palatal fragment (AMF 68751a, fig. 6D) retains the full length of the maxilla, from the medial suture with the premaxilla back to the posterior end of the alveolar portion, and preserves a complete midline palatal suture that includes a fragment of the palatine. Only the roots of the zygomatic and orbital processes are preserved. The right palatal fragment (AMF 68751b, fig. 6C) is less complete posteriorly but retains a larger portion of the antemolar palatal lamina. The specimen is partially mirrored in figure 7 to produce a composite that illustrates the major features of the palate. A left zygomatic plate from the same excavation unit probably derives from the same individual (AMF 68751c, fig. 6A–B). Though no direct contact exists between this specimen and the left maxilla, the two specimens are complementary and show an identical state of preservation and discoloration. Two other reasons for accepting this association are: (1) the basal portion of the plate is consistent with this

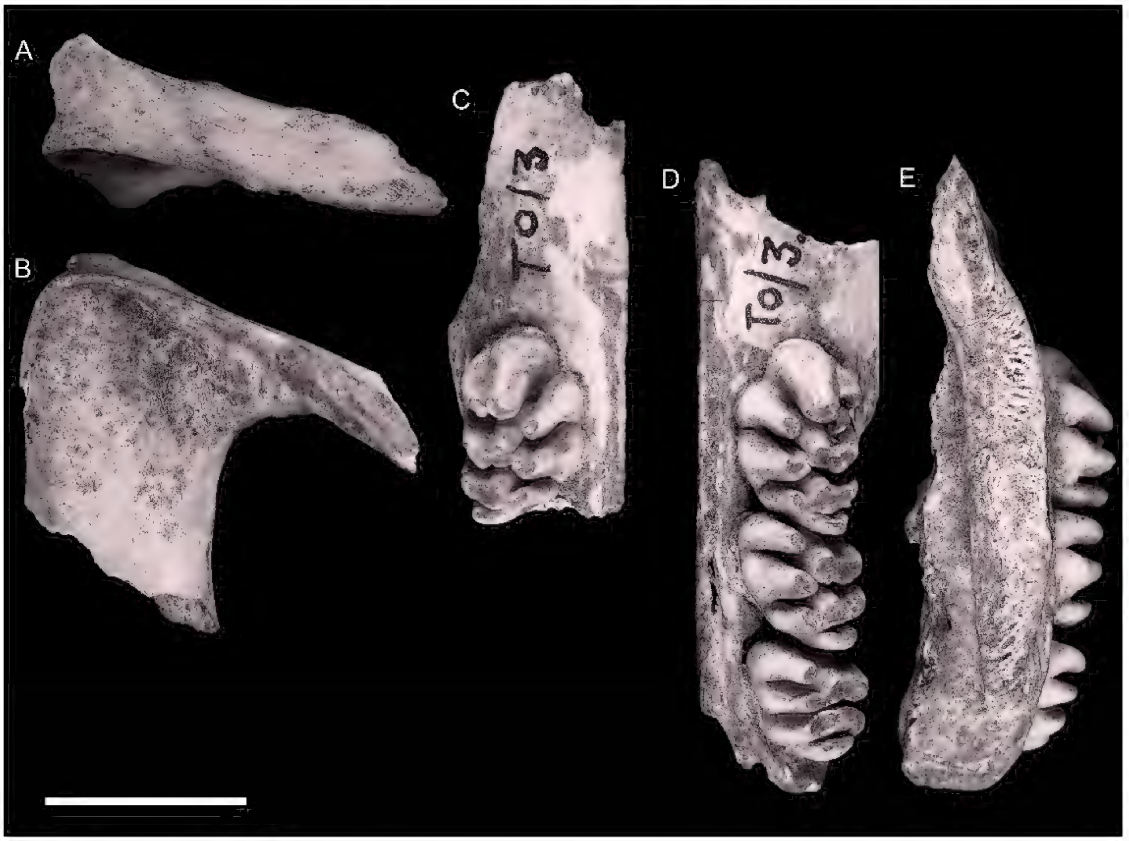

Fig. 6. Palatal specimens referred to *Coryphomys buehleri*. All fragments very likely derive from the same individual. The left zygomatic plate (AMF 68751c) is shown in lateral **(A)** and ventrolateral **(B)** views. The right maxillary fragment with M1 (AMF 68751b) is shown in occlusal view **(C)**. The left palatal fragment (AMF 68751a) includes portions of the maxilla and palatine bones, and M1–3; this is shown in occlusal **(D)** and medial **(E)** views. The right maxillary fragment extends forward to the premaxillary-maxillary suture (**pms**) and preserves the posterior notch (**ifn**) of a short and narrow incisive foramen. The left palatal fragment preserves the posterior margin of the bony palate (**ppm**) and the posterior palatal foramen (**ppf**). Scale bar represents 10 mm and applies to all images.

region in the second species of *Coryphomys*, to be described below; and (2) the morphology of the zygomatic plate differs from that of confidently associated specimens of each of the three other genera.

The most prominent features of the palate are the exceptionally large size of the molar rows relative to the bony support structures, the narrowness of the palatal bridge that separates them, the midpalatal antemolar depression, the short posterior palatal bridge, and the short and extremely narrow incisive foramina.

The palatal lamina of the maxilla is extremely thick, measuring 3.8–4.0 mm in depth at the medial suture and only thinning rapidly toward the anterior suture with the premaxilla (fig. 6E). The sutural contact between the palatine and maxilla, visible on the medial palatal suture, is situated level with the center of M2. The rear of the bony palate is level with cusp t4 of M3. The anterior sutural contact with the premaxilla is located 11.1 mm forward of the anterior face of M1. The total length of the maxilla is reconstructed as 33.3 mm, compared with the M1–3 alveolar length of 19.8 mm.

A deep palatal groove extends from the rear of the bony palate through to just forward of M1. Situated within this groove is the posterior palatal foramen, located approximately level with the front of M2. A

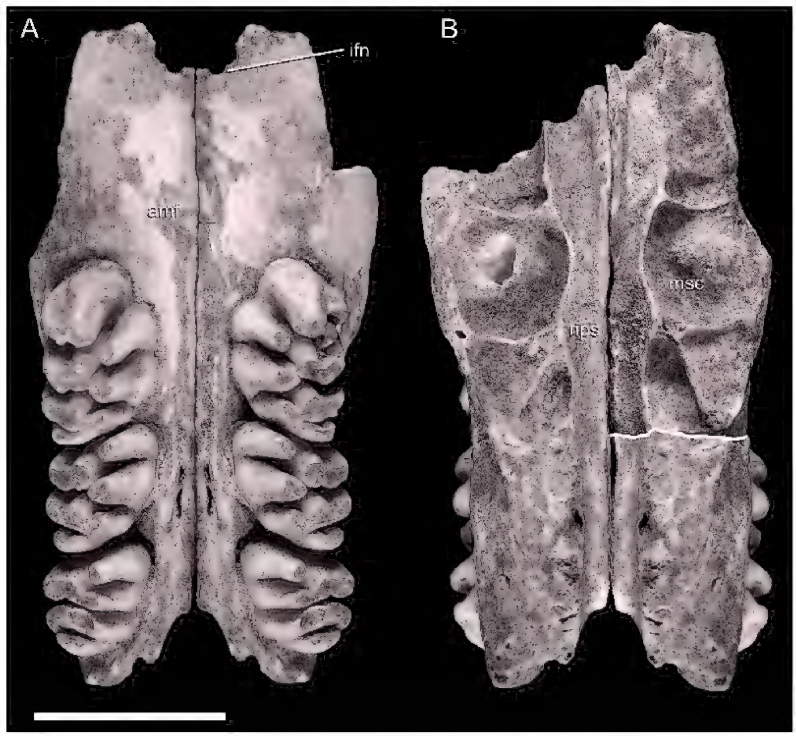

Fig. 7. Reconstructions of palatal structures of *Coryphomys buehleri* based on reciprocal mirroring of the left and right palatal fragments of specimen AMF 68751. The specimen is shown in **(A)** ventral and **(B)** dorsal views. The ventral view dramatically illustrates the extremely large size of the molars relative to the osseous structures, the very short and narrow nature of the paired incisive foramina (**ifn**) and the broad antemolar palatal fossa (**amf**). The dorsal view illustrates the marked narrowing of the nasopharygeal sulcus (**nps**) between the molar rows and the elaborate nature of the maxillary sinus complex (**msc**). Scale bar represents 10 mm. White line is posterior margin of preserved right maxilla.

sulcus located behind M3 marks the position of a posterior palatal pit and associated foramen.

The antemolar palatal lamina of each maxilla is arched dorsally, creating a broad midpalatal antemolar fossa. This surface lacks vascular grooving. The anterior margin of the palatal lamina bears a 2.7 mm deep notch for the posterior border of the incisive foramen. These paired structures were evidently very short, terminating some 9.8 mm forward of the molar rows, and narrow, with a combined width of only 3 mm. The lateral margin of the antemolar fossa is marked by a short (3 mm) but sharply defined masseteric ridge, marking the ventral limit of insertion of the anterior portion of the deep part of the masseter. This ridge originates at the centre of the M1 alveolus and runs forward to the medial side of a rugose fossa situated 2.5 mm forward of the alveolus and aligned with the labial row of cusps of M1. This is identified as the superficial masseteric fossa (for attachment of the inferior zygomatic plate aponeurosis); it is positioned remarkably close to the M1, but we note a similar condition in *Mallomys*. No nutrient foramen is visible anterior to M1.

The alveolar body of the maxilla is unusually shallow, especially given the great size of the molars. The lateral surface is near vertical above M1, but it twists to face dorsolaterally above M3. This rotation parallels the helical twist of the occlusal plane of the molar row (see below).

The dorsal surface of the maxilla (figs. 7–8) is divided into two major regions: (1) an endocranial region, representing the ventrolateral portion of the posterior rostral cavity; and (2) an orbitotemporal region, represent-

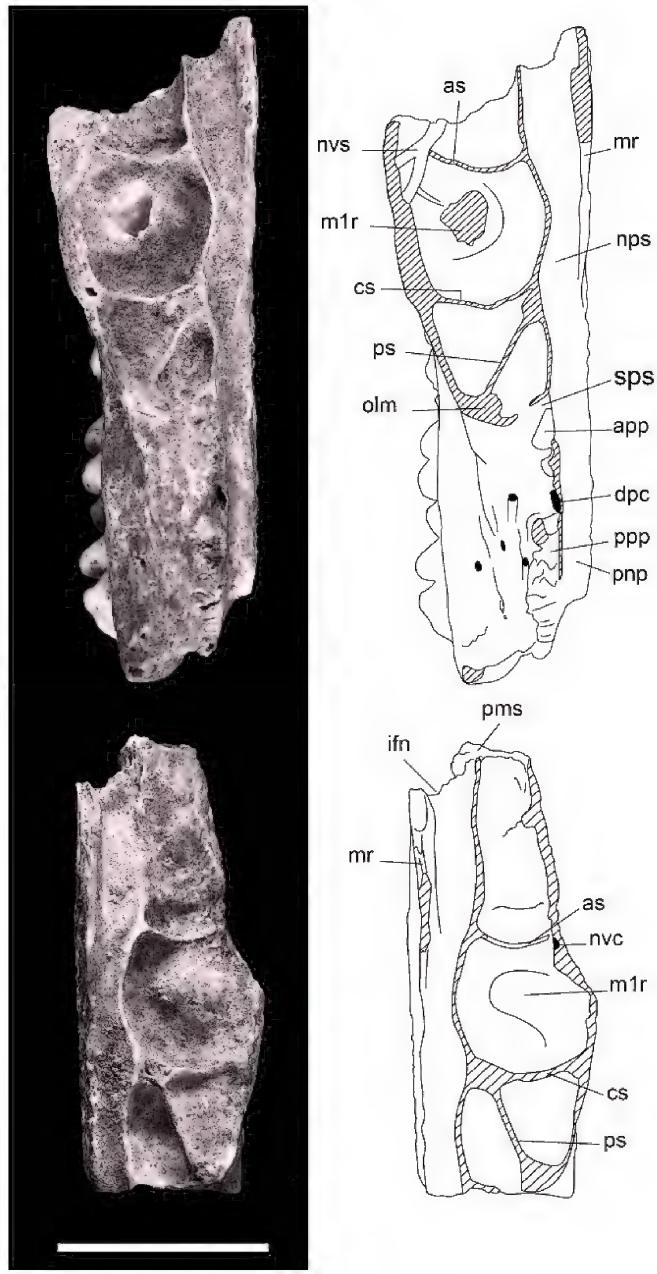

Fig. 8. Dorsal surface of the left (top) and right (bottom) palatal fragments of *Coryphomys buehleri* (AMF 68751a), with an interpretive diagram for significant anatomical features of the maxillary sinus complex and the floor of the orbitotemporal fossa. *Abbreviations*: **app**, anterior palatine process; **as**, anterior septum of maxillary sinus; **cs**, central septum of maxillary sinus; **dpc**, descending palatine artery and nerve canal; **ifn**, incisive foramen posterior notch; **nps**, nasopharyngeal sulcus; **m1r**, bulge covering anterior root of M1; **mr**, raised medial rim of maxilla; **nvc**, neurovascular canal; **nvs**, neurovascular sulcus; **olm**, orbital lamina of maxilla; **pms**, premaxilla-maxilla suture; **pnp**, posterior nasopharynx; **ppp**, posterior palatine process; **ps**, posterior septum of maxillary sinus; **sps**, sphenopalatine sulcus. Scale bar represents 10 mm and applies to both images.

ing the floor of the orbitotemporal fossa. These regions are separated by several maxillary contributions to the medial wall of the orbitotemporal fossa, namely its orbital lamina and palatine processes.

The endocranial surface features the nasopharyngeal sulcus, running along the medial side, and an elaborate series of depressions (herein termed the "maxillary sinus complex"), situated anterolaterally (fig. 8). The nasopharyngeal sulcus is relatively narrow throughout its length but narrows further in the zone between the molar rows. Anterior of the molar rows, the sulcus has an elevated medial rim that presumably supported the maxilloturbinate. Behind this point, the sulcus is unenclosed medially, indicating an undivided posterior nasopharynx. The maxillary sinus complex is a large and elaborate depression. It extends from just behind the premaxilla-maxilla sutural zone, back to above the front of M2, and laterally onto the root of the zygomatic plate, and it is partially subdivided by three low septa. The anterior septum is transverse and located well forward of the molar row. The central septum, also transverse, is level with the central loph of M1. The posterior septum is oblique, sharing a common medial origin with the central septum and terminating laterally at the level of the anterior loph of M2. Although the lateral margin of the maxillary sinus complex is mostly lost through damage, it is clear that it was enclosed by an extensive orbital lamina of the maxilla that crossed the root of the maxillary zygomatic plate. The floor of the maxillary sinus is marked by a short neurovascular sulcus that marks the passage of nasal branches of the infraorbital artery and superior alveolar nerve (see Discussion). On the left maxillary fragment, this sulcus passes obliquely across the lateral end of the anterior septum, while on the right fragment it is represented by an intraosseous canal exposed on the fractured edge. In various other murines surveyed by us (e.g., *Rattus* spp., *Mus musculus*, *Uromys caudimaculatus*, *Mammelomys lanosus*, *Paramelomys platyops*, *Bandicota indica*), this canal passes forward within the body of the maxilla to exit on the maxillary-premaxillary suture. The sutural surface in the fossil specimen is partially filled with matrix and the exact location of the anterior end of this canal cannot be determined without risk of damage.

The orbitotemporal surface takes the form of a narrow ledge above the posterior molars. This surface is irregular and includes several matrix-filled pits that probably represent foramina for branches of the superior alveolar nerves and vessels that supplied the upper molars. Anteriorly, it is delimited by the curving orbital lamina of the maxilla, and posteromedially, by two short palatine processes, aligned one in front of the other, and separated by a 1.75 mm gap. The orbital lamina and anterior palatine process are separated by a short sulcus that marks the position of the sphenopalatine foramen. The two palatine processes are rugose and represent sutural contacts with the orbital lamina of the palatine. The gap between the two palatine processes represents the dorsal palatine foramen. Medial to and aligned with this gap is a slitlike foramen that represents the orbital end of the intraosseous canal for the descending palatine artery and corresponding nerve.

The associated zygomatic plate (fig. 6A–B) is tall and relatively narrow, with a length of 9.7 mm at the narrowest point and a minimum height of 12.5 mm measured from the anteroventral border to the dorsal rim of the masseteric fossa. The anterior margin of the plate is thin and was either vertical or sloped slightly forward from the ventral root. The posterior margin of the plate is rounded and relatively thin, as appropriate to accommodate the lateral expansion of the maxillary sinus complex, as described above. The dorsal border of the masseteric fossa is more deeply excavated posteriorly than anteriorly. Although the dorsal root of the zygomatic arch is damaged posteriorly, enough survives to show that it was broad, with a shallow zygomatic notch that was probably no more than 1.5 mm in depth. The dorsal surface of the root is smooth and lacks the shallow fossa seen in some murines (e.g., *Rattus* spp.) for insertion of the frontalis muscle. The attached, anterior portion of the zygomatic arch is extremely robust, with a depth of 4.5 mm. It is distinctly rugose at the point of union with the plate, presumably advertising

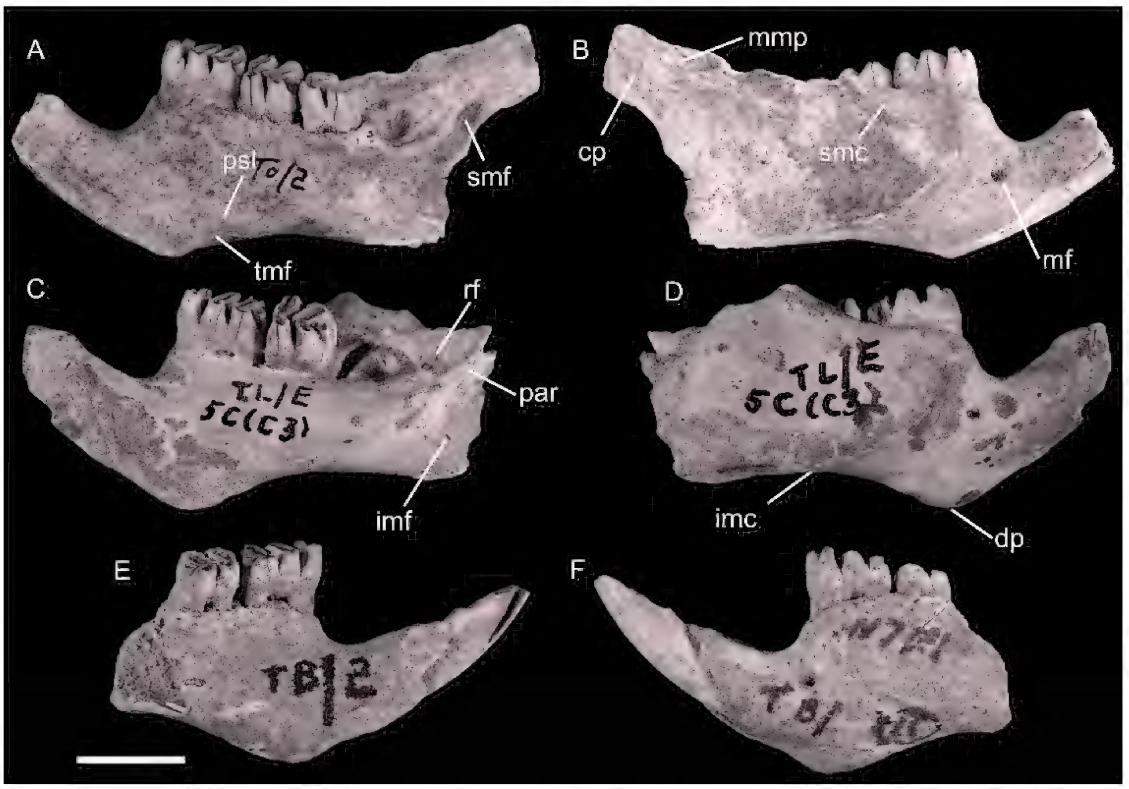

Fig. 9. Three partial dentaries referred to *Coryphomys buehleri*. AMF 68831: a right dentary fragment with m1–3 in medial **(A)** and lateral **(B)** views. AMF 68850: a right dentary fragment with m1–3 in medial **(C)** and lateral **(D)** views. AMF 68789: a left dentary fragment with lower incisor and m1–2 in medial **(E)** and lateral **(F)** views. Scale bar represents 10 mm and applies to all images. *Abbreviations*: **cp**, condylar process; **dp**, digastric process; **imc**, inferior masseteric crest; **imf**, inferior mandibular foramen; **mf**, mental foramen; **mmp**, fossa for insertion of posterior part of medial layer of masseteric muscle; **par**, postalveolar ridge; **psl**, ridge for attachment of posterior symphyseal ligament; **rf**, retromolar fossa; **smc**, superior masseteric crest; **smf**, superior mandibular foramen; **tmf**, fossa for deep part of transverse mandibular muscle.

the attachment of the medial zygomatic plate aponeurosis. This latter feature is also evident on two other fragmentary zygomatic plates referred at generic level (see below).

DENTARY: Three new dentaries are referred to *C. buehleri* (fig. 9). Notable features of this element are the large size of the molars relative to the bony framework, the deep and robustly formed symphyseal process that surrounds a stout lower incisor, and the well-developed retromolar fossa. The more delicate processes of the posterior ramus are absent in each case; the articular condylar is preserved in the holotype (Schaub, 1937: fig. 1).

The body of the ramus is deepest below the first molar, then shallows posteriorly along the molar row before deepening again onto the angular process. This creates a distinctly concave ventral border of the ramal body. The lateral surface bears a prominent and anteriorly expansive masseteric fossa, defined ventrally by a strong inferior masseteric crest and dorsally by a less prominent superior masseteric crest. The anterior union of these crests is located below the anterior root of m1 and is variably V-shaped or U-shaped. The mental foramen is situated at the intersection of the ramal body and the symphyseal process, just forward of the anterior root of m1, well below the diastemal border and well forward of the masseteric fossa.

The molars are large relative to the bony framework of the dentary, and the third molar is only slightly smaller than the second. To support the relatively large posterior molars, a prominent alveolar shelf overhangs the medial surface of the dentary. This shelf is linked to the medial surface of the ascending ramus by a well-developed postalveolar ridge that terminates at the mandibular foramen. The anterior margin of the ascending ramus arises lateral to the anterior root of m2, partially obscuring this tooth in lateral view. The trough between the molar row and the medial surface of the ascending ramus is narrow alongside m2 but opens posteriorly into a broad and well-developed retromolar fossa. This muscular insertion area is enclosed medially by the alveolar rim and posteriorly by the postalveolar ridge and presumably signifies hypertrophy of the posterior portion of the anteromedial portion of the anterior part of the temporal muscle.

Although the ascending ramus is damaged in all specimens, enough remains to demonstrate that the posterior end of the incisor alveolus is contained within the ascending ramus, without formation of a distinct tubercle. Damaged specimens indicate that the alveolus terminates level with the posterior end of the alveolar shelf and forward of a well-developed fossa for the posterior part of the medial layer of the masseter muscle.

The articular condylar, as preserved on the holotype and illustrated by Schaub, is supported by a broad condylar process, weakly incised behind by a broadly concave sigmoid notch. The condylar process on AMF 68831 (fig. 9A) is appropriately deep and stout. A low ridge on the lateral surface of the condylar process represents a continuation of the inferior margin of the muscular fossa. The medial surface of the condylar process is flat and lacks any equivalent buttressing. The angular process is also incomplete on all specimens. Surviving portions indicate that the internal pterygoid fossa was deeply excavated dorsally, below the postalveolar ridge, but smoothly continuous anteriorly with the medial surface of the ramal body. A small inferior mandibular foramen is preserved in two specimens, situated low and well forward in the internal pterygoid fossa.

The symphyseal process of the dentary rises at a steep angle relative to the molar row and ramal body. It is deep and robust, reflecting the stout nature of the lower incisor, and terminates posteroventrally in a prominent, triangular digastric process that has its apex located below the anteroconid of m1. The mandibular symphysis occupies much of the medial surface of the symphyseal process. It is broadest anteriorly and narrows to terminate on the digastric process. The anterior and posteroventral portion of this surface is highly rugose, marking the position of the symphyseal cartilage anteriorly, and of the anterior symphyseal ligament posteriorly. A discrete low ridge situated posterior and dorsal to the digastric process indicates the presence of a separate posterior symphyseal ligament. This ridge and the posterior end of the symphysis are separated by a sulcus that would have carried the submental artery and vein. Judging from the condition in other murines, the posteroventral rim of the digastric process would have provided attachment for two muscle units: anteromedially, for the aponeurosis of the anterior digastric muscle; and posterolaterally, for a straplike superficial portion of the transverse mandibular muscle. A small fossa located on the inner surface of the digastric process, just behind the symphysis, is interpreted as the point of origin of the deep portion of the transverse mandibular muscle. A low but continuous crest running along the dorsolateral margin of the symphyseal process marks the insertion of the pars orbicularis of the buccinator muscle.

Coryphomys musseri, sp. nov.

HOLOTYPE: ANWCP32: Matja Kuru 1 (MK1/AA/21), an unburnt left dentary with m1–3 in an early stage of wear (figs. 11O, 16A–B). The incisor is missing from its alveolus. The pterygoid, coronoid, and articular processes of the dentary are broken away. The specimen was excavated from Spit 21 of Square AA at the cave site of Matja Kuru 1 by S. O'Connor, and is understood to be early Holocene in age.

REFERRED SPECIMENS: AMF 68765: Uai Bobo 1 (TO2/G), L Dentary with m1–3; AMF 68851: Uai Bobo 1 (TO1/3), R Dentary

with m1–3; AMF 68753: Uai Bobo 1 (TO1/3) R Dentary with m1–3; AMF 68812: Uai Bobo 1 (TO1/3), R Dentary with m1–3; ANWCP9: Matja Kuru 2 (MK2/D/44), R Dentary with m1–2; AMF 68752: Uai Bobo 1 (TO1/3), L Dentary with i1 m1–2; AMF 68763: Uai Bobo 1 (TO1/4), L Dentary with m1–3; AMF 68789: Bui Ceri Uato (TB/2), L Dentary with m1–3; AMF 13CM10: Uai Bobo 1 (TO1/G), L Dentary with m1–3; AMF 68789: Uai Bobo 1 (TO1/G), R m1; ANWCP10: Matja Kuru 1 (MK1/AA/14), R Dentary with m1–3; ANWCP11: Matja Kuru 1 (MK1/AA/16), L Dentary with m1–3; ANWCP12: Matja Kuru 1 (MK1/AA/20), R Dentary with m1–3; ANWCP13: Matja Kuru 1 (MK1/AA/22), R Dentary with m1–2; ANWCP14: Matja Kuru 1 (MK1/AA/11), R M1; ANWCP15: Matja Kuru 1 (MK1/AA/8), R Dentary with m1–3; ANWCP16: Matja Kuru 1 (MK1/A/15), L m1; ANWCP17: Matja Kuru 1 (MK1/AA/19), L m1; ANWCP18: Matja Kuru 2 (MK2/D/43), R m1–3; ANWCP19: Matja Kuru 1 (MK1/A/28), L M1; ANWCP20: Matja Kuru 1 (MK1/A/13), R Dentary with m1–2; ANWCP21: Matja Kuru 1 (MK1/AA/12), R Dentary with m1–3; ANWCP22: Matja Kuru 1 (MK1/AA/12), R m2; ANWCP23: Matja Kuru 1 (MK1/A/29), L m2; ANWCP24: Matja Kuru 1 (MK1/AA/18), R M1; ANWCP25: Matja Kuru 1 (MK1/A/29), L M1; ANWCP26: Matja Kuru 1 (MK1/A/31), R and L Maxillae with RM2 and LM3; AMF 68770: Uai Bobo 1 (TO1/4), L Maxilla with M1–3; AMF 68756: Uai Bobo 1 (TO1/3), R Maxilla with M1; AMF 68768: Uai Bobo 1 (TO1/F), R Maxilla with M1; ANWCP27: Jerimalai (JM/B/26), L Dentary with i1 and m1; ANWCP28: Matja Kuru 1 (MK1/AA/8), L m1 and L m2; ANWCP29: Matja Kuru 1 (MK1/A/10), R m1; AMF 68831: Uai Bobo 1 (TO1/I), edentulous left dentary.

Diagnosis: Differs from *C. buehleri* in having molars slightly smaller on average in actual dimensions and proportionally much smaller relative to osseous structures; M1–3 with smaller posterior cinguli; i1 with concave dorsolabial surface; m1 with anterocentral cuspid undivided in majority of specimens; m2–3 with smaller posterior cinguli; maxilla with anteriorly shallower medial palatal suture and longer antemolar region, with superficial masseteric fossa located significantly further forward relative to M1; and dentary with more prominent digastric process, stronger inferior masseteric ridge, a larger fossa for deep portion of transverse mandibular muscle, and a postalveolar ridge that runs dorsal to superior mandibular foramen.

Etymology: We take the greatest pleasure in naming this species after Guy Musser, in appreciation of his meticulous and inspirational studies of murine rodents.

Description

Upper Molars (fig. 10, table 2): The upper molar cusp and root arrangements compare closely with those of *C. buehleri*. The root pattern of M2, as illustrated by ANWCP26, is shown to consist of a broad, kidney-shaped anterior root, supporting the anteroloph and with its concavity facing to the rear, a small circular root on the lingual side of the tooth, supporting cusps t4 and t7, and a larger circular posterolabial root, supporting cusps t8 and t9 and the associated posterior cingulum. The M3 of ANWCP26 has two roots and lacks the accessory labial root seen in *C. buehleri*.

M1: This tooth is represented by a total of six specimens (fig. 10A–F). The cuspal arrangement differs from that of *C. buehleri* in two respects: (1) each of the lingual cusps is positioned slightly further forward, creating a more transverse alignment of cusps in each lamina; and (2) the posterior cingulum is less bulky and more closely associated with the posterior surface of cusps t8–9.

As in *C. buehleri*, the posterior cingulum displays some variation in structure. On AMF 68770 (fig. 10A) it has a strong lingual connection to cusp t7 but is deeply separated from the rear of cusp t8 at the labial end; a small pimplelike cusp is present midway along the cingulum. On AMF 68756 (fig. 10C) the cingulum is an elevated ridge, deeply separated from each of cusps t7 and t8, and with three pimplelike cusps along its length and poor. Three other specimens have a simpler, lenticular posterior cingulum that is also deeply separated from each of cusps t7 and t8 (fig. 10B, D–E).

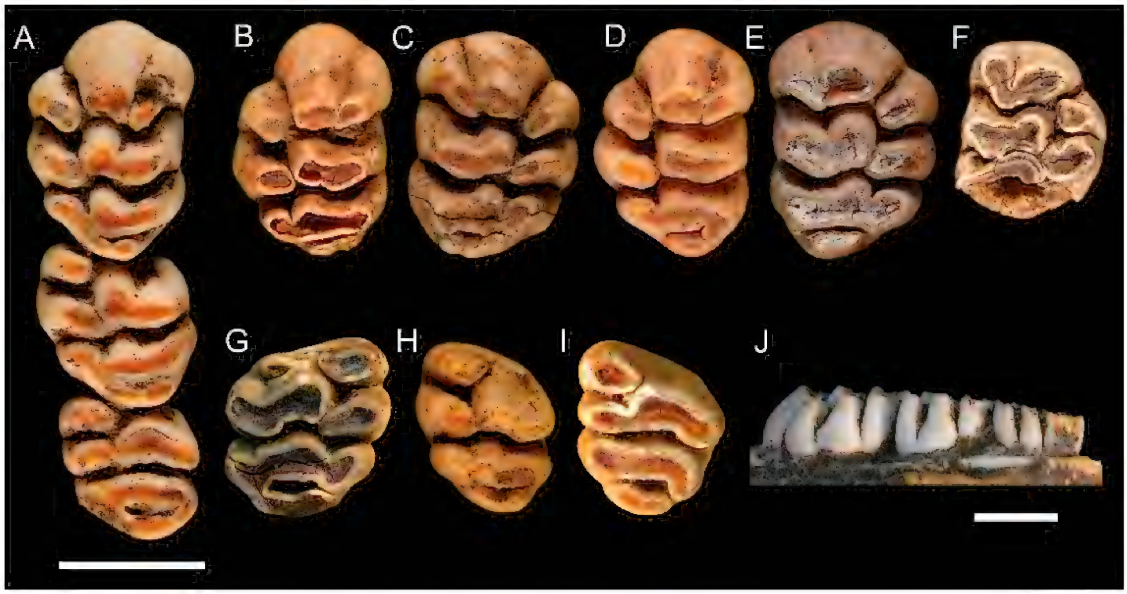

Fig. 10. Occlusal views and one lingual view of upper molars referred to *Coryphomys musseri*. Occlusal views: **A,** AMF 68770: associated left M1–3; **B,** ANWCP19: a left M1; **C,** AMF 68756: a right M1; **D,** ANWCP25: a left M1; **E,** AMF 68768: a right M1; **F,** ANWCP24: a right M1 (lacking the rear of the posterior lamina); **G,** ANWCP26a: a right M2; **H,** ANWCP22: a left M3; **I,** ANWCP26b: a left M3. Lingual view: **J,** AMF 68770: associated left M1–3. The lingual view illustrates the moderate hypsodonty and serial trends in inclination of molar cusps in *C. musseri*. Scale bar beneath A also applies to B–I and represents 5 mm. A separate 5 mm scale bar is provided for J.

M2: Three examples are available (figs. 10A, G–H). Cusp t3 is entirely absent on AMF 68770 (fig. 10A), is represented by a small nubbin positioned near the crown base on another (ANWCP22; fig. 10H), and is represented by a larger nubbin in the same position on the third (ANWCP24; fig. 10F).

The posterior cingulum is a broader on M2 than on M1. In all three examples it shows a more elevated lingual connection to cusp t7 and a deeper labial separation from cusp t9. Two specimens have a pimple-like cusp at the labial end of the cingulum; the condition on the third is obscured by damage. Compared with *C. buehleri*, the posterior cingulum is less bulky and more closely approximated to the rear of cusp t8.

M3: Two specimens are available, both associated with an M2 (figs. 10A, I). The occlusal area of M3 appears to be smaller relative to M2 in these specimens than in the few examples of *C. buehleri*. In part, this is due to the less bulky nature of the posterior cingulum, continuing the pattern observed on M1–2.

Neither M3 of *C. musseri* has any trace of cusp t3. The posterior lamina on AMF 68770 (fig. 10A) resembles that of *C. buehleri* with cusp t9 projecting backward to meet the elevated labial end of the posterior cingulum. On ANWCP26 (fig. 10I) cusp t9 is broadly united with cusp t8 and more deeply separated from the posterior cingulum.

Lower Incisor: Two dentaries preserve more or less complete lower incisors (fig. 11, table 2), but one of these is a young individual, with a correspondingly slender i1. Five others retain the base of a broken tooth. Although comparisons are difficult from a predominantly broken sample, the i1 appears to be slightly less robust than that of *C. buehleri*, due mainly to a more concave dorsolateral surface, and the medial surface appears to be flatter. The occlusal facet in the adult specimen is 10.52 mm in length and has a broadly concave posterior termination. The anterior margin of the facet curves to a medial point.

Lower Molars (fig. 11, table 2): The complete lower molar series is retained in 12

TABLE 2

Measurements of Upper and Lower Dentition in Specimens Attributed to *Coryphomys musseri*

Measurements are molar lengths (L) and widths (W) and the breadth (IB) and depth (ID) of the lower incisor. Sample sizes (n), means, standard deviations (s.d.), and ranges are also shown.

Upper dentition	Symmetry	M1–3	M1 L	M1 W	M2 L	M2 W	M3 L	M3 W		
CP26a	L						5.06	4.93		
CP26b	R				5.06	5.33				
CP25	L		8.12	5.69						
CP22	R				5.52	5.11				
CP19	L		8.54	5.71						
CP24	R			5.19						
AMF 68756	L		7.73	5.61						
AMF 68768	R		8.01	5.68						
AMF 68770	L	17.09	8.29	5.43	5.93	5.13	5.32	4.47		
mean		17.09	8.14	5.55	5.50	5.19	5.19	4.70		
s.d.			0.303	0.205	0.435	0.122	0.184	0.325		
Range			7.73–8.54	5.19–5.71	5.06–5.93	5.11–5.33	5.06–5.32	4.47–4.93		
N		1	5	6	3	3	2	2		
Lower dentition		M_{1-3}	M_1L	M_1W	M_2L	M_2W	M_3L	M_3W	IB	IH
AMF 68753	L	18.13	7.56	4.86	5.31	5.36	5.44	5.07		
AMF 68751	R	18.67	7.49	4.82	4.95	5.5	5.34	5.1		
AMF 68763	L	18.18	7.38		4.58	5.13	4.5	4.91		
AMF 68812	R	18.47	7.21	4.79	4.92	5.53	5.51	5.52		
AMF 68752	L		7.14	4.43	4.99	5.17			2.99	4.76
AMF 68789	R		7.92	4.86						
AMF 68765	L	17.93	7.36	4.7	4.73	5.07	4.97	4.8		
AMF 68759	L				5.13	5.14	5.17	4.84		
AMF 68789	L	17.71	7.35	4.72	4.97	5.27	5	5.19		
CP27	L		6.98	4.62					1.91	3.29
CP10	R	18.6	7.66	5.05	5.2	5.69	5.30	5.69		
CP17	L		7.63	4.9						
CP12	R	17.75		4.75	4.35	5.21	4.73	5.16		
CP9	R		7.59	5	5.77	5.78				
CP18	R		7.73	4.86	5.3	5.27	5.49	5.15		
CP29	L		7.54	4.67					3.32	
CP20	R	17.27	7	4.63	5.03	5.09				
CP11	L	18.76	7.5	4.7	4.81	5.31	5.37	5.47	3.31	

TABLE 2
(Continued)

Lower dentition		M_{1-3}	M_1L	M_1W	M_2L	M_2W	M_3L	M_3W	IB	IH
CP32	L		7.42	4.62	4.72	5.32	5.61	5.1		
CP13	R		7.58	5	5.19	5.68				
CP15	R	17.43	7.46	4.62	4.46	5.12	5.23	4.98		5.01
CP28	L			5	5.57	5.59				
CP14	R		7.72	4.96						
CP23	L				5.23	5.32				
CP16	L		7.63	4.93						
CP21	R	17.18	7.34	4.41	4.85	4.91	4.8	4.92		
Hooijer No 3	L	17.6		4.7		5.2		5		
Mean		18.01	7.46	4.78	5.00	5.32	5.18	5.14	2.88	4.35
s.d.		0.551	0.234	0.178	0.352	0.236	0.331	0.263	0.666	0.929
Range		17.18–18.76	6.98–7.92	4.41–5.05	4.35–5.77	4.91–5.78	4.5–5.61	4.8–5.69	1.91–3.32	3.29–5.01
N		12	22	23	20	20	14	14	4	3

dentaries, and six other specimens have two associated molars. Isolated lower molars are referred to this species on the basis of size and relative width. Molar root pattern appears identical to that described for *C. buehleri* except for the presence of a small accessory lingual root in two of 24 examples of the m1. Individual length and width measurements of m1 show slight overlap between *C. musseri* and *C. buehleri* (table 1–2). Overlap is more extensive in dimensions of m2 and even more so for m3.

m1: This tooth is represented by 21 examples (fig. 11A–S), two of which are too heavily worn to show details of cuspal arrangements. The cuspal arrangement is essentially similar to that in *C. buehleri* but with the following minor differences: (1) the anterocentral cuspid is divided in two (10.5%) specimens (ANWCP20, fig. 11B; and ANWCP29, fig. 11I) (the cuspid is divided in 67% in *C. buehleri*, including the holotype and Hooijer's specimen no. 2); (2) no specimen has small accessory cuspules attached to the rear of the anteroconid, though several (e.g., ANWCP13, fig. 11A) have a buttresslike ridge extending forward from the base of the protoconid to produce a partial cingulum across the base of the anterolabial flexid (33% have accessory cuspules in *C. buehleri*); (3) among the 16 examples where this relation can be scored, four (25%) show overlap of the hypoconid past the entoconid, 11 (69%) show the hypoconid and entoconid abutting without overlap, and one (6%) shows overlap of the entoconid in front of the hypoconid (60% of specimens show overlap of the hypoconid past the entoconid in *C. buehleri*); and (4) the posterior cingulum is slightly smaller in all specimens.

Of 16 lesser worn examples of m1 that illustrate the relationship between the protoconid and metaconid, 11 (69%) show the two cusps abutting anteriorly without overlap, and five show the protoconid overlapping the front of the metaconid. The five specimens of *C. buehleri* (including Hooijer's specimen no. 2) show two (40%) with overlap and three (60%) abutting without overlap.

The posterior cingulum is discrete in all but the most heavily worn example of m1

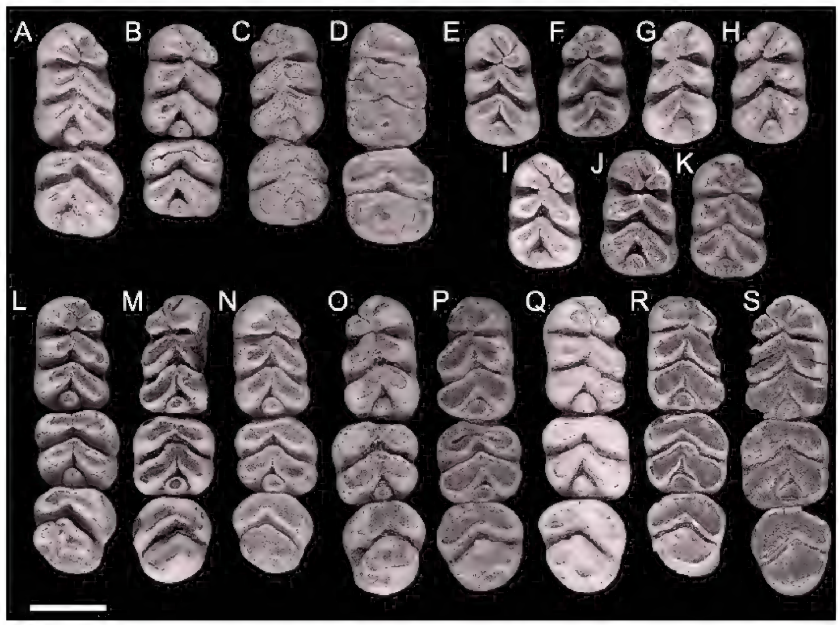

Fig. 11. Occlusal views of lower molars referred to *Coryphomys musseri*. **A,** ANWCP13: associated right m1–2; **B,** ANWCP20: associated right m1–2; **C,** AMF 68752: associated left m1–2; **D,** ANWCP9: associated right m1–2; **E,** ANWCP14: an isolated right m1; **F,** ANWCP27, an isolated left m1; **G,** ANWCP17: an isolated left m1; **H,** ANWCP16: an isolated left m1; **I,** ANWCP29: an isolated right m1; **J,** ANWCP18: associated right m1–3; **K,** AMF 68789: an isolated right m1; **L,** ANWCP10: associated right m1–3; **M,** AMF 68763: associated left m1–3; **N,** ANWCP15: associated right m1–3; **O,** ANWCP32 (holotype of *C. musseri*): associated left m1–3; **P,** ANWCP11: associated left m1–3; **Q,** CM4: associated right m1–3; **R,** CM2: associated right m1–3; **S,** AMF 68753: associated right m1–3. Scale bar represents 5 mm and applies to all images.

(ANWCP9, fig. 11D), where it is united by a common dentin pool to the hypoconid.

m2: The m2, represented by 20 new specimens (e.g., fig. 11A–D, L–S), is similar in proportions and cuspal arrangement to this tooth in *C. buehleri*. The main points of distinction other than smaller average size are the smaller size of the posterior cingulum and the less frequent suggestion of a fused or incipient anterolabial cuspid. The latter structure is moderately well indicated in two (14%) of the total of 14 specimens with an appropriate degree of wear, weakly indicated in four others (29%), and not expressed at all in eight (57%). In *C. buehleri* this structure is moderately well indicated in two specimens (40%) and weakly indicated in three (60%), including Hooijer's specimen no. 2. A groove on the posterior surface of the protoconid may also be less frequent in *C. musseri*, being present in two specimens only (ANWCP18, fig. 11J; and ANWCP10, fig. 11L).

The posterior cingulum in the most heavily worn example of m2 (ANWCP9, fig. 11D) is united by a common dentin pool to both the hypoconid and entoconid.

m3: This tooth is represented by 15 specimens (e.g., fig. 11L–S). Among nine specimens with lesser degrees of wear, the anterior margin of the protoconid bears a clear fold, suggestive of an amalgamated anterolabial cuspid, in one example (AMF 68812, fig. 11Q) (11%); it is angular in four others (44%), and smoothly rounded in the remaining four (44%).

The posterior lamina varies considerably in width and cuspal morphology. Only one specimen of nine (11%) matches the condition described for C. *buehleri*, wherein anterior and posterolingual grooves clearly mark the union of the hypoconid and entoconid. Six specimens (55%) have a posterolingual groove in the same position but lack any anterior groove. In two specimens (22%) the

posterolophid is more evenly divided by a posterior groove, with a small posterior cingulum at the base. The cingulum is best developed and most discrete in ANWCP12 (fig. 11Q); in ANWCP21 (not shown) it is united to the posterolingual surface of the hypoconid. Another specimen (AMF 68789, not shown) shows the unusual feature of a small but distinct posterolabial cusplet, defined by a narrow groove on the anterolabial face of the hypoconid.

MAXILLA (figs. 12–15): Partial maxillae of four individuals, two with attached portions of the palatine, together provide a fairly complete picture of palatal morphology in *C. musseri*. The most complete specimen (AMF 68770, figs. 12A–C, 13–15) illustrates the full length of the maxilla, from the suture with the premaxilla back to the posterior end of the alveolar portion, and retains all but the anterior portion of the midline palatal suture, including the palatine portion. The root of the zygomatic process is also preserved. The total length of the maxilla on AMF 68770 is reconstructed as 33.4 mm (essentially identical to *C. buehleri*), with an M1–3 alveolar length of 17.3 mm (19.8 mm in *C. buehleri*). This specimen is mirrored in figure 13 to illustrate the major features of the palate in comparison with *C. buehleri*.

Features shared with *C. buehleri* include: (1) the generally large size of the molar rows relative to the bony support structures and consequent narrowness of the palatal bridge that separates them; (2) the thickened nature of the palatal lamina (measuring 3.1 mm in depth at the medial suture between M1 and 3.9 mm between M2); (3) the short posterior palatal bridge (level with cusp t4 of M3); and (4) the morphology of the anterior palate which has a comparable midpalatal depression (antemolar palatal fossa) and lacks vascular grooving much beyond the anterior face of M1.

Key points of distinction between the two *Coryphomys* species (compared side by side in fig. 14) are the proportionally smaller size of the molars in *C. musseri*, relative to palatal structures, the greater degree of narrowing of the posterior nasopharyngeal margin (anterior margin of mesopterygoid fossa), and the proportionally longer antemolar palatal extent of the maxilla. Essentially, *C. buehleri* is a "megadont" version of *C. musseri*, with a degree of differentiation that greatly exceeds the bounds of normal intraspecific variation among murine rodents.

The anterior sutural contact with the premaxilla is located 13.1 mm forward of the anterior face of M1. Though damage to the anterior end of the maxilla on AMF 68770 and AMF 68756 has removed all trace of the anterior palatal foramen, it is clear that this was extremely short, probably much as in *C. buehleri*. The palate anterior to the molar row is considerably thinner in *C. musseri* than in *C. buehleri*, and this contrast is confirmed by a total of three specimens of *C. musseri*. The sutural contact between the palatine and maxilla, visible on the medial palatal suture of AMF 68770 (fig. 12A), is situated level with the embrasure between cusps t1 and t4 of M2, slightly forward of its relative position in *C. buehleri*.

Though only the root of the zygomatic plate is preserved on AMF 68770 (fig. 12B, C), enough survives to show that it was relatively small and lightly built, especially considering the moderate wear of the molars in this individual. It measures 9.5 mm in length and its posterior margin is level with the anterior face of M1. The anterior root is closely occluded by the rostral lamina of the maxilla, creating a slitlike anteroventral aperture for the infraorbital fissure. As in *C. buehleri*, the posterior root of the zygomatic plate is thinned to accommodate the lateral expansion of the posterior rostral skeleton, reflecting enlargement of the maxillary sinus complex (figs. 13, 15).

A shallow depression situated just behind and ventral to the anterior root of the zygomatic arch on AMF 68770 is identified as the superficial masseteric tubercle (fig. 12C). The posterior margin of the tubercle lies 6.5 mm forward of the anterior face of M1, more than twice the distance in *C. buehleri*. A sharply defined masseteric ridge, aligned with the lingual cusp series of M1, originates 3.3 mm forward of M1 and terminates medial to the tubercle. A nutrient foramen cannot be identified in this region of the maxilla on AMF 68770, but a small foramen might be obscured by encrusted sediment. A second maxillary fragment AMF 68756 has a nutrient foramen located just

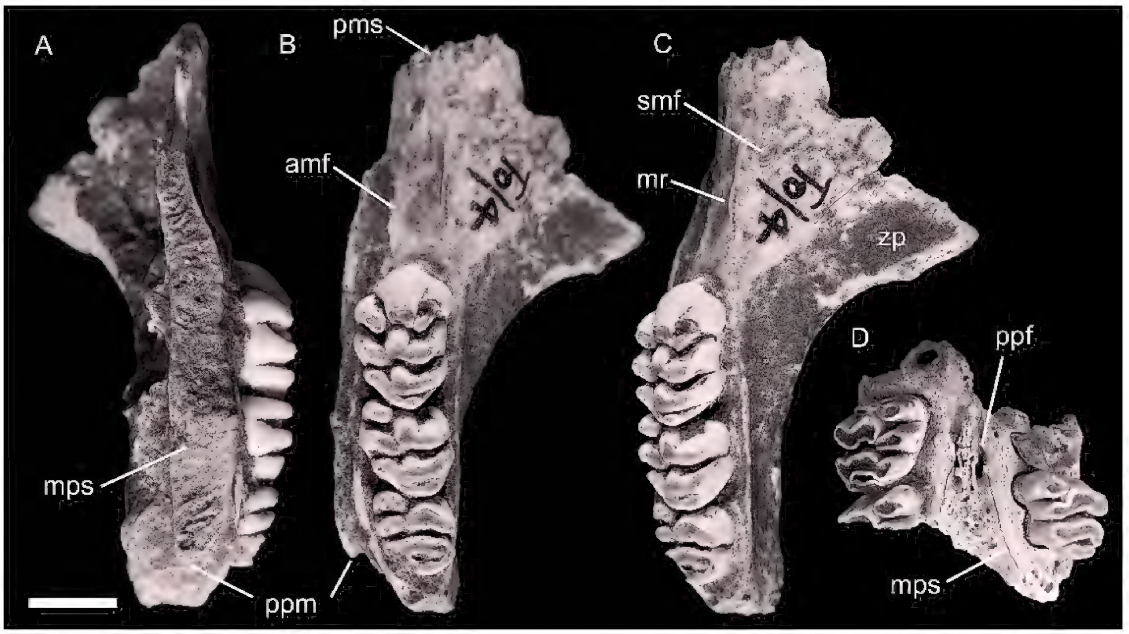

Fig. 12. Palatal specimens referred to *Coryphomys musseri*. **A–C,** AMF 68770, a left palatal fragment with portions of the maxilla and palatine bones, and M1–3; this is shown in medial **(A),** occlusal **(B),** and ventrolateral **(C)** views. **D,** ANWCP26, a posterior palatal fragment with portions of left and right maxillae and palatine bones, and variably damaged right and left M2–3; this is shown in ventral view. *Abbreviations*: **amf**, antemolar palatal fossa; **mps**, maxilla-palatine suture; **mr**, masseteric ridge; **ppf**, posterior palatal foramen; **ppm**, posterior palatal margin; **pms**, premaxilla-maxilla suture; **smf**, superficial masseteric fossa; **zp**, zygomatic plate. Scale bar represents 10 mm and applies to all images.

forward of M1 and lateral to the masseteric ridge.

The alveolar body of the maxilla is deeper than in *C. buehleri*, and the lateral surface maintains a near vertical orientation above the entire molar row. The position of the posterior palatal foramen is obscured by cemented sediment on AMF 68770. On ANWCP26 (fig. 12D), a posterior palatal fragment with conjoined portions of both maxillae and palatines, the posterior palatal foramen is level with cusp t7 of M2. This specimen also shows that the palatal surface of the palatine bone is perforated by numerous vascular canals, suggestive of a highly vascularized anterior portion of the soft palate.

The well-preserved dorsal surface of AMF 68770 (figs. 13 and 15) illustrates the full lateral development of the maxillary sinus complex, including its extension onto the dorsal surface of the root of the zygomatic arch. It also shows the entire course of the neurovascular sulcus for the nasal branch of the infraorbital artery (and associated nerve). The following minor differences are seen in comparison with *C. buehleri*: the neurovascular sulcus in *C. musseri* appears to traverse the maxillary sinus complex somewhat more medially and posteriorly, suggesting an origin farther back within the intraorbital sulcus; and the medial rim of the anterior nasopharyngeal sulcus in *C. musseri* is lower anteriorly, and less extensive posteriorly.

DENTARY (fig. 16): All 15 dentaries attributed to this taxon are damaged and no specimen preserves either the coronoid or angular processes or the articular condyle. The holotype (ANWCP32, fig. 16A–B) and three other specimens at contrasting wear stages illustrate the changes in mandibular form that occur through life (fig. 16).

The dentary is similar in size and general morphology to that of *C. buehleri*. Comparison of specimens of equal wear stages reveals the following points of contrast: (1) the molar

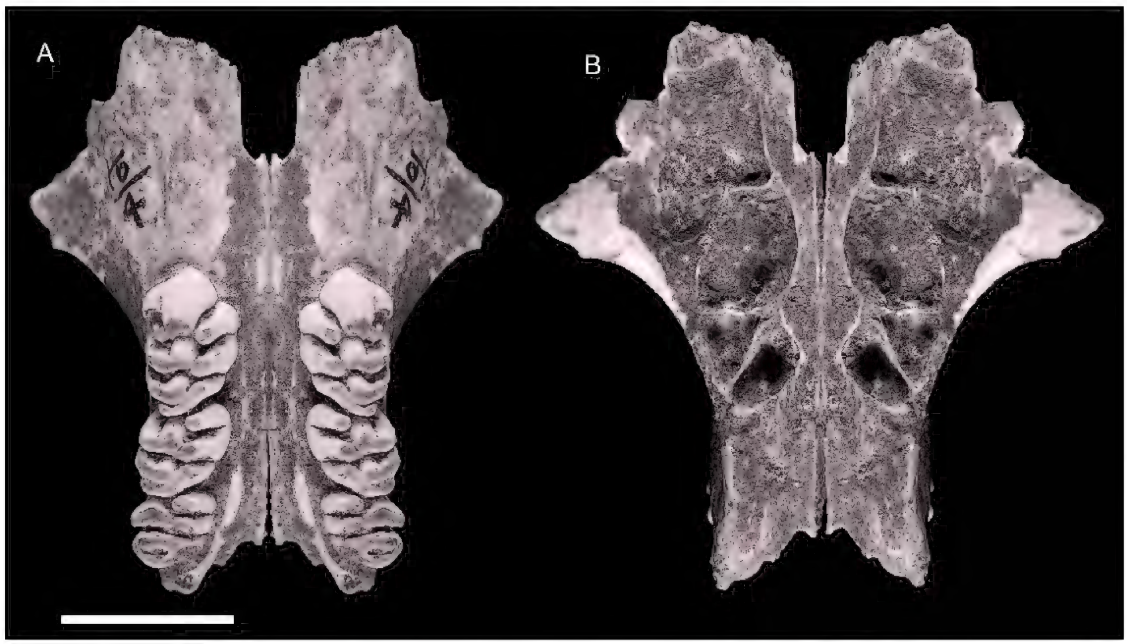

Fig. 13. Reconstructions of the palatal anatomy of *Coryphomys musseri* in ventral **(A)** and dorsal **(B)** views, based on mirroring of the left palatal specimen AMF 68770. Comparison with figure 7 illustrates the difference in size of the cheekteeth relative to osseous structures between the two species of *Coryphomys*. Scale bar represents 10 mm.

row is smaller in proportion to the dentary; (2) the inferior masseteric crest is more prominent; (3) the digastric process is more prominent and has a more pronounced posterior rim; (4) the fossa for the deep portion of the transverse mandibular muscle is substantially larger; and (5) the postalveolar ridge runs dorsal to the superior mandibular foramen and extends further onto the neck of the condylar process.

In combination, these features reflect a more powerfully developed masticatory musculature in *C. musseri*, compared with the larger-toothed *C. buehleri*. Enlargement of the fossa for the deep portion of the transverse mandibular muscle is particularly noteworthy. In laboratory rats this muscle is particularly active during adduction of the mandible (Weijs and Dantuma, 1975), with muscular contraction causing spreading of the anterior and superior borders of the symphysis and relieving compression on the symphyseal cartilage (Beecher, 1979).

One specimen (ANWCP12, not shown) with m1–3 retained has a clearly defined alveolus positioned behind the m3. This is as broad as the posterior lamina of m3 and presumably held a peglike tooth on a substantial root. Supernumerary fourth molars are rare in rodents generally, and seem to be especially so in Murinae (summarized by Johnson, 1952).

One edentulous dentary (AMF 68831, not shown) is referred to *Coryphomys* on the basis of the well-developed retromolar fossa, and tentatively assigned to *C. musseri* on the basis of inferred molar dimensions. The deep ramal body and strong development of the alveoli for m3 suggest an aged individual. The m1 in this specimen bore a small accessory root, midway along the lingual side of the tooth, in addition to a large anterior root with its posterolabial extension and a broad posterior root. Each of the m2 and m3 was supported by transversely widened anterior and posterior roots. The lingual margin of each alveolus is vertical, but the labial margins are splayed distally to provide enhanced anchorage. The anterior alveolus of each of m2 and m3 is bilobed in its deepest expression. Partially separate labial and lingual anterior roots are also observed in

Fig. 14. Side-by-side comparison of reconstructed palatal anatomy of *Coryphomys buehleri* **(A)** and *C. musseri* **(B)** illustrates the marked difference in proportional molar size relative to osseous structures. The two specimens are at approximately the same stage of tooth wear, hence the differences are not a product of contrasting individual age. *Coryphomys buehleri* is effectively a "megadont" version of *C. musseri* and this produces a more crowded palate and a shorter antemolar region. The apparent difference in the morphology of the incisive foramina is illusory; this region is damaged in the specimen of *C. musseri* and the posterior margin of the foramen is not preserved.

the shallower alveoli of a young individual of *C. musseri* (ANWCP27, fig. 16C–D) that has lost m2–3.

Coryphomys, sp. indet.

A number of specimens are referred with confidence to the genus *Coryphomys*, but due to lack of direct association with cheek teeth, cannot be determined to species. Nevertheless, this material adds significantly to our knowledge of the genus and warrants description under a generic banner.

The most significant specimens are: AMF 68822: Uai Bobo 1 (TO/2), a partial left premaxilla; AMF 68760: Uai Bobo 1 (T0/3a), a fragmentary left zygomatic plate; AMF 68747: Uai Bobo 1 (T0/3a), a fragmentary right zygomatic plate; AMF 68864: Lie Siri (TL/A c), an isolated left frontal bone; ANWCP30: Matja Kuru 2 (MK2/D/31), an isolated right petrosal with minor abrasion; ANWCP31: Matja Kuru 1 (MK1/D/31B), an isolated and burnt left petrosal missing most of the pars cochlearis.

Premaxilla: A partial left premaxilla (AMF 68822; fig. 17A–C) is referred on the basis of its simple D-shaped incisor morphology (described below), which parallels that seen in the lower incisor. The specimen also differs in both incisor and bony morphology from a directly associated premaxilla of a species of Mahoney's Genus A. The specimen retains the broken stump of the incisor and is complete from the narial rim back to the maxillary suture; this dimension measures 20.44 mm. The palatal process is abraded such that the symphysis and details of the incisive foramen cannot be discerned. The dorsal suture between the narial process and the nasal bone is also lost.

The surviving portion, oriented with reference to the anterior surface of the incisor, suggests a relatively narrow rostrum that is not expanded lateral to the incisor gyrus (contra examples referred to Mahoney's Genus A). The bony sheath of the incisor projects forward and downward from the palatal surface of the premaxilla, suggesting a weakly proodont incisor orientation (sensu Thomas, 1919).

Upper Incisor: This tooth in AMF 68822 has a simple D-shaped cross-section (fig. 17C). It measures 5.51 mm in depth and 3.55 mm in width, giving a depth to width ratio of 1.57. Pale orange enamel is restricted to the anterior half of the outer surface. The inner surface of the tooth is flat; the posterior surface is rounded.

Zygomatic Plate of Maxilla: Two fragmentary zygomatic plates (AMF 68760 and AMF 68747, not shown) are allocated to *Coryphomys* on the grounds of their close resemblance to this structure in a specimen referred to *C. buehleri*. In both the plate is tall and narrow, with a trapezoidal shape, and

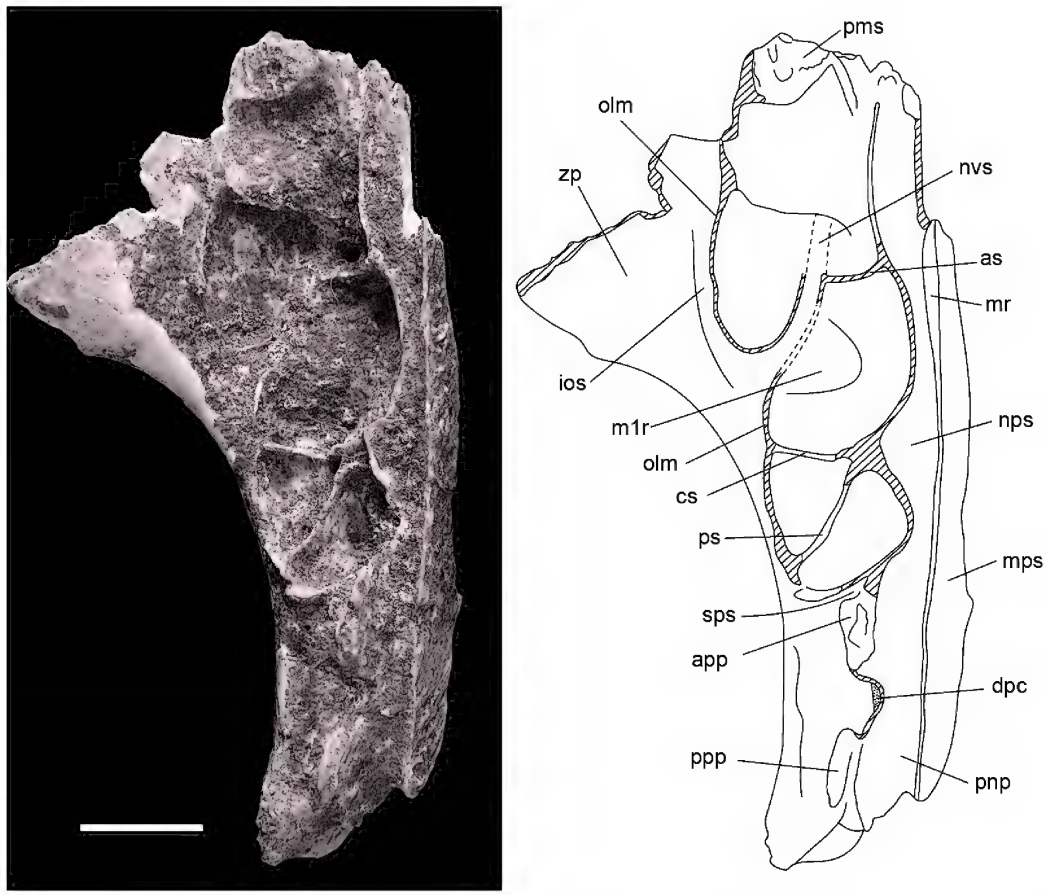

Fig. 15. Dorsal surface of AMF 68770, a left palatal fragment of *Coryphomys musseri* with an interpretive diagram for significant anatomical features of the maxillary sinus complex and the floor of the orbitotemporal fossa. *Abbreviations*: **app**, anterior palatine process; **as**, anterior septum of maxillary sinus; **cs**, central septum of maxillary sinus; **dpc**, descending palatine artery and nerve canal; **ios**, infraorbital sulcus; **mps**, median palatal suture; **m1r**, bulge covering anterior root of M1; **mr**, raised medial rim of maxilla; **nps**, nasopharyngeal sulcus; **nvs**, neurovascular sulcus; **olm**, orbital lamina of maxilla; **pms**, premaxilla-maxilla suture; **pnp**, posterior nasopharynx; **ppp**, posterior palatine process; **ps**, posterior septum of maxillary sinus; **sps**, sphenopalatine sulcus; **zp**, zygomatic plate. Scale bar represents 5 mm.

the dorsal margin displays the unusual feature of a strongly rugose and weakly overhanging posterior margin of the masseteric fossa. AMF 68760 preserves the full ventral root of the plate, which measures 10.2 mm in length, and a slightly damaged dorsal root with an indicated width of 6.05 mm. The height of the plate, measured from the inferior notch of the anterior infraorbital fissure to the highest point on the superior rim of the masseteric fossa, is 12.9 mm.

FRONTAL: An isolated left frontal bone (AMF 68864; fig. 17D) is referred to *Coryphomys*. The specimen is virtually complete save for some damage to the ventral margin of the orbital lamina.

The dorsal surface of the frontal is longitudinally rather flat, but it shows a very slight midline doming anteriorly and a slight midline depression posteriorly. The orbitotemporal ridge is sharp posteriorly where it narrowly overhangs the orbitotemporal fossa. It fades anteriorly as it passes onto the rostral portion of the bone. The minimum interorbital width (midline suture to orbitotemporal ridge) is 5.5 mm, giving a full interorbital width of 11 mm.

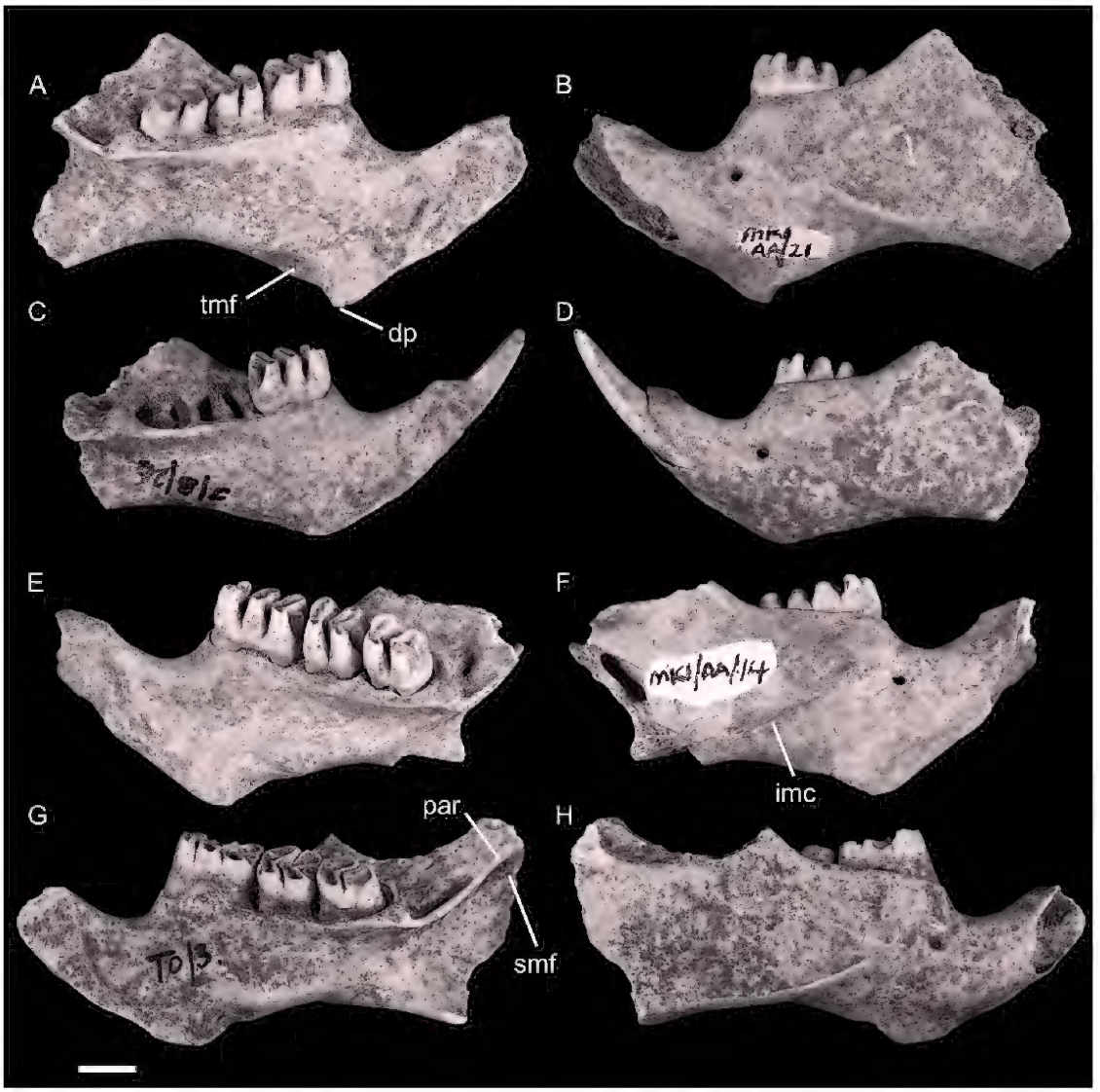

Fig. 16. Four partial dentaries referred to *Coryphomys musseri* ANWCP32 (holotype): a left dentary fragment with m1–3 in medial **(A)** and lateral **(B)** views; ANWCP27: a left dentary fragment with lower incisor and m1 in medial **(C)** and lateral **(D)** views; ANWCP10: a right dentary fragment with m1–3 in medial **(E)** and lateral **(F)** views; AMF 68753: a right dentary fragment with m1–3 in medial **(G)** and lateral **(H)** views. Scale bar represents 5 mm and applies to all images. *Abbreviations*: **dp**, digastric process; **imc**, inferior masseteric crest; **par**, postalveolar ridge; **smf**, superior mandibular foramen; **tmf**, fossa for deep part of transverse mandibular muscle. Scale bar represents 5 mm and applies to all images.

The anterior margin of the frontal is a simple V-shape with the apex facing anteriorly. This margin is comprised of two vertical, interdigitated sutures—the medial side is the nasofrontal suture, while the lateral suture is the maxillofrontal suture. The former suture is more finely interdigitating than the latter. The posterior margin of the frontal also bears a composite suture, the medial portion representing vertical, interdigitated contact with the parietal, and the lateral portion bearing a flattened facet for an overlying cranial lamina of the squamosal.

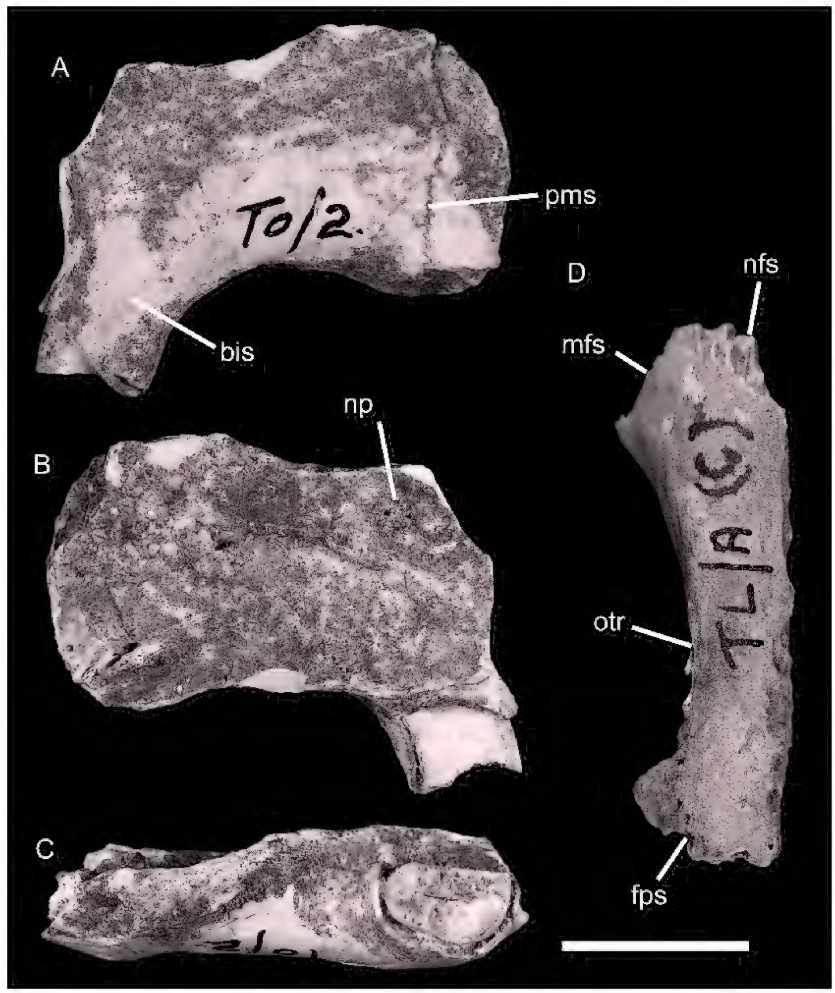

Fig. 17. Isolated cranial elements referred to the genus *Coryphomys* but without specific determinations. AMF 68822, a partial left premaxilla with a damaged upper incisor, shown in lateral **(A),** medial **(B),** and ventral **(C)** views. AMF 68864, an isolated left frontal bone in dorsal **(D)** view. *Abbreviations*: **bis**, bony incisor sheath; **fps**, frontoparietal suture; **mfs**, maxillofrontal suture; **nfs**, nasofrontal suture; **np**, narial process; **otr**, orbitotemporal ridge. Scale bar = 10 mm and applies to all images.

The orbital lamina of the frontal shows a relatively weak vertical fossa marking the broad fleshy origin of the orbital part of the temporal muscle. The ethmoid foramen is not present in the surviving part of the lamina and there is no sign of a dorsally placed foramen for the frontal diploic vein.

Petrosal Bone (figs. 18–19): The more complete of two specimens referred to *Coryphomys* (ANWCP30; fig. 18A–D) is a right petrosal with slight abrasion of the mastoid surface and the medial margin of the epitympanic wing. Important features of the tympanic surface (fig. 18A) are: (1) presence of a broad sulcus on the anterior pole of the pars cochlearis, presumably marking the passage of the internal carotid artery to the carotid canal; (2) absence of an obvious sulcus for the stapedial artery (the passage of a much reduced stapedial artery is possibly indicated by a small notch in the horizontal bony ridge that emanates from the ventral margin of the fenestra vestibuli and forms the medioventral lip of the stapedius fossa); (3) deep excavation of the tensor tympani fossa into the anterolateral surface of the promon-

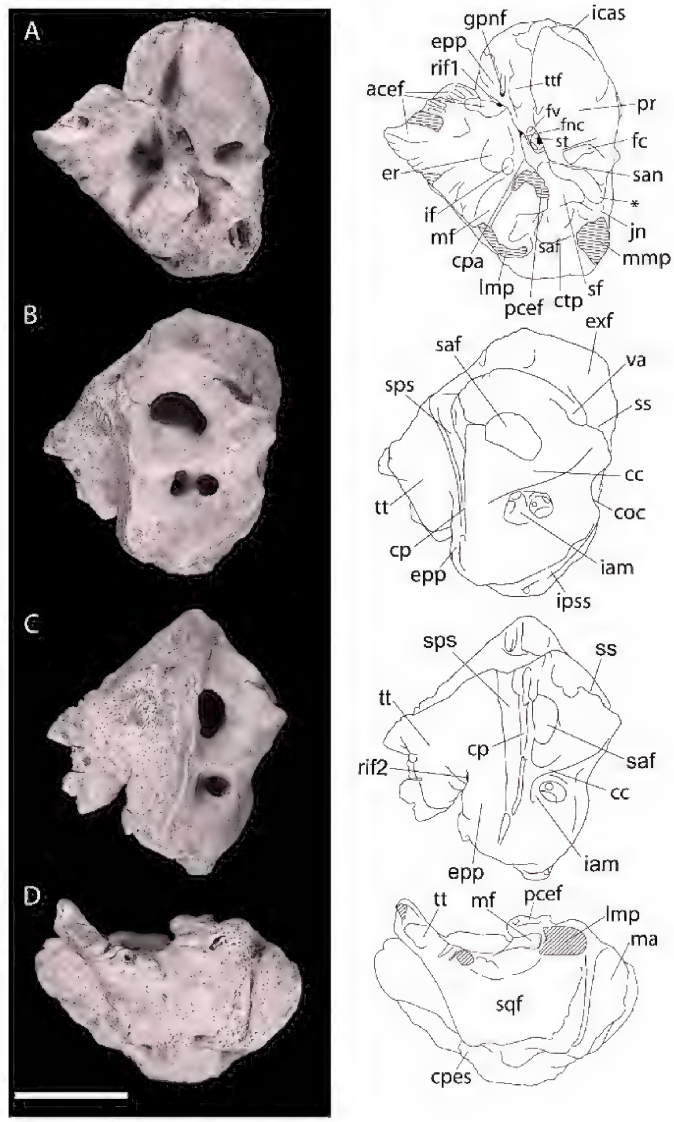

Fig. 18. Isolated right petrosal bone (ANWCP30) referred to the genus *Coryphomys*, and tentatively assigned to *C. musseri*. The four views are of **A,** the tympanic surface; **B,** the posterior endocranial fossa surface; **C,** middle endocranial fossa surface; and **D,** lateral surface. Nomenclature of anatomical features is based on the scheme of Wible (e.g., Wible, 1990). *Abbreviations*: **acef**, anterior crus of ectotympanic facet; **cc**, crus commune; **co**, cochlea; **coc**, cochlear canicularis (for cochlear aqueduct); **cp**, crista petrosa; **cpa**, crista parotica; **cpes**, capsuloparietal emissary vein sulcus; **ctp**, caudal tympanic process; **epp**, epitympanic process of petrosal; **er**, epitympanic recess; **exf**, exoccipital facet; **fc**, fenestra cochleae; **fnc**, facial nerve canal; **fv**, fenestra vestibuli; **gpnf**, greater petrosal nerve foramen; **iam**, internal auditory meatus; **icas**, internal carotid artery sulcus; **if**, incudal fossa; **ipss**, inferior petrosal sinus sulcus; **jn**, jugular notch; **lmp**, lateral mastoid process; **ma**, mastoid; **mf**, meatal fossa; **mmp**, medial mastoid process; **pcef**, posterior crus of ectotympanic facet; **pr**, promontorium; **rif1**, ramus inferior of stapedial artery foramen (intratympanic); **rif2**, ramus inferior of stapedial artery intratympanic (endocranial); **saf**, subarcuate fossa; **san?**, possible stapedial artery notch; **sf**, stapedial fossa; **sps?**, possible superior petrosal sinus sulcus; **sqf**, squamosal facet; **ss**, sigmoid sinus sulcus; **tt**, tegmen tympani; **ttf**, tensor tympani fossa; **va**, vestibular aqueduct; **ve**, vestibule; *, bony process partially occluding medial end of postpromontorial fossa. Scale bar represents 5 mm.

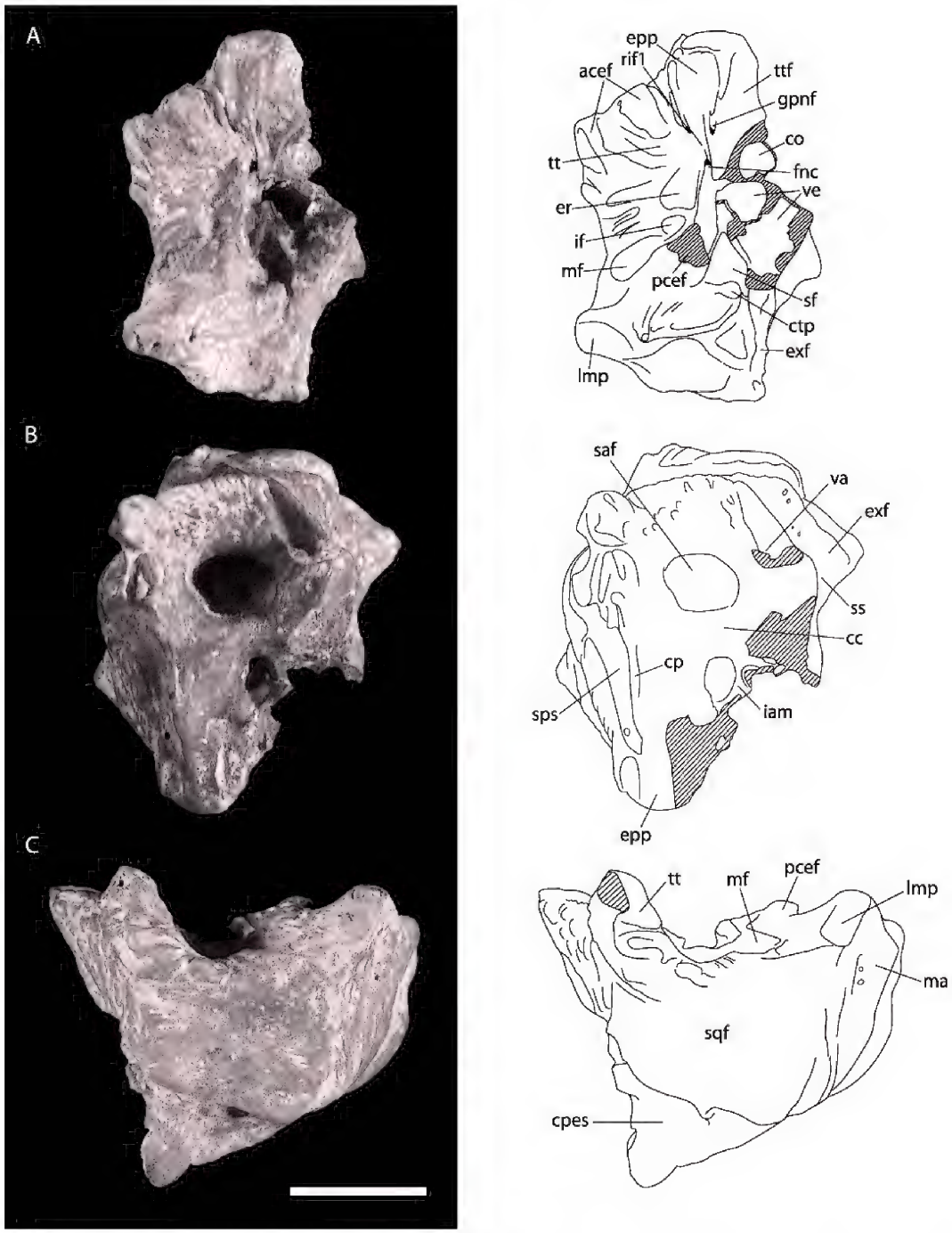

Fig. 19. Isolated right petrosal bone (ANWCP31) referred to the genus *Coryphomys*, and tentatively assigned to *C. buehleri*. This specimen is burnt and has lost much of the pars cochlearis; other parts are well preserved and appear undistorted. The three views are of **A,** the tympanic surface; **B,** the posterior endocranial fossa surface; and **C,** lateral surface. Crosshatched areas are fractured or abraded. Abbreviations as in figure 17. Scale bar = 5 mm.

torium; (4) incomplete fusion of the tegmen tympani and the epitympanic process of the petrosal above the facial nerve canal; (5) presence of very small foramina within the zone of union of the tegmen tympani and epitympanic process of the petrosal, one on each of the tympanic and endocranial surfaces (both are distinct from the foramen for the greater petrosal nerve, which opens onto the tympanic surface of the epitympanic process of the petrosal); (6) robust nature of the tegmen tympani, supporting a broad area of fibrous attachment to the anterior crus of the ectotympanic (not preserved); (7) deep excavation of the stapedius fossa above a bony ridge that links the ventral margin of the fenestra vestibuli and the medial end of the caudal tympanic process; (8) presence of a shallow epitympanic recess with a distinct incudal fossa at its rear; (9) presence of an elongate, transversely oriented meatal fossa, presumably marking the limits of attachment of the pars flaccida of the tympanic membrane; (10) weak development of the caudal tympanic process behind the posterior tympanic sinus; and (11) medial end of the posterior tympanic sinus is partially enclosed by a thickened bony lamina that narrows the connection with the jugular notch.

The medial and endocranial surfaces (fig. 18B–C) show several features of note: (1) a broad, rugose surface marking the zone of contact with the exoccipital; (2) a broad sulcus for the sigmoid sinus, leading to a prominent jugular notch; and (3) a short sulcus, anterior of the vestibular aqueduct, presumably for the inferior petrosal sinus. The endocranial surface also presents two notable features: (1) a conspicuously large vestibular aqueduct (for the endolymphatic duct) passing into the body of the pars vestibularis of the petrosal behind and slightly above the subarcuate fossa; and (2) a broad, deeply impressed sulcus running anterior to the crista petrosa. Though the latter sulcus is located in an appropriate position to mark the passage of a prootic sinus, this vessel appears to be lost in later development of all placental mammals studied by embryological methods to date (Wible, 1990; Wible and Hopson, 1995), with its drainage diverted into a capsuloparietal emissary vein (= petrosquamous sinus of human anatomy; e.g., Diamond, 1992). In the *Coryphomys* petrosal a sulcus for the capsuloparietal emissary vein is visible in lateral view (fig. 18D), directed as in other murines toward a postglenoid foramen located between the petrosal and the squamosal bones. Given this observation, the additional sulcus in *Coryphomys* most likely marks the course of an enlarged superior petrosal sinus (connecting the cavernous sinus with the transverse sinus; Greene, 1968). Another feature of note seen in lateral view is a small, unidentified vascular channel that emerges out of the posterior tympanic sinus behind the lateral mastoid process.

The vascular impressions on ANWCP30 advertise an arterial arrangement characterized by strong reduction of the stapedial artery and its branches, and by a largely extracapsular course for the internal carotid artery. This is a derived arterial arrangement among muroid rodents but is one that has evidently originated on a number of separate occasions across several families (see Discussion). Much less comparative information is available on the pattern of endocranial venous drainage of muroids. However, our preliminary comparisons have failed to find a parallel morphology in any other murine taxon.

The second specimen (ANWCP31, fig. 19) is a burnt left petrosal missing most of the pars cochlearis. This specimen is noticeably larger than the more complete example, but it is otherwise very similar in morphology. Most notably, it displays the highly diagnostic feature of the broad endocranial venous sulcus anterior to the crista petrosa. One minor point of difference is the more prominent development of the lateral mastoid process, though we note that that this process is somewhat abraded in ANWCP30. The larger specimen is tentatively referred to *C. buehleri* and the smaller specimen to *C. musseri*.

DISCUSSION

Our taxonomic studies of the Timorese murines provide new insights into their anatomy, evolutionary history, paleoecology, and sadly, for the majority of taxa, their extinction. Many of these issues will be

explored more fully in later contributions of this series, following completion of the primary descriptive works. Here we limit our discussion to three issues specific to the genus *Coryphomys*, namely the case for recognition of two species, the phylogenetic relationships of the genus, and its paleoecology.

Species Diversity in *Coryphomys*

Because our decision to recognize two biological species in the *Coryphomys* sample differs from the conclusions of previous researchers, we first provide some explicit arguments in support of this action.The most striking contrasts within the *Coryphomys* sample relate to the form of the posterior cingulum on M1, and the correlated contrast in molar size relative to skeletal structures. The lower molars also are divisible into two groups based on the morphology of the anteroconid on m1 and the form of the posterior cingulum on m1–2, again correlated with an absolute size distinction. Using these dental contrasts to divide the sample of maxillae and dentaries, a contrast in skeletal robusticity is then apparent, as well as subtle differences in masticatory anatomy. Significantly, it is the relatively smaller-toothed species that displays the more robust craniomandibular morphology. Contrasts of this kind and magnitude are commonly observed between congeneric species of murine rodents, typically associated with contrasting ecological specializations. However, a number of alternate explanations of the observed metric and nonmetric variation also warrant consideration, namely: (1) sexual dimorphism; (2) "insularization" or resource-based polymorphism; and (3) sample heterochroneity.

Sexual dimorphism. Muroid rodents generally do not show dimorphism in characters under sexual selection, such as occur for example in primates and artiodactyls (Weckerly, 1998). In contrast, weak dimorphism in adult body weight is not uncommon among muroids, especially in the largest taxa (Reiss, 1989). Probably because of this lack of overt sexual dimorphism, relatively few published taxonomic studies on muroids rodents give separate craniodental measurements for each sex. However, the few that do (e.g., Aoki and Tanaka, 1938; Kemper and Schmitt, 1992; Helgen, 2007) confirm that dimorphism is weak or absent in the teeth, and is very marked only in cranial dimensions among the largest taxa. In our experience, this general lack of sexual dimorphism also extends to all details of cuspal morphology.

If variation in the *Coryphomys* sample were due to sexual dimorphism, we would expect to see a bimodality of dental measurements. However, unless the feeding ecology of the sexes were significantly different, we would not expect to see any associated morphological differences in the tooth crowns. Finally, we would also expect the larger-toothed sex to display the more robust cranial morphology. In the *Coryphomys* sample we see not only size-linked morphological differences, but it is the smaller-toothed morphotype that displays the more robust skeletal morphology. For these reasons, we reject sexual dimorphism as an explanation for the observed morphometric variation.

Exceptional intrapopulational variability. Island populations of mammals commonly show divergent morphologies compared with continental relatives (Lomolino, 1985, 2005). The best-known examples involve either pronounced miniaturization or gigantism (Foster, 1964; Dayan and Simberloff, 1998), with island populations of rodents typically showing a slight increase in body size relative to continental populations (Van Valen, 1973; Adler and Levins, 1994; Lomolino, 2005). An increased level of sexual dimorphism in body weight is also reported in some island mammal populations, such as the long-tailed field mouse, *Apodemus sylvaticus*, in the Scilly Isles (Delany and Healy, 1967) and Channel Isles (Hedges, 1969), and Irish populations of several mustelids (Dayan and Simberloff, 1994).

Most attempts to explain these trends point to special features of island mammal communities, such as decreased numbers of competitors and predators, or to intrinsic properties of an island context, such as finite food resources and limited opportunities for dispersal (reviewed by Dayan and Simberloff, 1998).

The niche-variation hypothesis of Van Valen (1965) posits a relationship between

niche width and morphological variation. Under this model, island populations, released from the influence of specific competitors or predators, should display enhanced levels of morphological variability. The legitimacy of this notion has been challenged on the basis of weak evidential support across several groups of vertebrates (e.g., Soulé and Stewart, 1970; Malmquist, 1985) and also on population genetic grounds for sexually reproducing species (Roughgarden, 1972). Murine rodents, with their abundant representation on island systems throughout the Old World, represent an ideal group in which to explore the generality of this model. However, the relevant data compilations and analyses have not been performed, even on a regional level.

Intuitively, we suggest that an elevated level of morphological variation due to character release would be characterized by continuous morphometric variation (i.e., a lack of morphometric substructure) and by absence of character covariance beyond that which is ontogenetically determined (e.g., variation in paranasal sinus morphology would not be covariant with differences in cuspal morphology on molars). At the same time, we must remain mindful of the high levels of morphological integration that exist within the mammalian skull and dentition, due both to genetic and external influences on individual ontogenies.

Resource-based polymorphism (the maintenance of discrete morphotypes within a genetically cohesive species) is believed to be a product of divergent selection acting on discrete morphological variation within a heterogeneous environment (Skúlason and Smith, 1995; Smith and Skúlason, 1996). This phenomenon appears to be particularly common in "insular" populations, including both oceanic islands and geologically young lakes. Among the best-studied examples are discrete large- and small-billed morphs of the African Finch (*Pyrenestes ostrinus*; Smith, 1987, 1993) and the left- and right-handed versions of scale-eating cichlids (each of which allows feeding on one side only of target prey; Hori, 1993). In each of these examples, the key variable trait appears to be determined by a single locus with two alleles. In other examples, the polymorphism is environmentally determined ("polyphenism") with external stimuli at critical times causing a switch in developmental pathways (Scheiner, 1993). In either event, most examples of resource polymorphism involve components of the feeding apparatus (Hanken and Hall, 1993), though in some instances, as in the case of the asymmetrical cichlids, there is a more pervasive morphological change.

Examples of resource-based polymorphism among mammals remain elusive, perhaps because the prolonged intrauterine development of mammals serves to buffer the embryo against extreme environmentally determined phenotypic plasticity of the kind seen in many other vertebrates (e.g., Pfennig, 1992), and perhaps also because the relatively large individual home ranges of most mammals dictates against narrow dietary or habitat specialization of the kind that seems to underpin many examples of true resource-based polymorphism. Skúlason and Smith (1995) cite one possible instance, apparently involving contrasting patterns of habitat use and diet in ecomorphs of the deer mouse, *Peromyscus maniculatus* (Wimberger, 1994). Unfortunately, a detailed account of this example is pending. However, we should note that an earlier study of two *Peromyscus* species (*P. boylii* and *P. truei*) did find significant correlations between variation in body proportions (especially tail length and foot length), diet and degree of arboreality (Smartt and Lemen, 1980), thereby supporting the notion that intraspecific morphological variation in this genus has measurable adaptive significance.

Smith and Skúlason (1996) emphasized the essential uniformity of evolutionary process between resource-based polymorphism and sympatric speciation. The main point of distinction is whether gene flow is restricted in any way between the morphologically divergent subpopulations. This can arise in various ways, including simple spatial or temporal segregation of reproductive activity, assortative mating or pleiotropy and/or genetic hitchhiking (Rice and Hostert, 1993). Importantly, however, complete genetic isolation is not necessary for speciation to proceed, provided selection is strong and

the trait under selection is correlated in some way with rates of interbreeding (Bolnick and Fitzpatrick, 2007). Well-documented examples of sympatric speciation remain rare (Coyne and Orr, 2004), but many examples of resource-based polymorphism might be reconsidered as examples of incipient sympatric speciation (Dayan and Simberloff, 2005). Indeed, it is probably no coincidence that most examples of both phenomena are located in precisely the same geologically young environmental contexts that host some of the most spectacular recent adaptive radiations (e.g., cichlid fishes; anoles).

In the case of the Timorese murines, we regard taxon diversity as a more likely explanation for the observed morphological variation than resource-based polymorphism. However, this conclusion does not automatically imply that sympatric speciation has occurred. Timor is a relatively large island with varied habitat and a discontinuous central range and it seems just as likely that speciation occurred on Timor through allopatric divergence, perhaps involving chromosomal rearrangements of the kind that have very likely underpinned taxic diversification in other groups of murines (e.g., Baverstock et al., 1981, 1983; Robson, 2002; Rickart and Heaney, 2002; Steppan et al., 2003).

Sample heterochroneity. Many mammals underwent significant adjustments of both body size and morphology in response to the severe climatic perturbations that characterized the Quaternary (e.g., Kurtén and Anderson, 1980; Lister, 1989; Vartanyan et al., 1993; Helgen et al., 2006). Failure to account for variation in the age of fossil samples undoubtedly has led to unwarranted splitting of many fossil lineages, and the inability to control for this factor is an ongoing source of frustration in understanding taxon diversity in many groups (e.g., Anguillan caviomorphs: Biknevicius et al., 1993; dasyuromorph marsupials: Dawson, 1982a, 1982b).

As introduced above, the Timorese murine fossil samples range in age from nearly 40,000 years to recent, and thus span a period of significant global cooling, the last glacial maximum (LGM; ca. 33,000–15,000 BP), as well as the warmer and more stable conditions of the postglacial period. In eastern Indonesia the LGM probably generated significant aridity (O'Connor and Aplin, 2007) and it is reasonable to assume that terrestrial mammal lineages would have shown corresponding adjustments, perhaps including a significant metrical response in one or more taxa. A temporally unconstrained assemblage spanning this period could thus appear excessively variable and potentially polymodal, especially if the sample was nonrandomly derived with respect to age. However, in samples with good stratigraphic context and dating controls, variation related to temporal adjustments in size or morphology should be evident as a structured pattern.

The good stratigraphic provenance of many of the *Coryphomys* specimens allows us to confidently reject sample heterochroneity as an explanation for the observed morphological variability. Both putative species were obtained from stratigraphic contexts that date to relate to the early part of the LGM (e.g., ANWCP9 and ANWCP18 of *C. musseri* and ANWCP6 and ANWCP7 of *C. buehleri*) and both are well represented in levels that date to the mid-Holocene (e.g., AMF 68765, AMF 68851, AMF 68753 and ANWCP10, ANWCP11 of *C. musseri* and AMF 68831, AMF 68789, and AMF 68751a, b of *C. buehleri*). In neither species is there any obvious change in size of the teeth through time within the sample from a given site, nor is there any systematic variation between sites. However, it should be noted that sample sizes for each of the two *Coryphomys* species are inadequate to detect any subtle variation in tooth or skeletal dimensions that might have existed either across the altitudinal or temporal range.

Phylogenetic Affinities of *Coryphomys*

Previous assessments of *Coryphomys* have produced a variety of opinion as to its phylogenetic relationships. Schaub (1937) compared the lower molar structure of *Coryphomys* with each of *Lenomys*, *Mallomys*, *Apodemus*, and *Pithecheir*, but did not claim any special resemblance to any one genus. Stehlin and Schaub (1951) compared *Coryphomys* most closely with *Lenomys* but regarded the fossil murine as an extremely isolated lineage, largely due to the complex

nature of the m1 anteroconid. Hooijer (1965) studied additional specimens (including examples of Mahoney's genus A) and contested the significance of the m1 anteroconid. To Hooijer (1965: 129), the more significant observation regarding *Coryphomys* is that "there are no accessory basal tubercles in M_{1-3}, not even indications of an anterior buccal cingulum in M_{2-3}, while the posterior loph of M_3 is straight and undivided." Moreover, he noted that the former character linked *Coryphomys* to *Mallomys* and *Crateromys* alone "among the gigantic complex-toothed murines," while the latter feature was present also in *Papagomys*. Hooijer (1965) also compared *Coryphomys* with *Lenomys*, *Apodemus*, and *Spelaeomys*, each of which displays a relatively complex molar pattern. Misonne (1969) grouped all of the complex-toothed murines within his *Lenothrix-Parapodemus* division and characterized the lower molar dentition of *Coryphomys* as showing some advanced features over the three inferred primitive genera, *Lenothrix*, *Lenomys*, and *Pithecheir*. Musser (1981b), having examined at least some of the Glover material, suggested a possible relationship between *Coryphomys* and *Spelaeomys*, as elements of a larger assemblage of murines endemic to Melanesia to the east. Musser and Carleton (2005) identified each of *Coryphomys* and *Spelaeomys* as part of "an early radiation of New Guinea endemics" and further promoted this notion by placing both genera within their *Pogonomys* division.

The new material described herein, including the first upper molars and associated cranial elements, confirm the general resemblance of *Coryphomys* to the broadly defined assemblage of complex-toothed murines. However, detailed comparisons with extant murine genera such as *Lenothrix*, *Pithecheir*, *Lenomys*, *Apodemus*, *Pogonomys*, and *Spelaeomys*, and likewise, with various extinct Murinae, reveal a patchwork of similarities and differences, with no particularly compelling resemblance to any one genus. While this situation clearly invites the use of parsimony- or likelihood-based methods (e.g., Kitching et al., 1998; Lewis, 2001) to identify plausible phylogenetic topologies involving *Coryphomys*, in our view, any enthusiasm for such a route must be tempered by two considerations. The first is the general acknowledgment (e.g., Tate, 1951; Ellerman, 1941; Misonne, 1969; Musser and Newcomb, 1983) that homoplasious (i.e., independently evolved) morphological change is very likely rampant within the craniodental morphology of Murinae, owing to repeated dietary specializations (e.g., seed eating, insectivory) within different regional radiations, coupled with a high level of underlying morphological conservatism. If homoplasy is a dominant feature of morphological change within a group of organisms, then no form of unconstrained character-based analysis will reliably retrieve an underlying phylogeny (Felsenstein, 1978).

The second reason behind our reluctance to undertake a quantitative assessment based on morphological evidence is our belief that suites of morphological characters derived from one anatomical region, in this case the skull and teeth, are likely to be correlated in complex ways on account of ontogenetic interrelations and functional linkages (Jernvall and Jung, 2000; Kangas et al., 2004). As such, they are unlikely to satisfy one of the primary assumptions of character-based methods of phylogenetic analysis—the principle of character independence. Indeed, the contrary condition of profound character interdependence is more compelling for murine rodents than for any other group of vertebrates, owing mainly to their predominance as experimental animals. For example, recent work on the development of molar crowns, primarily in laboratory mice (*Mus musculus*), has shed light on the genetic and ontogenetic influences that lead to the initiation of dental placodes, the differentiation of the primary and secondary enamel knots, and the formation of accessory crests and basins that create species-specific dental morphologies (Keränen et al., 1998; Jernvall and Jung, 2000; Salazar-Ciudad and Jernvall, 2002; Kassai et al., 2005; Cai et al., 2007; Obara and Lesot, 2007). In particular, these studies make it abundantly clear that the murine genome does not contain code that "individualizes" particular cusps or other dental structures, but rather that these structures emerge as a consequence of developmental cascades involving complex, sequential molecular and cellular events. Simi-

lar work on the molecular basis of development of other cephalic tissues likewise point to the pervasive role of developmental cascades (e.g., Ahlberg and Köntges, 2006; Gross and Hanken, 2008; Kuratani, 2005; Nagase et al., 2008), and to the need for new approaches to morphological evidence based on a unification of the sciences of embryology and genetics (or more properly, genomics) (Hamburger, 1980; Van Valen, 1982; Hanken, 1993; Gilbert, 1994; Gilbert et al., 1996; West-Eberhard, 1998).

Previous skeptics of unconstrained morphological character analysis have encouraged the use of independently derived phylogenetic frameworks to investigate the pattern and process of morphological change (e.g., Soltis et al., 1999; Scotland et al., 2003). While this approach is still somewhat dependent on a reductionist, character-based approach to morphology, it does offer some hope for discrimination of homoplasious from nonhomoplasious changes within a group, for the identification of ancestral character states, and possibly also for disentangling patterns of covariation among characters. Despite these potential advantages, this approach has not often been applied on any large scale. One reason is that reliable, well-resolved organismal phylogenies have only recently started to appear for many groups, mirroring the rapid advance in both sequencing technology and analytical methods and capacity.

Murine rodents are one group about which knowledge of phylogenetic relationships has improved enormously within the past few years, with many of the key lineages represented by multiple mitochondrial and nuclear gene sequences (Michaux et al., 2001; Lecompte et al., 2002a, 2008; Jansa and Weksler, 2004; Steppan et al., 2004, 2005; Rowe et al., 2008). Lecompte et al. (2008) recently reviewed the commonality among the various molecular and other datasets and proposed a formal classification that recognizes 10 tribes within Murinae, grouped into several larger, informal clades (content of tribes is summarized in table 3). Several of Lecompte et al.'s (2008) murine tribes are equivalent in content to individual "divisions" of Musser and Carleton's (2005) arrangement. However, the majority is more inclusive and contains members of two or more "divisions."

We have extended the phylogenetic conclusions and classification of Lecompte et al. (2008) to more fully incorporate the major findings of Rowe et al.'s (2008) multigene phylogenetic analysis of murine evolution (summarized in fig. 20). Most importantly, Rowe et al. (2008) analysed representatives of two significant Asian murine genera (*Chiropodomys* and *Vandeleuria*) as well as a large number of Australo-Papuan genera. Their results confirm the unity of the Hydromyini but identify *Chiropodomys* as a likely basal member of this clade. *Vandeleuria* was found to be a more isolated lineage that probably warrants segregation at tribal level; it appears to be a sister lineage to a large clade comprised of Murini, Praomyini, Apodemurini, and Malacomyini.

A number of potentially significant murine genera still remain unstudied by molecular methods. Unfortunately, this includes a number of Southeast Asian murines that display a general resemblance in molar morphology to *Coryphomys*, namely *Lenothrix*, *Pithecheir*, *Pithecheirops*, *Lenomys*, *Vernaya*, and *Hapalomys*. Among these genera, *Lenothrix*, *Pithecheir*, *Pithecheirops*, and *Lenomys* form a dentally cohesive group (Misonne, 1969) that appears to be well removed from any of the 10 tribes recognized by Lecompte et al. (2008). For convenience we refer to this cluster of genera by the informal term "*Lenothrix* group." *Hapalomys* is highly modified in dental structure (Musser, 1972) and has obvious close relatives, while *Vernaya* is superficially similar in dental morphology to each of the distantly related *Chiropodomys* and *Vandeleuria* (Misonne, 1969; Heaney et al., 2009). In the absence of firm phylogenetic evidence for placement of any of these taxa or clusters, we treat each of them as potentially isolated lineages within Murinae.

We have selected a total of eight features for special consideration and assess the evolution of each feature against the consensus phylogeny illustrated in figure 20. Several of the selected features were given special emphasis in the prior literature on *Coryphomys*, while others are mentioned as potentially significant phylogenetic indicators

TABLE 3

Tribal Level Classification of Extant Murinae, Largely after Lecompte et al. (2008) but with Certain Additional Taxa Included on Basis of Rowe et al. (2008) Results

Recognition of a possible "*Lenothrix* Group" is based on an overall resemblance in dental morphology among the included genera. Among the "Murinae incertae sedis," *Chiropodomys* is probably the sister taxon to the Hydromyini, while *Vandeleuria* appears to be equally remote from all other lineages.

Tribes	Confirmed members	Divisions of Musser and Carleton (2005)	Other likely members
Arvicanthini	*Aethomys*, *Micaelamys*	*Aethomys* Division	
	Arvicanthis	*Arvicanthis* Division	
	Desmomys		
	Lemniscomys		
	Mylomys		
	Pelomys		
	Rhabdomys		
	Dasymys	*Dasymys* Division	
	Golunda	*Golunda* Division	
	Dephomys	*Hybomys* Division	
	Hybomys		
	Stochomys		
	Grammomys	*Oenomys* Division	*Lamottemys*
	Oenomys		
	Thallomys		
	Thamnomys		
Otomyini	*Myotomys*	Subfamily Otomyinae	
	Otomys		
	Parotomys		
Millardini	*Cremnomys*	*Millardia* Division	*Diomys*
	Millardia		*Madromys*
Apodemurini	*Apodemus*	*Apodemus* Division	
	Tokudaia		
Malacomyini	*Malacomys*	*Malacomys* Division	
Praomyini	*Colomys*	*Colomys* Division	*Nilopegamys*
	Zelotomys		
	Heimyscus	*Stenocephalemys* Division	
	Hylomyscus		
	Mastomys		
	Myomyscus		
	Praomys		
	Stenocephalemys		
Murini	*Mus*	*Mus* Division	*Muriculus*
Hydromyini	*Apomys*	*Chrotomys* Division	
	Archboldomys		
	Chrotomys		
	Rhynchomys		
	Crossomys	*Hydromys* Division	*Baiyankamys*
	Hydromys		*Microhydromys*
	Parahydromys		*Paraleptomys*
	Conilurus	*Pseudomys* Division	
	Leggadina		
	Leporillus		
	Mastacomys		
	Mesembriomys		
	Notomys		
	Pseudomys		
	Zyzomys		

TABLE 3
(Continued)

Tribes	Confirmed members	Divisions of Musser and Carleton (2005)	Other likely members
	Anisomys	*Pogonomys* Division	*Abeomelomys*
	Chiruromys		*Coccymys*
	Hyomys		*Pogonomelomys*
	Macruromys		
	Melomys	*Uromys* Division	*Protochromys*
	Paramelomys		
	Solomys		
	Uromys		
	Leptomys	*Xeromys* Division	*Mirzamys*
	Pseudohydromys		
	Xeromys		
	Lorentzimys	*Lorentzimys* Division	
Rattini	*Crunomys*	*Crunomys* Division	*Sommeromys*
	Chiromyscus	*Dacnomys* Division	*Anonymomys*
	Dacnomys		
	Leopoldamys		
	Niviventer		
	Maxomys	*Maxomys* Division	
	Margaretamys	*Pithecheir* Division	
	Micromys	*Micromys* Division	
	Abditomys	*Rattus* Division	*Kadarsanomys*
	Bandicota		*Nesoromys*
	Berylmys		*Palawanomys*
	Bullimus		*Taeromys*
	Bunomys		*Tryphomys*
	Diplothrix		
	Komodomys		
	Limnomys		
	Nesokia		
	Papagomys		
	Paruromys		
	Paulamys		
	Tarsomys		
	Rattus		
	Sundamys		
	Melasmothrix	*Melasmothrix* Division	*Tateomys*
Phloeomyini	*Batomys*	*Phloeomys* Division	
	Carpomys		
	Crateromys		
	Musseromys		
	Phloeomys		
Murinae *incertae sedis*	*Echiothrix*	*Echiothrix* Division	
	Hadromys	*Hadromys* Division	
	Chiropodomys	*Micromys* Division	
	Haeromys		
	Hapalomys		
	Vandeleuria		
	Vernaya		
	Eropeplus	*Pithecheir* Division	
'Lenothrix' Group	*Lenomys*	*Pithecheir* Division	
	Lenothrix		
	Pithecheir		
	Pithecheirops		

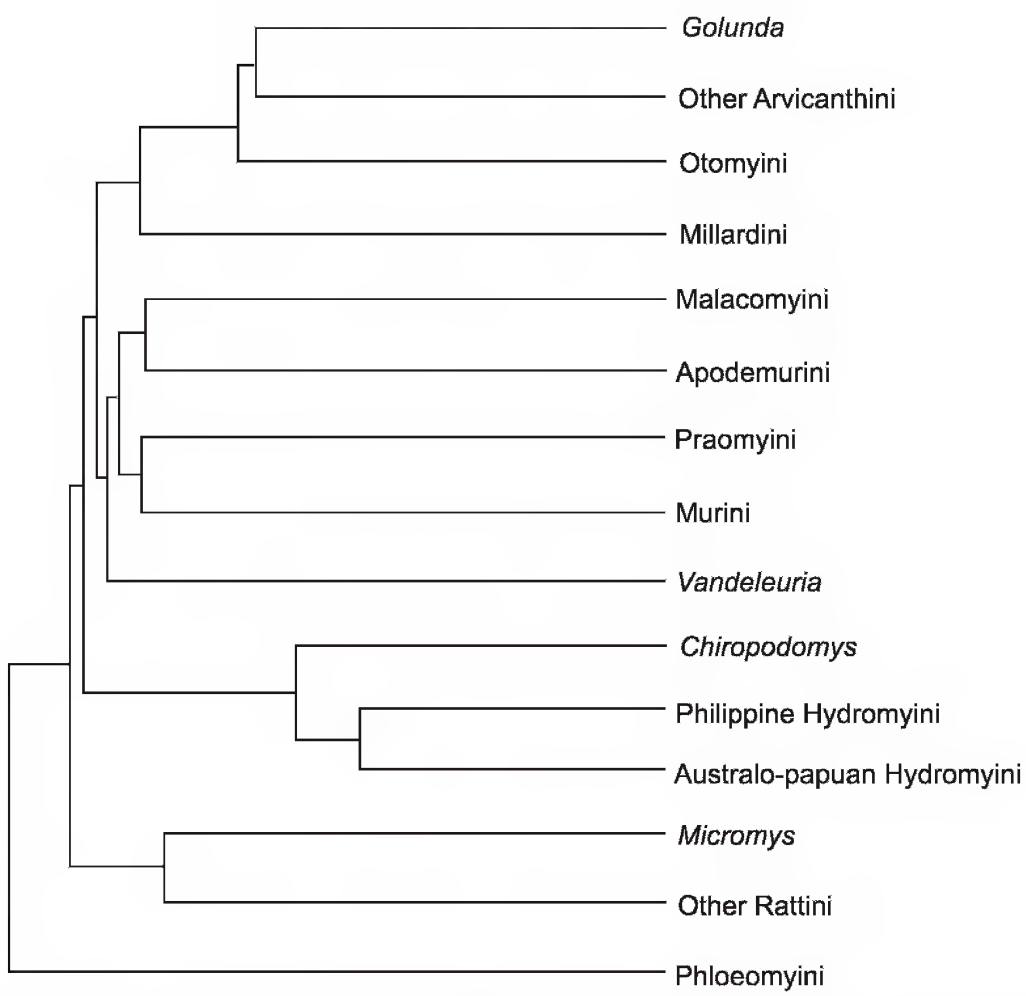

Fig. 20. Hypothesis of phylogenetic relationships among the major lineages of Murinae, based on the findings of recent molecular studies of multiple mitochondrial and nuclear genes (Michaux et al. 2001; Lecompte et al., 2002a, 2008; Jansa and Weksler, 2004; Jansa et al., 2006; Steppan et al., 2004; Rowe et al., 2008). Branch lengths are scaled according to the chronogram presented by Lecompte et al. (2008: fig. 2). The placement of *Chiropodomys* and *Vandeleuria* on this topology is based on the multigene phylogeny published by Rowe et al. (2008); branch lengths for these placements are approximate. The taxonomic content of each Tribe is summarized in table 3.

in previous reviews of murines (e.g., Ellerman, 1941; Misonne, 1969; Musser and Heaney, 1992). For one cranial character (maxillary sinus elaboration), we currently lack sufficient comparative data to explore the phylogenetic significance of the observed morphological variation. To assist with assessment of character polarity, we occasionally consult the condition in other muroid subfamilies, including the two groups—Gerbillinae and Deomyinae—that are identified on molecular grounds as the closest relatives to Murinae (Adkins et al., 2003; Jansa and Weksler, 2004; Steppan et al., 2004, 2005).

Presence of Cusp t7 on Upper Molars: A significant number of murine rodents, *Coryphomys* among them, possess a third cusp in the lingual series of the upper molars, labelled cusp t7 under Miller's (1912) scheme. Winge (1881: 17; as cited by Thomas, 1906: 84) identified this cusp in *Micromys* as a new development that promoted the anterior displacement of the two original

internal cusps. Thomas observed that the "same structure" is present in the upper molars of widely scattered murines, including genera with Palearctic, African, Philippine, New Guinean, and Australian distributions, and promoted the alternative view that "(even if [it is a] later growth as compared with the very primitive Cricetine series of Muridae), it is an early development within the true Murinae, occurring here and there within the group, and has then been reduced in some forms and lost in others ..." (Thomas, 1906: 85). Misonne (1969: 58–62) reviewed the distribution of this structure across all extant and then known fossil Murinae and usefully observed that, because addition of cusp t7 effectively squares off the teeth, it is one way of increasing the continuity of the occlusal surface of the molar row as a whole (the other way is to increase the degree of molar overlap; Misonne, 1969: 60, fig. E). Misonne (1969: 59) concluded that "a classification based upon the presence or absence of t7 is wrong," citing its variable occurrence on homologous teeth even within some genera and species, and sometimes between different molars in the series. Like Michaux (1967), he also cited the absence of this cusp in the earliest (then known) fossil murines (species of *Progonomys*) as evidence for its being a neoformation. Subsequent discovery of earlier and seemingly more primitive murines has only reinforced this view, with the earliest known murine, *Antemus chinjiensis*, showing no cuspal development in this position (Jacobs, 1977; Jacobs et al., 1989, 1990). Absence of cusp t7 in all members of the outgroup taxa (Deomyinae and Gerbillinae; Petter, 1959, 1972, 1973, 1983; Misonne, 1969; Denys and Michaux, 1992) also strongly supports the notion that cusp t7 is a novel development within Murinae. Musser and Newcomb (1983: 537, table 38) and Chaimanee (1998) both scored the presence of a cusp t7 on upper molars as a derived character within Murinae.

The broad phylogenetic distribution of cusp t7 (table 4) suggests a complex pattern of character evolution, with undeniable evidence for multiple origins or losses within Murinae. However, the more interesting question of whether cusp t7 was present in the common ancestor of all living murines is not so clearly resolved. Evidence favouring an early development of cusp t7, followed by multiple subsequent losses, includes the likely presence of this cusp in all members of the Phloeomyini (Musser and Heaney, 1992: 66, fig. 34; Musser et al., 1998a: 18–19, figs. 12–13), in a number of other phylogenetically isolated genera (*Vandeleuria*, *Micromys*, *Chiropodomys*; Misonne, 1969; Musser, 1979), and in various phylogenetically unallocated but highly distinctive genera (e.g., *Hapalomys*, *Vernaya*, members of the "*Lenothrix* group"; Misonne, 1969; Musser, 1972, 1981a; Musser and Newcomb, 1983). Evidence favouring an alternative history, involving multiple origins, could include the presence of cusp t7 in crown members only of certain groups (e.g., *Thamnomys* within the Arvicanthini, Misonne, 1969: figs. 38–39; and in *Leptomys*, *Chiruromys*, *Pogonomys*, and *Hyomys* within the Australo-Papuan branch of the Hydromyini; Misonne, 1969; Musser et al., 2008).

Other evidence that might help decide this issue comes from variation in the morphological relations of cusp t7. Among extant murines, three main variants of cusp t7 are found, involving: (1) an anterior connection to cusp t4; (2) a labial connection to cusp t8; or (3) isolation from both cusps or a weak anterolabial connection to cusp t5. These contrasting conditions show a variable degree of constancy within the major murine lineages. In Phloeomyini, all genera show strong labial connection of cusp t7 to cusp t8, while in the speciose genus *Chiropodomys*, cusp t7 is invariably connected to cusp t4. Within the Australo-Papuan branch of the Hydromyini, contrasting patterns of connection are found in different genera (e.g., to cusp t4 in *Leptomys*; to cusp t8 in *Pogonomys*, *Hyomys*, *Zyzomys*, and *Conilurus*; isolated in *Mesembriomys*; isolated or connected to cusp t5 in *Chiruromys*). Similarly, among the genera tentatively associated here as the "*Lenothrix* group," cusp t7 is connected to cusp t8 in *Lenomys* and *Pithecheir*, but to cusp t4 in *Lenothrix*.

Further evidence for the multiple derivations of cusp t7 is observed within certain extant genera and fossil lineages. In species of *Leptomys*, for example, cusp t7 is variable in

TABLE 4

Distribution of Various Derived Craniodental Character States across All Major Groups of Extant Murines and in Some of the Earliest Fossil Murinae from the Late Miocene

A "Y" means that the taxon shares the derived condition with *Corphyomys*, an "N" signifies a more plesiomorphic (i.e., less derived) condition, and a combination of N and Y means that members of the taxon possess both ancestral and derived character states. Whichever letter (Y or N) is written first represents the more typical condition in the group. Sources for the morphological information are mentioned in relevant parts of the main text.

	M^X with cusp t7	M_x with antero-labial cuspids	M_x with accessory labial cuspids	M_1 anteroconid elaboration	Enlarged posterior molars	M^X posterior cingular enlargement	Incisive foramen reduction	Stapedial artery reduction
Phloeomyini	Y	N/Y	N	Y	N/Y	N/Y	N/Y	Y/N
Micromys	Y	Y	Y	Y	N	N	N	N
Other Rattini	N	Y/N	Y/N	N/Y	N	N	N	N/Y
Chiropodomys	Y	Y	Y	Y	N	N	N	N
Australo-papuan Hydromyini	N/Y	N/Y	N/Y	N/Y	N/Y	N/Y	N/Y	N/Y
Philippine Hydromyini	N	N	N	N/Y	N	N	N/Y	N/Y
Vandeleuria	Y	Y	Y	Y	N	N	N	N
Murini	N	Y/N	N	N/Y	N	N	N/Y	N
Praomyini	N	Y/N	N/Y	N/Y	N	N	N	N
Apodemurini	Y	Y	Y	Y	N	N/Y	N	N
Malacomyini	N	N	N	N	N	N/Y	N	N
Millardini	N	Y	N	N	N	N/Y	N	N
Golunda	N	Y	N	N	N	N/Y	N	N
Other Arvicanthini	N/Y	Y/N	N	N/Y	N/Y	N/Y	N	N
Otomyini	N	N	N	N	Y	Y	N	N
Lenothrix	Y	Y	Y	Y	Y	Y	N	N
Lenomys	Y	N	Y	Y	Y	Y	N	N
Pithecheir	Y	N	Y	Y	Y	N	N	N
Hapalomys	Y	Y	Y	Y	N	N	Y	N
Vernaya	Y	Y	N	Y	N	Y	N	?
Antemus	N	Y	Y	N	N	N	?	?
Progonomys	N/Y	Y	Y	Y/N	N	N	?	?

its degree of differentiation from a posterior spur that emanates from cusp t4 (Musser et al., 2008). Within *Micromys*, the extant *M. minutus* and the majority of Plio-Pleistocene species show a well-developed cusp t7 with firm attachment to cusp t8 (reviewed by Storch and Dahlmann, 1995). However, in the earliest known species of *Micromys* (*M. chalceus* of the latest Miocene) cusp t7 is absent and its position is occupied either by a low cingulum between cusps t4 and t8 or by a ridge that emanates from cusp t8 but fails to reach cusp t4 (Storch, 1987). In the slightly younger *M. paricioi* an incipient cusp t7 is present on the cingulum or ridge in the majority of specimens (Mein et al., 1983; Adrover et al., 1988). Within the complex genus *Apodemus*, cusp t7 is variably connected to cusp t4 or cusp t8, though the latter is more usual (Michaux, 1969; Mártin Suárez and Mein, 1998; de Bruijn et al., 1999). Among fossil *Apodemus*, large dental samples often show morphological variation in cusp t7. For example, in *A. orientalis* of the late Miocene of Inner Mongolia (Storch, 1987), individual M1 can have a simple spur from t4, a discrete cusp t7 situated on a cingulum-like ridge that links cusps t4 and t8, or a discrete cusp t7 attached to cusp t8.

Judged on this suite of evidence, it seems certain that cusp t7 has evolved repeatedly among the extant Murinae, perhaps building on more primitively shared structures in this corner of the upper molar crown, including buttresslike ridges from cusps t4 and t8, and/or a basal cingulum passing between these cusps. Nevertheless, it remains pertinent to ask whether the detailed form and relations of cusp t7 in *Coryphomys* might reveal anything of its phylogenetic affinities. As described earlier, cusp t7 in *Coryphomys* is united high on the crown to cusp t8, but with a deep anterior groove giving definition to each cusp. In contrast, cusps t7 and t4 are separated by a deep cleft and there is no associated ridging or cingulum. Among extant murines, a fundamentally comparable morphology is observed in representatives of many tribes: *Crateromys*, *Batomys*, and *Carpomys* of the Phloeomyini; *Thamnomys* of the Arvicanthini; *Chiropodomys* (sister lineage to the Hydromyini; Rowe et al., 2008) and *Micromys* of the Rattini; and *Apodemus* and *Tokudaia* of the Apodemurini. Other murines that share an essentially similar cusp t7 include the potentially phyletically isolated *Hapalomys*, *Pithecheir*, and *Vernaya*, and the fossil *Spelaeomys florensis* (Musser, 1981b: 109, fig. 19). Probable further developments on this pattern are found in several other murine genera, including *Hyomys* where cusp t7 is amalgamated into a transverse lamina but identified by a narrow anterior groove. In *Phloeomys*, the laminae show no delimitation of component cusps and the evolutionary incorporation of a formerly discrete cusp t7 can only be inferred (Musser and Heaney, 1992). In contrast, species of *Bandicota* and *Nesokia* seem to have achieved a similar lamellate condition through expansion of a lingual spur from cusp t8 (Musser and Brothers, 1994: 20, fig. 9), though without producing a discrete cusp t7.

Absence of Labial Accessory Cuspids on Lower Molars: Hooijer (1965: 129) made special note of the absence of "accessory buccal tubercles" on the lower molars of *Coryphomys* and used this characteristic to focus his comparisons on two other genera of "giant" rats, *Mallomys* and *Crateromys*. Misonne (1969: 77) considered that the anterolabial cuspid (his cone Sv) of *Coryphomys* is "traceable in M_2 and M_3, though already included in Epd" (= metaconid). The new material described here confirms that the labial cuspids are consistently absent in both species of *Coryphomys*, except perhaps for a weak inflection of the anterior surface of the protoconids, as observed by Misonne (1969: 77).

The labial cuspids of murine lower molars are generally treated in two distinct categories. Cusps found at the anterolabial corner of each of m2 and m3 are widely regarded as serial homologs of the anterolabial cuspid of the m1 anteroconid (= cusp Sv of Vanderbroek's [1961] scheme) and as possible homologs of the anteroconid of certain other muroids (sensu Wood and Wilson, 1936; = anteroconulid of Hershkovitz, 1962: 75). In contrast, other cusps (usually called "cusplets") or cingular structures on the labial margin m2–3 and in all positions on the labial margin of m1 are regarded as potentially neomorphic, and thus

without traceable homologs in other groups of muroids. On these criteria, the anterolabial cuspids might be identified as a plesiomorphic feature of the murine dentition, whereas labial cusplets and cinguli as either ancestral or derived, depending on exactly when during murine evolution they first appeared. Clearly then, the significance of these two classes of structures must be treated as separate issues.

ANTEROLABIAL CUSPIDS: Among muroids, discrete cusps or elevated cinguli are found in an equivalent position on m2–3 to the anterolabial cuspids of Murinae in representatives of most major clades, including some Deomyinae (e.g., *Deomys*), Cricetomyinae, Sigmodontinae, Mystromyinae, Delanymyinae, Pteromyscinae, Cricetinae, Dendromurinae, and Lophiomyinae and Calomyscidae (Petter, 1966a, 1966b, 1967, 1975). In some cases, this position is occupied by a weak cingulum, as in some Deomyinae (e.g., *Acomys*, *Lophuromys*; Misonne, 1969; Petter, 1983). Only among members of Gerbillinae is there no cusp or cingulum in this position (Petter, 1959, 1973).

Among living Murinae, most major lineages include at least some taxa with well-developed anterolabial cuspids (table 4). In a few genera, these structures are replaced by a cingular ridge (*Haeromys*, Musser and Newcomb, 1983: 563, fig. 103; *Pithecheir* and *Lenomys*, Misonne, 1969). Absence of any cusp or cingulum in this position occurs in examples of seven tribal level clades, namely the Phloeomyini, Rattini, Hydromyini, Malacomyini, Murini, Arvicanthini, and Praomyini, but in all but one of these clades (the monogeneric Malacomyini; Misonne, 1969), there is intragroup variation in regard to this character. Within Phloeomyini, *Carpomys* spp. are atypical in having well-developed anterolabial cuspids (Musser and Heaney, 1992). Among Rattini, anterolabial cuspids are present in the basal lineage *Micromys* (Misonne, 1969) and in many other genera including *Saxatilomys* (Musser et al., 2005), *Bandicota* (Musser and Brothers, 1994), *Sundamys* (Musser and Newcomb, 1983), *Taeromys* (Musser and Newcomb, 1983), *Bunomys* (Musser and Newcomb, 1983; Musser, 1991), *Bullimus* (Musser and Newcomb, 1983), *Komodomys* (Musser and Boeadi, 1980), *Paruromys* (Musser and Newcomb, 1983), *Tarsomys* and *Limnomys* (Musser and Heaney, 1992), and *Rattus* itself (e.g., Musser, 1981a, 1986; Musser and Heaney, 1992; Musser and Holden, 1991). The cuspids are absent in all species of *Maxomys*, *Leopoldamys* and *Niviventer* (Musser, 1981a; Musser and Newcomb, 1983), in *Crunomys* (Musser, 1982a) and in *Nesokia* (Musser and Brothers, 1994), and they are variably present or absent in different species of *Berylmys* (Musser and Newcomb, 1983). Anterolabial cuspids are also variable in occurrence within each of Arvicanthini, Murini, and Praomyini. For example, they are well developed in most arvicanthins but reduced in *Golunda* and *Mylomys* (Musser, 1987), and some *Arvicanthis* (Misonne, 1969). Similar variation is present among praomyins (for details see Lecompte et al., 2002a) and even within the genus *Mus* (often absent in members of subgenus *Nannomys*; Misonne, 1969). The majority of Australo-Papuan hydromyins and all Philippine representatives lack anterolabial cuspids. However, these cuspids are well developed in each of *Pogonomys*, *Chiruromys*, and *Hyomys*.

Where anterolabial cuspids are altogether absent, this is generally associated with simplification of molar patterns, either through production of lamellae (e.g., *Melomys*, *Apomys*) or of basin-shaped structures (e.g., *Hydromys*, *Chrotomys*). However, the presence of striking exceptions (e.g., well-developed cuspids present in *Hyomys*, with highly lamellate molars; and absent in *Mesembriomys*, with very cuspidate molars) makes it clear that any functional association is far from simple.

Anterolabial cuspids are present on m2–3 in almost all Miocene Murinae. In *Antemus chinjiensis* there is a prominent cingular ridge on each tooth, deeply separated from the protoconid at the labial end (Wessels et al., 1982; Jacobs et al., 1989, 1990). Well-developed anterolabial cuspids are a near constant feature in *Progonomys* and later Miocene genera including *Huerzelerimys*, *Occitanomys*, *Orientalomys*, *Linomys*, *Karnimata*, *Parapodemus*, *Apodemus*, *Rhagapodemus*, and *Hansdebruijnia* (Storch, 1987; Mein et al., 1993; Martín Suárez and Mein, 1998; Storch and Ni, 2002). One exception is

Leilaomys of the late Miocene of China, in which there is a cingular ridge but no discrete cusp (Storch and Ni, 2002).

OTHER LABIAL CUSPLETS AND CINGULI ON LOWER MOLARS: Accessory labial cusplets and cinguli are found on the lower molars of many Murinae and they also occur in various other muroid subfamilies (e.g., Deomyinae; Cricetomyinae, Mystromyinae, Dendromurinae, Sigmodontinae; Petter, 1966a; Misonne, 1969) and in some of the earliest known relatives of Muroidea (e.g., *Nonomys*; Emry, 1981). In all taxa, these structures are positioned below the level of the principal cuspids and may thus function initially as cinguli, with a possible role in protecting the gums. With increasing wear, the cusplets become incorporated into the occlusal surface and thenceforth serve to increase both the area, and in some cases the complexity, of the lophids.

Jacobs (1978: 29) alluded to the possibility that the posterolabial cusplet (C1; Cv5 of Misonne, 1969) of m1 may be homologous across Murinae, and later offered a firmer opinion: "We believe that the development of C1 is fundamental to the development of the murid masticatory system, as is the addition of lingual cusps in upper molars" (Jacobs et al., 1989: 164). More anterior cusplets on m1 (C2, C3) and all cusplets on m2–3 tend to be more variable in occurrence, both within species and between closely related forms (Misonne, 1969).

Labial cusplets and/or cinguli are absent in both species of *Coryphomys*. They are similarly absent in all members of several tribal lineages (table 4), notably the Phloeomyini (Musser and Heaney, 1992), Murini and Malacomyini (Misonne, 1969), and in all Philippine and Australo-Papuan representatives of the Hydromyini (Misonne, 1969; Musser and Heaney, 1992), but present in at least some members of the Rattini (e.g., *Leopoldamys*, Musser, 1981a), many *Rattus* species; Musser, 1981a, 1986; Musser and Holden, 1991), in Millardini (Misonne, 1969), in the majority of Praomyini and Arvicanthini (Misonne, 1969; Lecompte et al., 2002a) , and in various unallocated genera (e.g., *Hapalomys*, Musser, 1972; *Vernaya*, Misonne, 1969), and members of the "*Lenothrix* group" (Misonne, 1969; Musser and Newcomb, 1983). Among fossil Murinae, they are present in most genera of Miocene age, including the earliest recorded taxa included within *Antemus* (Wessels et al., 1982; Jacobs, 1977; Jacobs et al., 1989, 1990) and *Progonomys* (Mein et al., 1993).

The mosaic pattern of distribution among the various murine tribes of both the anterolabial cuspids and the accessory cusplets, together with their variable occurrence even within certain genera, provides incontrovertible evidence for their multiple acquisition and/or loss within Murinae.

ELABORATION OF THE ANTEROCONID OF m1: The presence of four cuspids on the anterior part of m1 of *Coryphomys buehleri* was touted by Stehlin and Schaub (1951) as a unique development within Murinae and the most distinctive feature of the genus. Hooijer (1965) attempted to show that the accessory cuspids were highly variable in *C. buehleri*, but his referred specimens included a specimen of Mahoney's Genus A and examples of both species of *Coryphomys*. More usefully, Misonne (1969: 77) noted that a division of the anterior cusp of the anteroconid of m1 could be found in other murines including "some *Chiropodomys*." Our greatly expanded series of *Coryphomys* show that an anterocentral cuspid is consistently present in both species of the genus. However, it also demonstrates considerable variation in the pattern and frequency of subdivision of this cusp, with a divided cusp less common in *C. musseri* than in *C. buehleri*.

Misonne (1969: 68) included the anterocentral cuspids (as cusp "Sm") in his reconstruction of the ancestral lower molar of Murinae. This view is the presence of well-developed anterocentral cuspids in many fossil murines, including some of the earliest species of *Progonomys*. However, anterocentral cuspids are absent in all other groups of muroids, including the immediate relatives of Murinae (Gerbillinae and Deomyinae), and they are also absent in the earliest recognized murine *Antemus chinjiensis* (Wessels et al., 1982). For these reasons, we remain unconvinced regarding the evolutionary polarity of this feature among extant Murinae, even though evidence for its early appearance within this group is incontrovertible.

The distribution of anterocentral cuspids among extant murines (table 4) makes it clear that these structures have been acquired or lost on multiple occasions. For example, the cuspid is variably present or absent among different genera among the Australo-Papuan Hydromyini (present in *Pogonomys*, *Chiruromys*, and *Hyomys*; absent in all other genera; Misonne, 1969) and within Arvicanthini (present in *Oenomys*, *Grammomys*, *Thamnomys*, *Thallomys*, *Hybomys*; very small or absent in *Arvicanthis*, *Pelomys*, *Golunda*; Misonne ,1969; Musser, 1987) and it is similarly variable between species within the genus *Rattus* (e.g., Musser and Holden, 1991). As a rule, taxa with an anterocentral cuspid also tend to have cuspidate molar patterns; however, there are notable exceptions to this (e.g., *Hyomys* has highly lamellate molars).

Variation in the morphology of anterocentral cuspids also suggests the possibility of multiple derivations of this structure. We have not attempted an exhaustive study of this structure but note the following major variants:

(1) anterocentral cuspid attached by a ridge, or "stalk," to the anterolabial cuspid. This condition is observed in *Hyomys* and some *Thamnomys* among living murines, in the extinct *Spelaeomys* of Flores (Musser, 1981b), and in some *Apodemus* and *Rhagapodemus* (e.g., Martín Suárez and Mein, 1998) among fossil taxa. The majority of specimens of both *Coryphomys* species conform to this pattern, with the variable subdivision of the anterocentral cuspid as a further elaboration. A possible precursor to this condition (or its relictual expression) is an anteriorly directed spur from the anterolabial cuspid, such as occurs in *Anonymomys*, *Crunomys*, *Archboldomys*, *Limnomys*, and some *Taeromys* (Musser, 1969, 1981a, 1982b; Musser and Heaney, 1992).

(2) anterocentral cuspid attached by a ridge, or "stalk," to the anterolingual cuspid. This condition is observed in *Lenothrix*, *Pogonomys*, *Grammomys*, *Thallomys*, and some *Thamnomys* among extant murines (Misonne, 1969) and in various extinct murines including *Ratchaburimys* (Chaimanee, 1998) and some *Progonomys*, *Apodemus*, and *Huerzelerimys* (Mein et al., 1993). An anteriorly directed spur from the anterolingual cuspid, analogous to the structure noted above, occurs in *Lenomys*, *Palawanomys*, *Tryphomys*, *Komodomys*, some *Rattus*, and some *Taeromys* (Musser, 1981b; Musser and Newcomb, 1983; Musser and Holden, 1991).

(3) anterocentral cuspid or cuspids that occupy a more isolated position between the anterolabial and anterolingual cuspids. In this pattern, the anterocentral cuspids either stand alone (e.g., *Hapalomys*, *Micromys*, and *Oenomys* among extant murines [Misonne, 1969; Musser, 1972] and *Rhagamys*, some *Rhagapodemus*, some *Paraethomys* among fossil murines [Castillo Ruiz, 1991; Martín Suárez and Mein, 1998]) or they are linked by a cingulum to each of the principal anteroconid cusps, thereby enclosing an anteroconid basin (e.g., *Chiropodomys*, *Vandeleuria*, *Haeromys*; Musser, 1979; Musser and Newcomb, 1983: fig. 103). Subdivision of the anterocentral cuspid also occurs as a variant of this pattern, as noted by Misonne (1969) for *Chiropodomys* and illustrated by Chaimanee in specimens referable to this genus (Chaimanee, 1998: pl. 5, fig. 4) and to *Hapalomys* (Chaimanee, 1998: pl. 3, fig. 4).

(4) anterocentral cusp in a central position but attached by a well-developed "stalk" to the point of union of the anterolabial and anterolingual cuspids. This pattern is less frequently observed but we note possible examples in *Hybomys* and in *Pithecheir*, including the fossil *P. peninsularis* (Chaimanee, 1998: pl. 4, fig. 10).

(5) anterocentral cuspid expanded in size and forming the anterior half of a distinctive, cordate anteroconid. This pattern, found only among members of the Phloeomyini, was described and illustrated by Musser and Heaney (1992: 61, 97–99: fig. 64). A variant on this pattern has the anterocentral cuspid subdivided into two subequal units (e.g., *Carpomys melanurus*; Musser and Heaney, 1992: fig. 64D). A cingulum and centrally located cuspid, as described above for *Haeromys* and *Chiropodomys*, may be a suitable precursor for the phloeomyin anteroconid morphology.

Apart from the unusual condition of being sometimes divided, the form of the anteroconid in *Coryphomys* is thus reproduced precisely in several extant murines spread across various major lineages, and paralleled more generally in many others. Like other dental characters assessed here, this feature does not provide unambiguous evidence of the phylogenetic affinities of *Coryphomys*.

Relative Sizes of the Posterior Molars: Proportionally large posterior molars (table 3), such as occur in *Corphyomys* (M3 of *C. buehleri* is 92% of M2 length; 90% in *C. musseri*), are traditionally treated as a primitive feature of dental morphology among Murinae (Ellerman, 1941: 44–45; Misonne, 1969; Musser and Newcomb, 1983). Apart from members of Otomyini, in which the M3 has been massively elongated through serial addition of extra laminae (Denys et al., 1987; Sénégas and Avery, 1998), the longest M3 among extant murines (relative to M2 length; data from Misonne, 1969: 70) occurs in a variety of taxa identified by Ellerman (1941) and Misonne (1969) as dentally archaic forms, including the Australo-Papuan hydromyin genera *Hyomys* (100%), *Pogonomys* (83%), and *Anisomys* (70%), the arvicanthin *Thamnomys rutilans* (81%), and the phylogenetically unassigned murines *Lenomys* (95%) and *Lenothrix* (90%). In general, taxa with a proportionally larger M3 also have an M1 that is relatively short compared with M2, though the relationship is far from straightforward.

Misonne (1969: 52–53) interpreted the trend toward lengthening of M1 and shortening of M3 as a means of shifting the entire molar series forward into a position of improved mechanical advantage (with M2 treated as effectively invariant in both relative size and position). An underlying assumption is that loss of the posterior premolar in basal muroids initially caused a posterior displacement of the cheek-tooth battery relative to the position of the combined P4–M3 of other rodents. Several objections can be raised against this model of molar evolution in Murinae. The first of these relates to the nature of molar gradients in both in fossil murines and outgroup taxa. In *Antemus chinjiensis*, the earliest fossil murine, the third molars (as reported by Wessels et al., 1982; Jacobs et al., 1989, 1990) are small, with a length that is only 68% that of the M2. Relatively small third molars are also reported from a variety of other Miocene murines, including *Huerzelerimys minor* (66%–71% in four samples; Mein et al., 1993: table 1, pl. 1) and *Rhagapodemus primaevus* (75%; Martín Suárez and Mein, 1998: fig. 3). Similarly, among each of the immediate outgroups to Murinae (Deomyinae and Gerbillinae), the third molar is moderately small (e.g., *Acomys* spp. in Deomyinae; Denys and Michaux, 1992; Denys et al., 1992) to very small (all Gerbillinae [Petter, 1959, 1973]; *Lophuromys* and *Uranomys* in Deomyinae [Denys and Michaux, 1992]). Further afield within Muroidea, relative third molar size varies considerably within each of Nesomyidae (e.g., small in Mystromyinae, Dendromurinae, and Petromyscinae; larger in Cricetomyinae and Nesomyinae (Petter, 1966a, 1967, 1975; Rosevear, 1969; de Graaff, 1981) and Cricetidae (e.g., small in Sigmodontinae; large in Cricetinae [Stehlin and Schaub, 1951; Gaunt, 1961; Weksler, 2006]), making it difficult to decide on a likely evolutionary polarity. At any rate, the combined evidence of the murine fossil record, the condition in the immediate sister lineages to Murinae, and the variability among other muroid lineages, seems to weigh against any simple acceptance of a proportionally large ancestral M3 within Murinae. Indeed, a case could well be made for the opposite view, with posterior molar enlargement being a derived character state within Murinae.

Two other objections to Misonne's model emerge out of recent studies of laboratory mice, based on the condition of the teeth in various "mutant" mouse strains and on direct experimental manipulation of the tooth-forming tissues. The first relates to the assumption that the three molars of a typical murine correspond in simple fashion to the M1–3 of a nonmuroid rodent, hereby implying loss of the posterior premolar. As argued by Peterkova et al. (2005, 2006), the ontogenesis of these teeth suggests that the anterior portion (anteroconid) of the first molar in *Mus*, rather than being an evolutionary neoformation, instead represents the posterior premolar of other rodents. A key element of this case is the observation that the anterior part of m1 originates as a discrete dental placode that subsequently unites with the remainder of m1 during normal development but either remains separate or fails to develop in various mutant strains. This observation differs from previous suggestions that saw the M1 of muroid rodents as equivalent in its entirety to the

posterior premolar of other rodents (e.g., Johnson, 1952; Sheppe, 1964).

Whether or not this new model of murine cheektooth homology is correct, it does serve to introduce the second objection that concerns the nature of the ontogenetic processes that regulate relative molar dimensions. As in other mammals, the murine cheekteeth develop sequentially, each successive molar passing through essentially the same processes but with a time delay from front to back of the jaw. Experimental manipulation of this process suggests that the initiation of posterior molars is determined by a balance between mesenchymal activation and intermolar inhibition, with a number of different signaling molecules involved (Kavanagh et al., 2007). Furthermore, it appears that the final size of each successive molar is tightly determined by its activation schedule, and that such effects are cumulative. Far from being the invariant tooth of Misonne's (1969: 52) conception—"wedged between M1 and M3 ... [so that it] ... cannot modify its length" —the murine M2 is a dynamic entity that owes its size and shape to the events that shape the M1, and in turn, has a powerful influence over final size and shape of the M3. Illustrating this point, Kavanagh et al. (2007) note that initiation of the M3 fails altogether when the M2 falls below half the size of M1 (a pattern paralleled among extant Murinae), whereas supernumerary molars tend to form when the M3 approximates the M2 in size. Supernumerary molars are very rare among extant murines and it is thus of particular interest that one specimen of *Coryphomys musseri*, a taxon with almost equal-sized m2–3, has a well-developed alveolus for a single rooted but sizeable fourth lower molar.

Kavanagh et al. (2007) postulated that relatively large posterior molars among murines are associated with specialized herbivory, whereas reduction and even loss of posterior molars are associated with specialized faunivory. This makes good sense in terms of the functional demands of each dietary adaptation, and it comes as no surprise that more herbivorous rodents also have a greater degree of coronal complexity than animal-eating rodents (Evans et al., 2006). Selection for increased masticatory efficiency, as conferred by increases in occlusal area and/or complexity, could lead to rapid phenotypic adjustment, provided of course that the ontogenetic system displays sufficient intrapopulational variability.

Expansion of the Posterior Cingulum on Each Upper Molar: A posterior cingulum (teloloph or Z of Misonne, 1969; cusp t10 of Lavocat, 1962; cusp t12 of Thaler, 1966) occurs in many living murines and is a near constant feature in the earliest fossil members of this group (Wessels et al. 1982; Jacobs et al., 1989, 1990; Mein et al., 1993). When present, it usually originates on the posterolabial surface of cusp t8 (Thaler, 1966) and takes the form of a cingular shelf behind cusp t9. A topologically identical structure is present in some Gerbillinae (e.g., *Gerbillus* but not *Taterillus*) and some Deomyinae (present in *Acomys* and *Deomys*, absent in *Lophuromys*), and in many other muroids (Stehlin and Schaub, 1951), and there can be little doubt that it represents a plesiomorphic feature among muroids in general. In the great majority of taxa, it occurs only on M1–2.

In *Coryphomys* the posterior cingulum of M1–2 is modified in two ways: (1) by a labial migration of its attachment to the point of union of cusps t8 and t7; and (2) by elevation and thickening of the cingulum to form a "posteroloph." These developments disrupt the primitive contact between cusp t8 of each of M1–2 and cusp t5 of M2–3, respectively, and also create a deepened "posterior fossette" between the posterior cingulum and cusp t9. A further specialization observed in *Coryphomys* is the addition of a substantial posterior cingulum to the rear of M3.

Among extant murines (table 4), these developments are most completely paralleled in *Carpomys* of the Philippines (Misonne, 1969; Musser and Heaney, 1992: 66, fig. 34). The structural resemblance between the taxa is considerable, even to the presence of a discrete, elevated posterior cingulum on M3, and is all the more remarkable for the general lack of close resemblance between *Coryphomys* and *Carpomys* in other details of molar morphology. For whereas the molars of *Coryphomys* are hypsodont and highly cuspidate, those of *Carpomys* are brachyodont and rather lamellate.

Hyomys of New Guinea is another murine genus with an enlarged posterior cingulum on each of M1–3 (Misonne, 1969). However, in this case, the structure shows a lesser degree of lingual displacement of cingular attachment than in *Coryphomys*, especially on the anterior molars, and a progressive increase in the size of the cingulum from M1 to M3. These two genera also share molar hypsodonty, but the molars of *Hyomys* are highly lamellate, rather than cuspidate as in *Coryphomys*. In other murine genera (e.g., *Vernaya*, *Tokudaia*, and *Chiruromys*; Misonne, 1969) enlargement of the posterior cinguli on M1–2 occurs without alteration of the point of attachment to cusp t8.

A posterior cingulum is present on the rear of M3 in a variety of other murines including *Lenothrix*, *Lenomys*, *Spelaeomys*, *Anisomys*, *Chiruromys*, and *Chiropodomys* (Misonne, 1969; Musser, 1981b; Musser and Newcomb, 1983). In every instance, the new structure is isolated from cusp t8, as it is in *Coryphomys*. This structure is largest in *Anisomys*, *Lenothrix*, and *Spelaeomys*.

The widely dispersed phylogenetic distribution of murine taxa showing enlargement and elaboration of the posterior cingulum leaves no doubt that this has occurred independently at least six times—in *Carpomys*, *Hyomys*, *Anisomys*, *Chiruromys*, *Chiropodomys*, and *Tokudaia*—and very likely on other occasions.

Shortening and Narrowing of the Incisive Foramen: The shortness and narrowness of the incisive foramen is a noteworthy feature of palatal morphology in *Coryphomys*. Among extant murines (table 4), a comparable condition is observed in *Phloeomys* of the Philippines and in several New Guinean hydromyins (*Anisomys*, *Hyomys*, and some *Uromys*). Similarly short but somewhat broader incisive foramina are observed in a larger number of extant murines including some Philippine Hydromyini (*Rhynchomys* and *Chrotomys*; Musser and Heaney, 1992: 75, fig. 42), a variety of other New Guinean hydromyins (*Pseudohydromys* [sensu Helgen and Helgen, 2009], *Microhydromys*, *Hydromys*, *Baiyankamys*, *Parahydromys*, *Chiruromys*, and *Pogonomys*), and the subgenus *Coelomys* of *Mus*. All other extant murines have longer incisive foramina, with more extensive penetration into the palatal lamina of the maxilla (e.g., Phloeomyini: Musser and Heaney, 1992); Praomyini: Lecompte et al., 2002b; Australo-Papuan Hydromyini: Tate, 1951; Flannery, 1995a, 1995b; Philippine Hydromyini: Musser and Heaney, 1992; Otomyini: Taylor et al., 2004; Rattini: Musser, 1981a, 1981b, 1986, 1991; and Musser and Newcomb, 1983). Information on palatal structures is available for only a small number of fossil murines (*Stephanomys* and *Malpaisomys*: López-Martínez et al. (1998) and not for any of the earliest members of the group.

Other groups of muroids typically have elongate incisive foramina that penetrate far into the maxilla (Wahlert, 1985: 314; also Quay, 1954, for Microtinae; Hershkovitz, 1962 for Phyllotinae; Carleton, 1980, for Neotominae and Peromyscinae; Voss, 1988, for Icthyomyinae; Weksler, 2006, for Sigmodontinae; De Graaff, 1981, and Rosevear, 1969, for Dendromurinae, Mystromyinae, Cricetomyinae, Petromyscinae, Gerbillinae). However, outside of Muroidea, short and narrow foramina are widely distributed among sciuromorph and hystricomorph rodent lineages (Wahlert 1985), and they also feature in the earliest members of Rodentia for which cranial remains are known (e.g., species of *Paramys* and *Sciuravus*; Wahlert, 1974).

To our knowledge, the anatomical and evolutionary significance of variation in the incisive foramina among muroid rodents has not been previously been reviewed. Specific anatomical information on this region comes from a variety of sources, including the general anatomy of *Rattus norvegicus* (Greene, 1968), a more detailed account of this region in the microtine *Ondatra zibethica* (Quay, 1954), and clinical studies of the anatomy of the vomeronasal organ and nasopalatine duct in laboratory murines (Vaccarezza et al., 1981; Salazar and Quinteiro, 1998). From these sources and our own observations, it is clear that the paired incisive foramina of muroids are largely floored by a dense fibrous membrane. At around the level of the premaxillary-maxillary suture this membrane is perforated by the paired nasopalatine ducts that pass from the palate to the vomeronasal organs, and by

small blood vessels that accompany these ducts to supply the mucosa of the nasal chamber.

In *Ondatra* the portion of the incisive foramina that lies behind the nasopalatine duct is underlain by an extensive venous plexus, with a separate, smaller plexus lying anterior of the duct (Quay, 1954). Though the function of these venous plexi in *Ondatra* has not been investigated, their positioning directly below the membrane suggests a possible heat exchange function, either to cool blood or to heat air within the nasal chamber. There is no mention of similar vascular specializations in general accounts of *Rattus norvegicus* (Greene, 1968) or in any other muroid taxon. However, it would seem reasonable to expect the elongate foramina of the majority of muroids to be associated with similar vascular features.

The broad evolutionary pattern of the incisive foramina thus seems to involve elongation of these structures as a novel morphological development, probably early during the evolution of Muroidea (although the foramina are not elongate in the early Oligocene muroid *Nonomys simplicidens*; Emry, 1981). Within Murinae, a return to short and narrow incisive foramina, as in *Coryphomys*, presumably represents a derived condition, albeit an evolutionary reversal to a more primitive rodent condition. As noted above, this condition is relatively rare within Murinae and its occurrence might be expected to shed light on phylogenetic relationships. Two unrelated murine lineages possess a similar derived condition for this character: the Philippine genus *Phloeomys* (other Phloeomyini have elongate incisive foramina); and several members of the Australo-Papuan Hydromyini (species of *Anisomys*, *Hyomys*, and *Uromys*). Recent molecular studies by Rowe et al. (2008) indicate that *Anisomys*, *Hyomys*, and *Uromys* are not particularly closely related within Hydromyini, and any special similarity in the form of the incisive foramina is presumably due to homoplasy. However, since the majority of Hydromyini, including both Australo-Papuan and Philippine members, show significant shortening of the incisive foramina (albeit with less narrowing, a condition that is also present in subgenus *Coelomys* of *Mus*), it might be concluded that the more meaningful comparison is with the Hydromyini as a whole, rather than with any specific lineage.

Reduction of the Stapedial Arterial System: The stapedial artery is present in early embryological stages in all mammals, except perhaps for the echidna, and its principal branches accompany each of the three divisions of the trigeminal nerve to the supraorbital, infraorbital, and mandibular regions (Wible, 1987). Few adult mammals retain this primitive pattern. Instead, it is modified in various ways during later ontogeny by anastomotic "capture" of the peripheral distribution by components of either the internal or external carotid artery. In many groups of mammals, including all marsupials and most ungulates (for a full treatment, see Wible, 1987, 1990), this process leads to complete replacement of the stapedial system, including ablation of the stem or "proximal" stapedial artery.

All rodents probably retain the stem of the proximal stapedial artery, with branches to the muscles and mucosal tissues of the middle ear (Bugge, 1980). In most rodent lineages, the proximal stapedial artery also retains at least some of its wider peripheral distribution. In these taxa, the vessel crosses the promontorium to pass through the obturator foramen of the stapes, then through the roof of the tympanic cavity to enter the cranial cavity before dividing into its superior and inferior rami (Wible, 1987). The ramus inferior exits the cranium almost immediately via the pyriform fenestra (= middle lacerate foramen of Wahlert, 1974). Among most murids, the ramus superior loses all or most of its peripheral distribution in the orbital fossa and nasal cavity due to anastomotic capture of these branches by branches of the external carotid artery (Bugge, 1980: 325, fig. 5; 1985). The ramus superior in these taxa either is ablated entirely or reduced to a mandibular supply (described by Bugge, 1980, for a murine [*Apodemus*] and a gerbilline [*Tatera*]). Exceptionally, in *Batomys russatus* of the Philippines, a patent ramus superior grooves the endocranial surface of the squamosal and alisphenoid bones, then exits the cranial cavity into the orbital fossa via a sphenofrontal foramen (Musser et al.,

1998a: 45, fig. 28). Although these relations are identical to those observed in many other groups of muroid rodents, Musser et al. (1998: 44–45) speculated that this "may be a new acquisition (reversal of a character state) rather than retention of a primitive character." We agree with this interpretation.

The osseous expression of the inferred primitive murid arterial pattern includes a large stapedial foramen enclosed between the petrosal and bullar process of the ectotympanic, a well-marked stapedial groove that traverses the promontorium ventral to the fenestra cochleae and terminates at the fenestra vestibuli, an enlarged facial canal (carrying both the facial nerve and the proximal stapedial artery), and a short "stapedial artery canal" (sensu Wahlert, 1974) that diverges at the level of the primary facial foramen and emerges on the intracranial surface of the petrosal. The extracranial course of the ramus inferior is usually marked by a groove on the posterior surface of the alisphenoid bone, medial to and paralleling the pterygoid ridge, and leading to the posterior opening of the alisphenoid canal (which shares a common dorsal margin with the primary foramen ovale). Loss of the ramus superior is indicated by the absence of an endocranial sulcus and of the sphenofrontal foramen.

Less commonly among muroids, all major peripheral elements of the embryonic stapedial artery appear to be annexed by the external carotid system. To date, the detailed anatomy of this arrangement has not been documented for any taxon. However, its occurrence is reliably inferred from the reduction in size of each of the stapedial foramen, the promontorial groove, and the "stapedial artery canal," and from remnants of dried vessels preserved on some crania (e.g., Musser, 1982b). This pattern is also indicated by changes in the pattern of vascular grooving on the alisphenoid (Musser, 1982b; Musser and Heaney, 1992).

The petrosal bones referred to *Coryphomys* advertise a relatively extreme version of this derived arterial pattern. The small caliber of the proximal stapedial artery is evident both from the indistinct promontorial groove and the slitlike nature of the intraosseous canals for the branches of the ramus inferior. Elsewhere within Murinae (table 3), a similar degree of reduction of the proximal stapedial artery is reported in the following taxa: (1) most members of the phloeomyin genera *Crateromys*, *Batomys*, *Carpomys* (Musser and Heaney, 1992: 61; the sole exception is *Batomys russatus*, Musser et al., 1998a: 44–45, figs. 27–28); (2) most species of the Philippine hydromyin genus *Apomys* (except for *A. datae*; Musser, 1982b); (3) species of the shared Philippine and Sulawesian rattin genus *Crunomys* (Musser, 1982a); (4) various Australo-Papuan hydromyins including species of *Leptomys*, *Xeromys*, and *Pseudohydromys* (sensu Helgen and Helgen, this volume), and species of *Lorentzimys* and *Mammelomys* (Musser and Heaney, 1992: 87); and (5) *Sundamys maxi* within the Rattini (Musser and Newcomb, 1983: fig. 56). The derived arterial pattern also features in a smattering of other muroid lineages, including the Neotropical sigmodontines *Rheomys hartmanni* (Voss, 1988: 296, fig. 18D), *Ichthyomys* spp. (Voss, 1988: 298) and *Oryzomys palustris* (Musser and Carleton, 1989: 38, fig. 21A).

The distribution of stapedial reduction as a character among muroid rodents and within Murinae in particular suggests that it has evolved on multiple, independent occasions. Accordingly, this feature is of ambiguous value in determining the wider phylogenetic affinities of *Coryphomys*.

Enlargement and Elaboration of the Maxillary Sinus: The large and internally complex maxillary sinus complex appears to be one of the more unusual morphological characteristics of *Coryphomys*. Indeed, comparisons thus far have failed to identify a comparable morphological development in any other genus of murine, though it must be emphasized that a full comparative survey of this region in other murines and other muroids remains to be made, given that this part of the cranium is accessible only in heavily damaged specimens or through use of internal imaging technology. Nevertheless, the maxillary structures are sufficiently interesting to warrant some preliminary discussion of their comparative anatomy and their possible functional significance.

The anatomy of this region of the cranium is partially documented for each of the two primary laboratory murines, *Rattus norvegicus* and *Mus musculus*, and these sources provide a sound basis for interpreting the condition in other murines including *Coryphomys*. In *Rattus norvegicus*, for which we have the most detailed account of the development and adult histochemistry of the maxillary sinus (Vidic 1971; Vidic and Greditzer, 1971; Uraih and Maronpot, 1990), the dorsal surface of the maxilla features a broad nasopharyngeal sulcus and a shallow, undivided maxillary sinus depression bounded medially by a raised septum, and posteriorly and laterally by low ridges (the lateral ridge is continuous posteriorly with the orbital lamina of the maxilla; a comparable anatomy is illustrated in fig. 21A–B for *Rattus rattus*). A broad infraorbital sulcus separates the lateral ridge from the zygomatic plate. No internal bony septa are present but the floor of the maxillary sinus complex is crossed by a broad neurovascular sulcus that transmits nasal branches of the infraorbital artery and the anterior superior alveolar nerve (Greene, 1968: 185, fig. 213). The generative capsule of the incisor hangs suspended above the anterior third of the depression, but leaves no osseous impression. The posterior two-thirds of the depression in *R. norvegicus* are occupied by the maxillary sinus (sensu Jacob and Chole, 2006), a "paranasal" chamber that communicates with the nasal cavity proper via an aperture, or "ostium," situated between the posterior end of the maxilloturbinate and the anterior end of the ethmoturbinates (Broman, 1921; Negus, 1958; Vidic and Greditzer, 1971; Jacob and Chole, 2006). The maxillary sinus is lined with submucosal glands and it is this feature that distinguishes it from all other spaces within the nasal cavity (Jacob and Chole, 2006).

Glandular tissue of the maxillary sinus is varied in type and origin. In *Rattus norvegicus*, the sinus represents an invagination of the lateral nasal wall at day 16 of embryonic development (Vidic, 1971). Development of the space is closely associated with differentiation and expansion of two glands, the lateral nasal gland, a body of serous tissue with a major duct that drains anteriorly into the nasal vestibule, and the maxillary gland, made up of numerous serous, tubulo-alveolar glands that drain directly into the posterior maxillary recess. In the early stages of development the two glands occupy discrete areas, the lateral nasal gland situated below the anterior maxillary recess, and the maxillary gland positioned above the posterior recess. However, both glandular masses expand to such a degree that the entire submucosa of the sinus eventually becomes infiltrated, and the topographical limits of each gland are blended.

Secretions of the serous maxillary gland contain a high concentration of water and probably serve to humidify air in the upper respiratory tract (Bojsen-Møller, 1964). In contrast, the lateral nasal gland secretion contains a greater proportion of mucosubstances that regulate fluid exchange between environment and tissues and protect epithelial cells against penetration by bacteria and other foreign particles. Targeted delivery of these secretions to the nasal vestibule suggests a primary protective function in murines.

The maxillary sinus complex of *Coryphomys* differs from that of *Rattus* and *Mus* in two main respects. The first is the considerable expansion of the complex in each of the medial, lateral, and posterior directions. Medial expansion results in the marked narrowing of the nasopharyngeal sulcus, while lateral expansion leads to the displacement of the orbital lamina of the maxilla onto the zygomatic plate, with consequent narrowing of the infraorbital sulcus. The second is the subdivision of the maxillary sinus complex by conspicuous bony septa. Among other murines surveyed to date, the great majority show only small departures from the maxillary sinus complex of *Rattus* (fig. 21A–B). The most notable departure, and the closest match with the condition in *Coryphomys*, is found in *Mallomys* (fig. 21C). In this taxon, the maxillary sinus is expanded laterally, resulting in a shift of the lateral wall of the maxillary sinus complex onto the root of the zygomatic arch and a marked narrowing of the infraorbital sulcus, and posteriorly, to a point level with the rear of M1. Unlike *Coryphomys*, there is no medial expansion of the maxillary sinus complex in *Mallomys*,

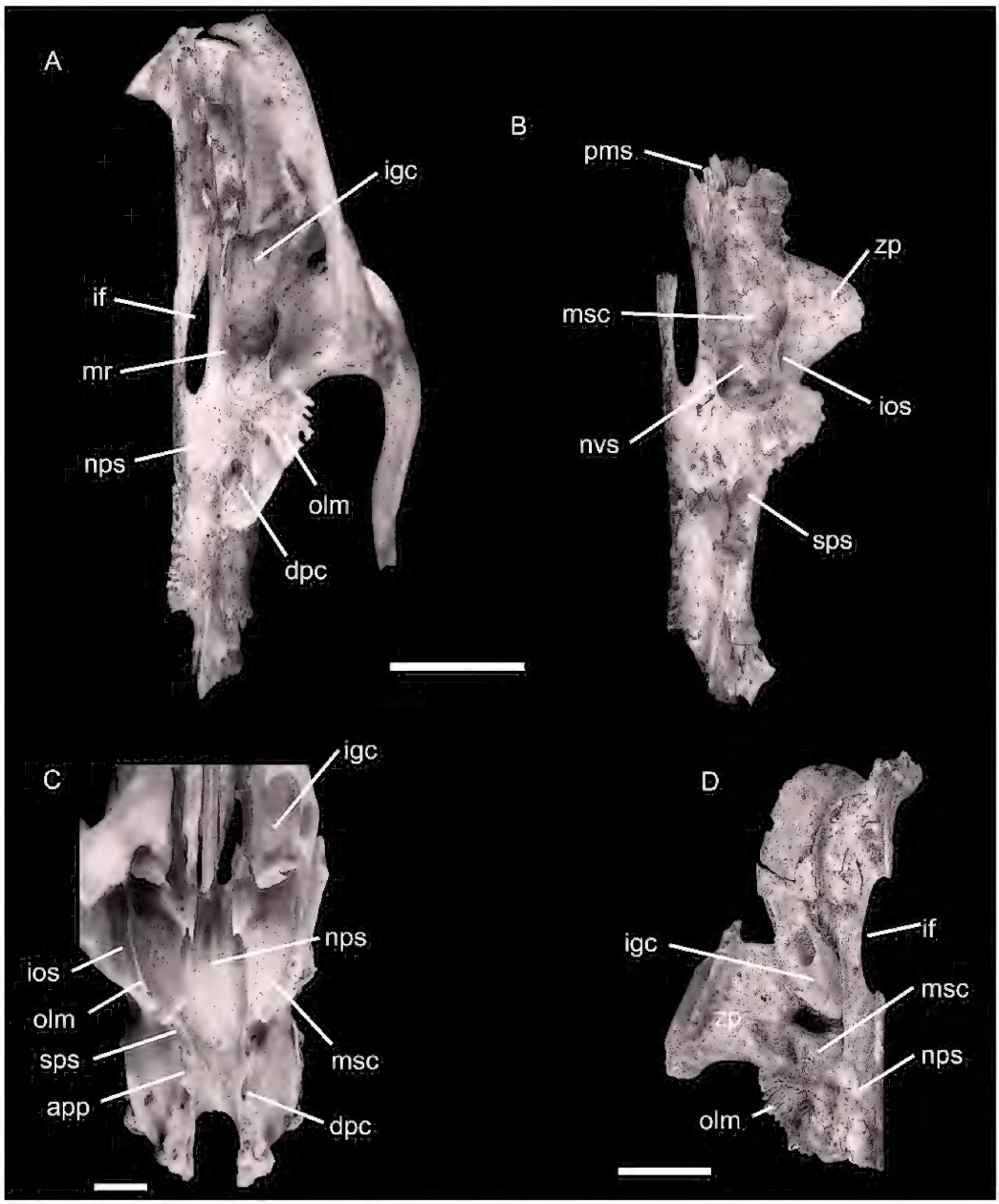

Fig. 21. Anatomical features of the maxilla and surrounding bones in four extant murine species. **A,** *Rattus rattus* (CM35627), right premaxilla, maxilla and palatine bones in dorsolateral view; and **B,** *Rattus rattus* (CM35628), right maxilla and palatine bones in dorsal view; **C,** *Mallomys gunung* (CM11715), rostral fragment of cranium with bones of roof removed to expose inner structures of narial chamber; and **D,** *Uromys caudimaculatus* (ANWCP34), right premaxilla, maxilla and palatine bones in dorsolateral view. *Abbreviations*: **app**, anterior palatine process; **dpc**, descending palatine artery and nerve canal; **if**, incisive foramen; **igc**, incisor generative capsule; **ios**, infraorbital sulcus; **mr**, medial ridge of maxillary sinus complex; **msc**, maxillary sinus complex; **nps**, nasopharyngeal sulcus; **nvs**, neurovascular sulcus; **olm**, orbital lamina of maxilla; **pms**, premaxilla-maxilla suture; **sps**, sphenopalatine sulcus; **zp**, zygomatic plate. Scale bars each represent 5 mm. One scale bar is shared by A and B.

hence no narrowing of the nasopharyngeal sulcus. A similar degree of posterior expansion of the maxillary sinus complex was also found in specimens of *Mammelomys* and *Paramelomys* (not shown) but without lateral expansion in either case. In each of these genera a small pocket near the posterior end of the space is defined by a low transverse septum. An important observation is that expansion of the maxillary sinus complex is not simply a function of large body size: the anatomy of this region in the large-bodied *Bandicota indica* (not shown) is essentially identical with that of *Rattus* spp., whereas the maxillary sinus complex in *Uromys caudimaculatus* is among the least expansive of all murines examined thus far, reaching only to the front of M1 (fig. 21D). The presence of multiple bony septa in the maxillary sinus complex of *Coryphomys* is without parallel among extant murines surveyed to date.

Expansion of the maxillary sinus complex presumably reflects an increase in the volume of the glandular tissues of the maxillary sinus. Depending on which of the two embryologically and functionally distinct glandular components are involved, this might reflect an increased demand for humidification of inhaled air and/or more subtle physiological or immunological evolutionary influences. However, pending more detailed anatomical and physiological studies of *Mallomys* and other large-bodied murines such as *Uromys*, further speculation on the role of these structures in *Coryphomys* is unwarranted.

The significance of bony septa within the maxillary sinus complex does warrant further comment. In particular, we note that bony septa within other cranial spaces (e.g., the tympanic cavity) generally arise within a general context of pneumatization and through the specific process of bone remodeling, with septa forming along the line of attachment of membranous sheets established early in ontogeny (MacPhee, 1981). Whether such membranous sheets are present in this region of the developing murine skull and, further, whether any such structures are related specifically to the embryologically and functionally distinct glandular components are questions that can be answered only by more detailed ontogenetic studies with a specific emphasis on the impact of maxillary sinus development on supporting skeletal structures.

SUMMARY OF PHYLOGENETIC ASSESSMENTS: Previous students of murine phylogeny clearly recognized the frequent occurrence of multiple, independent acquisitions and/or losses of craniodental traits within the group (e.g., Ellerman, 1941; Misonne, 1969; Musser and Newcomb, 1983). However, because their conclusions were based on the observation of incongruence among character distributions, it has remained uncertain which, if any, of the morphological characters might rate as the more reliable phylogenetic indicators. Our comparative assessments of morphological evolution within Murinae are among the first to be carried out with the benefit of an independent phylogenetic framework derived from analysis of multiple molecular markers (see also Michaux et al., 2007). As already noted, such an approach can help to identify instances of homoplasy, to decide upon character polarity, and to disentangle patterns of morphological covariation.

As documented above, each and every one of the morphological features of *Coryphomys* subjected to phylogenetic assessment shows incontrovertible evidence of multiple, independent acquisitions and/or losses among extant Murinae. Notably, this includes the acquisition in the upper molars of cusp t7, a feature that some prior students of murine evolution have regarded as a potentially good indicator of phylogeny (e.g,. Chaimanee, 1998). At the same time, our assessments also have highlighted the need for revision of current notions of character polarity for a number of key features of the murine cranium and teeth, most notably the molar size gradient and the form of the incisive foramina. However, the evidence in each case remains somewhat ambiguous, due in part to the intrinsic vagaries of ancestral state reconstruction (Cunningham et al., 1998) but also to the frequent strong contrasts in morphology between the members of the basal murine lineage, the Phloeomyini, and the immediate outgroups, the Deomyinae and Gerbillinae.

Despite this seemingly pessimistic outlook, the morphological evidence casts the spotlight on two lineages as potential phyloge-

netic affines of *Coryphomys*: the Phloeomyini and the Hydromyini. The majority of the derived morphological traits of *Coryphomys* (e.g., enlarged posterior cinguli on upper molars; reduction of the stapedial artery; loss of labial cuspids on lower molars) are replicated in members of one or both of these groups, and less frequently elsewhere within Murinae. One possible interpretation is that this simply reflects the large body size and ecologically specialized nature of many of the phloeomyins and hydromyins, features that they share with *Coryphomys*. Alternatively, the communality of morphological specializations might reflect a phyletically determined "propensity" to develop certain dental and cranial specializations (e.g., reduction of the stapedial artery, loss of labial cuspids on lower molars) but with the morphological pattern blurred as a consequence of homoplasy within the more speciose lineages. However, given that the Phloeomyini and Hydromyini do not represent sister taxa within the Murinae, any such "propensity" itself would have to be homoplasious!

The superficial resemblance noted by previous researchers in lower molar morphology between *Coryphomys* and members of the "*Lenothrix* group" (Schaub, 1937; Hooijer, 1965; Misonne, 1969) is confirmed in a very general sense for the upper molars. However, detailed comparison of the upper molars between *Coryphomys* and each of the members of the "*Lenothrix* group" reveals numerous differences in the shape, positioning and connections of the major cusps. Furthermore, none of the various cranial specializations described for *Coryphomys* are matched among the various members of the "*Lenothrix* group." Derivation of *Coryphomys* from within the "*Lenothrix* group" remains possible but seems unlikely.

Each of the three groups mentioned as possible relatives of *Coryphomys* is represented today in areas that bound the region of Wallacea: in the Philippines to the north, in the Australo-Papuan region to the east, or in the Sundaic region and Sulawesi to the west. If we can assume that murine rodents first evolved on continental Asia (Jacobs and Downes, 1994), then it is reasonable to infer that the ancestor of all three groups either evolved in or passed through the Sundaic region before engaging in overwater dispersal to reach their ultimate places of diversification (Aplin, 2006; Jansa et al., 2006; Rowe et al., 2008). In the case of easterly dispersal of murine rodents, this process was facilitated by late Miocene narrowing of the "Indonesian Seaway"—the deepwater trench between the colliding Australian and Asian continental plates (Linthout et al., 1997) and the progressive subaerial emergence of the numerous islands that make up the contemporary landscape of Wallacea. Colonization of Timor by murines including the ancestor of *Coryphomys* may have occurred during an initial easterly dispersal across the Indonesian Seaway or through a secondary process of back dispersal, either from the Philippines in the north or from Melanesia in the east. Judging from the broad regional tectonic framework, murine dispersal through this region could have commenced as early as 8 million years ago, and there can be little doubt that murine rodents were already well established and undergoing regional radiations in each of the Philippines and New Guinea by 6 million years ago (Lecompte et al., 2008; Rowe et al., 2008) and possibly even earlier (Jansa et al., 2006).

Attempts are currently underway to recover DNA from representatives of each of the prehistoric Timorese murines, including specimens of *Coryphomys*. Even if successful, these results are unlikely to lead to precise phylogenetic placement of all of the prehistoric murines. However, they may serve to constrain the phyletic affinities in ways that allow morphological characters that are globally homoplasious to assume phylogenetic significance within the context of specific subsections of the murine radiation.

Paleoecology of *Coryphomys*

Inferences regarding the paleoecology of extinct mammals can be based on various sources of information, including intrinsic attributes such as anatomical features including body size, chemical properties (e.g., stable isotopes) of bones and teeth, and patterns of dental microwear and skeletal pathology, and extrinsic attributes including the spatial and temporal patterns of distribution and abun-

dance, and the age and sex structure of death assemblages. All of these sources of information may eventually be consulted to produce a full paleoecological assessment of the extinct Timorese murine fauna (e.g., Bocherens et al., 2006). However, for the present contribution on *Coryphomys*, we limit our treatment to some preliminary comments based on the likely body size and features of craniodental anatomy, and their broad spatial distribution and abundance relative to other elements of the murine fauna. We close with some comparative remarks regarding patterns of "giant rat" diversity in other regions.

INFERENCES FROM BODY SIZE: Both species of *Coryphomys* were extremely large rats, equivalent in body size only to the very largest of extant murines—species of *Mallomys* and *Hyomys* in New Guinea, *Papagomys armandvillei* on Flores, and species of *Phloeomys* and *Crateromys* in the Philippines. Adult body mass in these genera falls in the range of 1200–2600 grams (Flannery, 1995a; Heaney, 2005; Helgen, 2007). Based on the currently available skeletal remains, we expect the two *Coryphomys* species to fall at (or even exceed) the upper limit of this range.

Murine rodents have a reputation as prolific breeders, characterized by rapid reproductive and recruitment cycles, and large litters (see Aplin et al., 2004, for a summary of information on agricultural pest and commensal murines). However, available information on the very largest murines suggests that they are considerably constrained in reproductive potential when compared with many smaller-bodied taxa. Most tellingly, murine species that achieve a body weight well in excess of 1000 grams typically have only a single pair of inguinal mammae (*Phloeomys* spp.) or two inguinal pairs (the largest species of *Hyomys*, *Uromys*, and *Solomys*), and available breeding records for these species suggest that they commonly raise only one young per litter (Flannery, 1995a, 1995b; Majnep and Bulmer, 2007). Exceptions are found in the genus *Mallomys*, whose species all appear to have three pairs of mammae (one axillary and two inguinal pairs) (Flannery, 1995a; Helgen, 2007). Yet, despite this greater teat number, published observations of *Mallomys* litters suggest that only a single offspring is raised in each litter (Helgen, 2007). We cannot find published information on the number of teats or breeding biology in *Papagomys armandvillei* of Flores or *Crateromys* spp. of the Philippines. The rattin *Bandicota indica*, with a body weight around 1000 grams, is exceptional in being one of the very few large murines to possess a high number of mammae (six pairs in total) and to produce large litters (typically 8–10 pups; data summarized by Aplin et al., 2004). Based on the available observations, we posit that the species of *Coryphomys* probably had small litters.

Small litters in the largest of murines render such species particularly susceptible to extinction in the face of widespread habitat modification, particularly when this factor is combined with targeted hunting for consumption by human populations. This combination of threatening factors is identified as the likely cause of the ongoing decline of large insular endemic rats in the Solomon Islands (Flannery, 1995b) and the Philippines (Oliver et al., 1993; Gonzales and Kennedy, 1996), and is likely to have been similarly important in the recent extinction of the "giant rat" fauna on Timor and in Holocene extinctions of other large rats in insular contexts throughout Wallacea and Melanesia (e.g., Flores, Musser, 1981b; Greater Bukida in the Solomon Archipelago, Flannery and Wickler, 1990).

INFERENCES FROM CRANIODENTAL ANATOMY: The craniodental anatomy of *Coryphomys* also provides some clues regarding paleoecology. From an ecomorphological standpoint, the most significant features of *Coryphomys* are its relatively short and broad rostrum, its powerful incisors, and its large, high-crowned, and highly cuspidate molars. Among extant murines, the closest ecomorphological approximation of *Coryphomys* can be found among the species of *Mallomys* and *Crateromys* (e.g., see figures of *Mallomys* and *Crateromys* skulls and teeth in Flannery et al., 1989; Flannery, 1995a; and Musser and Gordon, 1981). Species in both genera are herbivorous, nocturnal, arboreal or scansorial, primarily forest dwelling (but also may forage in grasslands adjacent to forests), and nest in tree hollows or in shallow under-

ground burrows. These similarities may offer broad clues to the lifestyle of the species of *Coryphomys*.

The four known species of *Crateromys* are distributed allopatrically (on four Philippine islands) and occur in primary and secondary forest habitats, both in lowland forest (*C. paulus* on Ilin Island, *C. australis* on Dinagat, and *C. heaneyi* on Panay) and in montane pine and oak formations (*C. schadenbergi* on Luzon). The species of *Crateromys* may be mostly arboreal (Oliver et al., 1993) and are reliant on forest but have also been taken in adjacent grassland contexts (Gonzales and Kennedy, 1996). Limited information on diet and nesting sites is available for two species—the relatively smaller-bodied *C. heaneyi* of Panay (1000 g) and the largest species, *C. schadenbergi*, from Luzon (weight TK g). Gonzales and Kennedy (1996: 37) reported that one individual of *C. heaneyi* was collected from a tree hollow, and that captive specimens "have a varied vegetable diet and are easy to keep. They prefer cabbage leaves *Brassica oleoracea* and bananas, which they peel before eating. They also show preference for fresh leaves of red mulberry (*Morus rubra*), and sunflower (*Helianthus*) seeds when available." Whether this reflects the diet of *C. heaneyi* in the wild is not yet clear. *Crateromys schadenbergi* occurs in mossy pine and oak forests above 2000 m on Luzon (recorded between 2000–2500 m; Heaney et al., 1998). It is also recorded to make nests in tree hollows (Whitehead, in Thomas, 1898; Taylor, 1934), but it also nests in burrows made among the roots of large trees (Whitehead, in Thomas, 1898) and in stick nests built in the tops of trees (Rabor, 1955). Rabor's (1955) examination of stomach contents from five individuals of *C. schadenbergi* revealed finely ground pine buds and young pinecones, in line with Taylor's (1934) earlier indication that the species eats young buds and bark of pine sprouts. Whitehead (in Thomas, 1898) indicated that this species may also feed on fruits in trees (but not fallen fruits on the ground).

The four currently recognized species of *Mallomys* are endemic to New Guinea's montane forests and alpine grasslands (Flannery et al., 1989; Musser and Carleton, 2005). They are nocturnal and scansorial, and eat leaves, epiphytes, fronds and shoots of gingers, ferns, pandanus, wild bamboo, and other grasses, as well as forest fruits and crops from native gardens, such as sugarcane (reviewed by Helgen, 2007). The species range in body size from *M. rothschildi* (averaging about 1200 g; data summarized by Helgen, 2007) to *M. istapantap* and *M. gunung* (1800–2000 g). Available evidence suggests that *M. rothschildi* is the most arboreal species, roosting primarily in tree hollows and foraging on leaves and shoots in the forest canopy (Helgen, 2007). Two larger species in the genus, *M. aroaensis* (averaging 1540 g) and *M. istapantap* (averaging 1888 g) are more scansorial, making nests of leaves and fronds in underground cavities among the roots of trees or under large rocks (especially at the boundary of montane forest and grasslands) and climbing forest trees in search of young fronds and fruits. The largest species of *Mallomys* is *M. gunung* (one specimen weighed 2000 g), a presumably scansorial species that exclusively occupies alpine grasslands in the western portion of New Guinea's expansive Central Cordillera (Flannery et al., 1989). Nothing is firmly recorded of the biology of this species, but its extremely high-crowned molars and environmental context suggest that abrasive ferns and grasses comprise a major part of the diet (Flannery, 1995a).

One other feature of craniodental anatomy in *Coryphomys* warrants some brief comments. This is the slightly proodont orientation of the upper incisor in a premaxillary specimen assigned only at generic level (fig. 17A–C). Incisor proodonty in rodents is typically associated with the use of the teeth for digging. As noted by Hershkovitz (1962: 102–104), proodonty is often associated with a reduction in bulk of the incisors and a general degeneration of the dentition, both commonly associated with small body size and a dietary specialization on earthworms and other soft-bodied invertebrates. In such groups, there is a clear shift in incisor functionality from gnawing to picking and manipulation of both soil and prey items. Incisor proodonty also combines with hypertrophy in some muroid lineages. The most extreme examples are found in Spalacidae, a family of medium-sized to large-bodied fossorial rodents that typically dig

large semipermanent burrows and feed on highly abrasive vegetative matter. However, comparable (though far less extreme) morphological adaptations are observed in a variety of murine genera, including *Mallomys gunung* (Flannery et al., 1989), *Berylmys berdmorei* (Musser and Newcomb, 1983: fig. 18B), *Bandicota bengalensis* (Musser and Brothers, 1994: fig. 6); *Chrotomys* (Musser and Heaney, 1992: fig. 43), *Protochromys fellowsi* (Menzies, 1996) and *Leggadina lakedownesis* (Watts, 1976). Among these taxa, the species of *Berylmys* and *Bandicota* are both medium-sized murines (body weights typically around 500 gm) and both excavate extensive burrow systems (literature summarized by Aplin et al., 2004), and the same behavior is suspected for the gigantic *Mallomys gunung* that lives above the tree line in New Guinea. More detailed observations of burrowing and feeding behavior are needed to determine whether the slight incisor proodonty in these taxa is related to the excavation and carrying of soil or to dietary items that perhaps require some degree of grasping and tearing, rather than the usual gnawing action of a typical rodent. However, that burrowing alone is almost certainly not a sufficient explanation is suggested by the fully opisthodont orientation in the other species of *Bandicota*, all of which excavate extensive burrows, sometimes in the same locality as *B. bengalensis* (Aplin et al., 2004).

Inferences from Distributions and Abundances: The various excavated sites provide an environmental transect from near coastal locations to a variety of inland habitats, at elevations between 300 m and 600 m. Though the available prehistoric samples are unlikely to fully sample the higher elevation forests of Timor, especially those of the upper montane zone above 1500 m, which harbour such remarkable endemism in other regional island contexts (Flannery, 1995a; Musser and Durden, 2002; Heaney et al., 1998; Heaney, 2001, 2005), they nonetheless provide some initial insights into the altitudinal ranges and the relative abundances of various extinct Timorese murines. For full treatment of this issue, we must await completion of our taxonomic studies of the remaining murine genera. However, based on the present contribution and our ongoing assessment of the other genera, we can offer some preliminary observations for *Coryphomys*.

The remains of *Coryphomys* were recovered from six sites, ranging in elevation from Jerimalai at ca. 150 m to the Uai Bobo sites at ca. 600 m. In all sites, *Coryphomys* is relatively scarce, matched for overall rarity only by Mahoney's Genus C. In the lowest altitude sites of Lene Hara and Jerimalai, *C. buehleri* and *C. musseri* are each represented by a single example from layers that date from the Late Pleistocene, and neither species is represented in samples of Holocene age in which Mahoney's Genus A alone is present in reasonable numbers. At the somewhat higher elevation sites of Bui Ceri Uato (175 m) and Lie Siri (240 m) on the Baucau Plateau, both species of *Coryphomys* are represented in samples of early to mid Holocene age, but they are greatly outnumbered by examples of Mahoney's Genus A and Mahoney's Genus B. Samples excavated at even higher elevations—around Lake Ila Lalaro at 334 m and on the flank of Mount Hatu Ariana at 600 m in the Central Highlands—yielded the bulk of the *Coryphomys* material, though again these are greatly outnumbered by specimens of Mahoney's Genus A and Mahoney's Genus B. In both of these areas, specimens of *C. musseri* are more than twice as abundant as examples of *C. buehleri*. In the two Matja Kuru sites, situated on the margin of Lake Ila Lalaro, both species of *Coryphomys* are represented throughout the stratigraphic profiles, from just before the time of the Last Glacial Maximum through into the mid-Holocene, but with a slightly greater proportion of *C. buehleri* in the Pleistocene layers (5 of 9 specimens) compared with *C. musseri* (6 of 21 specimens).

These preliminary observations suggest that the Timorese murine fauna displayed significant altitudinal zonation. A similar view was expressed by Mahirta et al. (2004), as part of an explanation for why large murine remains are not represented in the terminal Pleistocene deposit of Pia Hudale Rockshelter, on Roti Island. In their view,

> rodent diversity may well have been lowest in lowland habitats on Timor and, by association, on nearby Roti. ... In the lower altitude site of Lie Siri only one of the three giant rat species

> (identified as Genus A) is at all abundant, and the small rat fauna is also limited in diversity, with only one species of the *Melomys* / *Pogonomelomys* group certainly present. In contrast, the two higher elevation sites of Uai Bobo 1 and 2 have a more evenly balanced suite of giant rats (Genus B is most abundant in both sites) and a higher diversity of small rats (at least two species of the *Melomys* / *Pogonomelomys* group. (Mahirta et al., 2004: 389)

Mahirta et al. (2004: 389) also noted that "a similar altitudinal effect on rat diversity is found in New Guinea, Sulawesi and the larger Philippine Islands, each of which supports a diverse and highly endemic rodent fauna. In each case, rat diversity is highest in midmontane habitats, with fewer species in lowland rainforest, especially among the medium-sized to gigantic size range."

The pattern of distribution and abundance of *Coryphomys* suggests to us that it was primarily a genus of upland habitats on Timor. At certain times during the Late Pleistocene, perhaps in response to cooler (and drier?) conditions, it may have extended to lower elevations or increased in abundance in these habitats to the point where it became visible in the archaeological record. The relative scarcity of *Coryphomys*, even in the higher elevation sites, might reflect a natural rarity, perhaps related to dietary specialization. Alternatively, it might reflect some behavioral specialization that kept these species more often out of the hands of prehistoric Timorese hunters.

Observations on Sympatry among the Largest Extant Murines: Within the mountains of New Guinea, species of *Mallomys* exhibit complex patterns of sympatric co-occurrence among morphologically very similar species. Since this situation is analogous to the apparent geographic and temporal co-occurrence of *Coryphomys buehleri* and *C. musseri* in Timor, a consideration of the basis and expression of the sympatry in *Mallomys* might shed light on the prehistoric Timorese context. Three species of *Mallomys*—*Mallomys rothschildi*, *M. aroaensis*, and *M. istapantap*—occur in widespread syntopy in montane forests across most of the breadth of the Central Cordillera (Flannery et al., 1989; Helgen, 2007). What ecological factors mediate sympatry between these congeners? Differences in body size are important, but body size distinctions are not always clearly evident from dental, cranial, and mandibular comparisons. For example, despite a small average difference in overall cranial size, no significant difference in molar size, and few or no consistent distinctions in qualitative molar morphology, *Mallomys aroaensis* has a heftier body than *M. rothschildi* and averages 32% larger in body mass (Helgen, 2007). Even with the availability of large comparative samples of skins, skulls, and postcranial skeletons of *M. aroaensis* and *M. rothschildi* in world museums, and consistent differences between the two in fur color, tail length, and qualitative cranial characters, the covarying morphological distinctions between these two broadly sympatric biological species were not identified and appreciated by taxonomists until two decades ago and only then with the added benefit of genetic data (Flannery et al., 1989). These taxa would likely not be distinguished solely on the basis of molars and fragmentary dentary and maxillary material such as are available for *Coryphomys*. In body mass, *Mallomys istapantap* averages 22% larger than *M. aroaensis* and 62% larger than *M. rothschildi* (Helgen, 2007), but the maxillary tooth row of *M. istapantap* averages only 5% and 6% larger compared to these respective taxa. By way of comparison, the only complete maxillary tooth row available for *C. buehleri* (19.49 mm in length) averages 14% longer than the only complete maxillary tooth row available for *C. musseri* (17.09 mm in length). To us, these comparisons involving sympatric species of *Mallomys* provide a clear indication that the morphological distinctions we document between the two species of *Coryphomys* in Timorese fossil samples are sufficient to accommodate sympatry between these forms, and bolster our case that these taxa represent biological species rather than extraordinary morphological variation within a single interbreeding lineage.

Differences in habitat preference and microhabitat usage are also seemingly important in facilitating syntopic occurrence of *Mallomys* taxa. The craniodentally similar taxa *Mallomys rothschildi* and *M. aroaensis* have different but widely overlapping eleva-

tional ranges. The recorded elevational range of *M. rothschildi* in Papua New Guinea extends from 1450 to 3700 m (mean of 27 localities = 2278 m, median 2400 m, SD = 487 m); the recorded elevational range of *M. aroaensis* in Papua New Guinea overlaps broadly but is staggered lower than that of *M. rothschildi*, extending from 1100 m to 2700 m (mean elevation of 35 different localities = 1790 m, median 1818 m, SD = 398 m). The third broadly overlapping species, *M. istapantap*, has an essentially equivalent elevational range to *M. rothschildi* (1500 to 3850 m), but comparisons involving most available museum samples demonstrate that on average *M. istapantap* occurs more commonly at higher elevations (mean elevation of 19 vouchered sites = 2771 m, median 2700 m, SD 595 m) than *M. rothschildi* and *M. aroaensis*. Judging from their relative representation among museum material, *M. istapantap* appears to be less common than *M. aroaensis* throughout eastern New Guinea, though in a few areas *M. istapantap* appears to be relatively common and *M. aroaensis* genuinely uncommon. Further, in these rare areas of local overlap between *M. aroaensis* and *M. istapantap*, museum holdings demonstrate that *M. rothschildi* is uncommon or perhaps sometimes locally absent—a potentially illuminating insight into complex sympatric interactions of these three congeneric giant rats.

Potential differences in microhabitat usage among *Mallomys* species remain essentially unstudied. However, information gleaned from museum labels and rare field observations suggests that *M. rothschildi* is the most arboreal species, commonly nesting in tree hollows, and may be more folivorous, while *M. aroaensis* and *M. istapantap* appear to be more terrestrial, nesting especially in underground burrows, and possibly somewhat more frugivorous (summarized by Helgen, 2007). A spool-and-line tracking study of *Mallomys* in the Hagen Range reported by Berry et al. (1987) antedated the first modern taxonomic revision of this group by Flannery et al. (1989) and the species they studied (possibly more than one) cannot be determined. However, the reported body weights of tracked animals and the fact that *M. rothschildi* is the most abundant species of *Mallomys* in the Hagen Range (Helgen, 2007) suggests that most of their data pertain to this taxon. The observations of Berry et al. (1987) portray *Mallomys* as "an agile and capable climber" that travels both across the ground and through the canopy, forages principally off the ground, and rests in "tree holes or branch forks up to 10 m above the ground; holes in root compounds at tree bases and mud banks, and on the ground under dense vegetation," though they noted that "in each case, there was no evidence, such as the presence of dried leaves, of construction of a proper nest."

The widespread sympatric occurrence of three biological species of *Mallomys* in the mountains of New Guinea thus appears to be mediated by significant distinctions in adult body mass (not always clearly evident from dental and cranial comparisons alone), significant differences in average elevational occurrences (only evident once large geographic samples are assembled), and possibly by ecological differences such as degree of arboreality, choice of nesting sites, and diet. We expect that similar distinctions were important in facilitating the sympatric occurrence of *C. buehleri* and *C. musseri* in Timor.

More insightful review of the paleoecology of *Coryphomys* awaits the characterization of the remaining taxonomic components of the extinct large-bodied rodent community of Timor, all of which belong to currently undescribed genera and species.

CONCLUSIONS

The large collections of prehistoric animal bones recovered from archaeological cave deposits on Timor provide our only record of a remarkable slice of global mammalian diversity that is now all but gone. Just how this locally confined radiation of murine rodents came to produce many of the world's largest rats on such a small oceanic island, and exactly how these remarkable animals fared during their long interaction with prehistoric Timorese people, are big questions that resonate far beyond the immediate geographic and taxonomic context.

Clarifying the taxonomic content of the genus *Coryphomys* represents the first step

toward documenting the Timorese murine radiation. Interestingly, our primary conclusion in this regard—that the genus *Coryphomys* actually contained two biological species—is an outcome that was not anticipated by previous students of the Timorese fossil rodents. Whether our conclusion proves acceptable to the wider community remains to be seen. Suffice it to say here that we find the morphological (and distributional) evidence for the presence of two biological species of *Coryphomys* to be compelling, and that evidence further supports the presence of significant sympatric diversity in various large-bodied New Guinean murines, not only in *Mallomys* (Helgen, 2007) but probably also in other genera such as *Hyomys* and *Uromys* (ongoing studies by Helgen, Aplin, and others). Future contributions in this series will also emphasize the remarkable taxon diversity among the gigantic Timorese murines, with two or three species to be described in each of Mahoney's Genus B and Genus C.

The preliminary paleoecological discussions included in this work also lay the foundation for more detailed studies. By first delineating the species within each genus of both large and small murines, and then quantifying the relative abundances of each taxon across the various altitudinal and habitat gradients, we hope to establish a framework of testable hypotheses regarding the habitat preferences and ecological niche occupied by each taxon; hypotheses that can be tested through application of the full range of modern methods now available to a vertebrate paleoecologist. Our conclusion that *Coryphomys* was essentially a genus of upland murines represents a small step toward this goal, as does our speculation that it was a naturally uncommon element, at least at the midelevations sampled by the various archaeological sites.

ACKNOWLEDGMENTS

Both authors acknowledge the inspirational guidance and seemingly endless generosity of Guy Musser, whose monumental contributions in the field of murine systematics represent the common foundation on which so many of us now stand.

We also wish to acknowledge the contributions of the late Jack Mahoney who, together with Dan Witter, carried out much of the initial sorting and analysis of the Glover archaeozoological collection, and of Ian Glover, who not only excavated much of the fossil rodent remains from East Timor but also maintained an avid interest in the giant rat remains as they have progressed through various sets of hands. Aplin extends special thanks to Sue O'Connor, Peter Veth, and Matthew Spriggs for the opportunity to study the recently collected Timorese samples. For assistance with production of this paper, we are particularly grateful to Angela Frost who took all of the photographs and compiled the various plates and figures for this paper.

The reviewers of this manuscript are thanked for their valuable comments and suggested improvements.

REFERENCES

Adkins, R.M., A.H. Walton, and R.L. Honeycutt. 2003. Higher-level systematics of rodents and divergence time estimates on two congruent nuclear genes. Molecular Phylogenetics and Evolution 26: 409–420.

Adler, G.H., and R. Levins. 1994. The island syndrome in rodent populations. Quarterly Review of Biology 69: 473–490.

Adrover, R., P. Mein, and E. Moissenet. 1988. Contribución al conocimiento de la fauna de Roedores del Plioceno de la región de Teruel. Teruel 79: 91–151.

Adrover, R., P. Mein, and E. Moissenet. 1993. Roedores de la transición Mio-Plioceno de la región de Teruel. Paleontologia i Evolució 26–27: 47–84.

Aguilar, J.-P., and J. Michaux. 1996. The beginning of the age of Murinae (Mammalia: Rodentia) in southern France. Acta Zoologica Cracoviensia 39: 35–45.

Agusti, J., and M. Llenas. 1996. The late Turolian muroid rodent succession in eastern Spain. Acta Zoologica Cracoviensia 39: 47–56.

Ahlberg, P.E., and G. Köntges. 2006. Homologies and cell populations: a response to Sánchez-Villagra and Maier. Evolution and Development 8: 116–118.

Almeida, A. de., and G. Zbyszewski. 1967. A contribution to the study of the prehistory of Portuguese Timor – Lithic Industries. *In* W.G. Solheim, II (editor), Archaeology at the Elev-

enth Pacific Science Congress: papers presented at the XI Pacific Science Congress, Tokyo, August–September 1966. Asian and Pacific Archaeology Series 1: 55–67. Honolulu: Social Science Research Institute, University of Hawaii.

Aoki, B., and R. Tanaka. 1938. Biostatistical research on *Rattus losea* (Swinhoe, 1870), a Formosan wild rat, with special reference to its diagnostic characters for taxonomy. Memoirs of the Faculty of Science and Agriculture Tohoku Imperial University 23: 1–74.

Aplin, K.P. 2006. Ten million years of rodent evolution in Australasia: phylogenetic evidence and a speculative historical biogeography. *In* J.R. Merrick, M. Archer, G.M. Hickey, and M.S.Y. Lee (editors), Evolution and biogeography of Australasian vertebrates: 707–744. Sydney: Auscipub Pty Ltd, 942 pp.

Aplin, K.P., P.R. Brown, J. Jacob, C. Krebs, and G.R. Singleton. 2004. Field methods for rodent studies in Asia and the Pacific. ACIAR Monograph Series, 100, 1–397. Canberra, Australian Centre for International Agricultural Research.

Audley-Charles, M.G. 1968. The geology of Portuguese Timor. Memoirs of the Geological Society of London 4: 1–76.

Baverstock, P.R., M. Gelder, and A. Jahnke. 1983. Chromosome evolution in Australian *Rattus*—G-banding and hybrid meiosis. Genetica 60: 93–103.

Baverstock, P.R., C.H.S. Watts, M. Adams, and S.R. Cole. 1981. Genetical relationships among Australian rodents (Muridae). Australian Journal of Zoology 29: 289–303.

Beecher, R.M. 1979. Functional significance of the mandibular symphysis. Journal of Morphology 159: 117–130.

Bekele, A. 1983. The comparative functional morphology of some head muscles of the rodents *Tachyoryctes splendens* and *Rattus rattus*. I. Mammalia 47: 395–419.

Bellwood, P. 1997. Prehistory of the Indo-Malaysian Archipelago. Revised ed. Honolulu: University of Hawaii Press.

Berry, A.J., T.J.C. Anderson, J.N. Amos, and J.M. Cook. 1987. Spool-and-line tracking of giant rats in New Guinea. Journal of Zoology (London) 213: 299–303.

Berry, R., and A.E. Grady. 1981. Deformation and metamorphism of the Aileu Formation, north coast, East Timor and its tectonic significance. Journal of Structural Geology 3: 143–167.

Biknevicius, A.R., D.A. McFarlane, and R.D.E. MacPhee. 1993. Body size in *Amblyrhiza inundata* (Rodentia: Caviomorpha), an extinct megafaunal rodent from the Anguilla Bank, West Indies: estimates and implications. American Museum Novitates 3079: 1–25.

Bocherens, H., J. Michaux, F.G. Talavera, and J. Van der Plicht. 2006. Extinction of endemic vertebrates on islands: The case of the giant rat *Canariomys bravoi* (Mammalia, Rodentia) on Tenerife (Canary Islands, Spain). Comptes Rendus Palevol 5: 885–891.

Bojsen-Møller, F. 1964. Topography of the nasal glands in rats and some other mammals. Anatomical Record 150: 11–24.

Bolnick, D.I., and B.M. Fitzpatrick. 2007. Sympatric speciation: models and empirical evidence. Annual Review of Ecology, Evolution and Systematics 38: 459–487.

Bouma, G.A., and H.T. Kobryn. 2004. Change in vegetation cover in East Timor, 1989–1999. Natural Resources Forum 28: 1–12.

Broman, I. 1921. Über die Entwicklung der konstanten grösseren Nasenhölendrüsen der Nagetiere. Zeitschrift fur Anatomie und Entwicklungsgeschichte 60: 439–586.

Brown, P., T. Sutikna, M.J. Morwood, R.P. Soejono, Jatmiko, E. Wayhu Saptomo, and Rokus Awe Due. 2004. A new small-bodied hominin from the Late Pleistocene of Flores, Indonesia. Nature 431: 1055–1061.

Bugge, J. 1980. The contribution of the stapedial artery to the cephalic arterial supply in muroid rodents. Acta anatomica 76: 313–336.

Bugge, J. 1985. Systematic value of the carotid arterial pattern in rodents. *In* W.P. Luckett and J.L. Hartenberger (editors), Evolutionary relationships among rodents, a multidisciplinary analysis: 355–379. New York: Plenum Press.

Burney, D.A., and T.F. Flannery. 2005. Fifty millennia of catastrophic extinctions after human contact. Trends in Ecology and Evolution 20: 395–401.

Cai, J., S.-W. Cho, J.-W. Kim, M.-J. Lee, Y.-G. Cha, and H.-S. Jung. 2007. Patterning the size and number of tooth and its cusps. Developmental Biology 304: 499–507.

Carleton, M.D. 1980. Phylogenetic relationships in neotomine-peromyscine rodents (Muroidea) and a reappraisal of the dichotomy within New World Cricetinae. Miscellaneous Publications Museum of Zoology University of Michigan 157: 1–146.

Castillo Ruiz, C. 1991. *Paraethomys belmezensis* nov. sp. (Rodentia, Mammalia) du Pliocène de Córbona (Espagne). Geobios 25: 775–780.

Chaimanee, Y. 1998. Plio-Pleistocene rodents of Thailand. Thai Studies in Biodiversity 3: 1–303.

Chappell, J., and H.H. Veeh. 1978. Late Quaternary tectonic movements and sea-level changes at Timor and Atauro Island. Geological Society of America Bulletin 89: 356–368.

Charlton, T.R. 1991. Postcollision extension in arc-continent collision zones, eastern Indonesia. Geology 19: 28–31.

Cheema, I.U., S.M. Raza, L.J. Flynn, A.R. Rajpar, and Y. Tomida. 2000. Miocene small mammals from Jalalpur, Pakistan, and their biochronologic implications. Bulletin of the National Science Museum Series C (Geology and Paleontology) 26: 57–77.

Coiffait, B., P.-E. Coiffait, and J.-J. Jaeger. 1985. Découverte en Afrique du Nord des genres *Stephanomys* et *Castillomys* (Muridae) dans un noveau gisement de microvertébrés néogènes d'Algérie orientale: Argoub Kemellal. Proceedings of the Koninklijke Nederlandse Akademie van Wetenschappen Series B Physical Sciences 88: 167–183.

Corbet, G.B., and J.E. Hill. 1992. The mammals of the Indomalayan region: a systematic review. Oxford: Oxford University Press.

Coyne, J.A., and H.A. Orr. 2004. Speciation. Sunderland, MA: Sinauer, 545 pp.

Cunningham, C.W., K.E. Omland, and T.H. Oakley. 1998. Reconstructing ancestral character states: a critical reappraisal. Trends in Ecology and Evolution 13: 361–366.

Dawson, L. 1982a. Taxonomic status of fossil devils (*Sarcophilus*, Dasyuridae, Marsupialia) from late Quaternary eastern Australian localities. *In* M. Archer (editor), Carnivorous marsupials: 517–525. Sydney: Royal Zoological Society of New South Wales.

Dawson, L. 1982b. Taxonomic status of fossil thylacines (Thylacinus, Thylacinidae, Marsupialia) from late Quaternary deposits in eastern Australia. *In* M. Archer (editor), Carnivorous marsupials: 527–536. Sydney: Royal Zoological Society of New South Wales.

Dayan, T., and D. Simberloff. 1994. Character displacement, sexual size dimorphism, and morphological variation among the mustelids of the British Isles. Ecology 75: 1063–1073.

Dayan, T., and D. Simberloff. 1998. Size patterns among competitors: ecological character displacement and character release in mammals, with special reference to island populations. Mammal Review 28: 99–124.

Dayan, T., and D. Simberloff. 2005. Ecological and community-wide character displacement: the next generation. Ecology Letters 8: 875–894.

de Bruijn, H., G. Sarac, L.W. van den Hoek Ostende, and S. Roussiakis. 1999. The status of the genus name *Parapodemus* Schaub, 1938; new data bearing on an old controversy. Deinsea 7: 95–112.

de Smet, M.E.M., A.R. Fortuin, S. Tjokrospaoetro, and J.E. van Hinte. 1989. Late Cenozoic vertical movements of non-volcanic islands in the Banda Arc area. Netherlands Journal of Sea Research 24: 263–275.

Delany, M.J., and M.J.R. Healy. 1967. Variation in the long-tailed field-mouse (*Apodemus sylvaticus* (L.)) in the Channel Islands. Proceedings of the Royal Society of London Series B Biological Sciences 166: 408–421.

Denys, C., and J. Michaux. 1992. La troisième molaire supérieure chez les Muridae d'Afrique tropicale et le cas des genres *Acomys*, *Uranomys* et *Lophuromys*. Bonner Zoologische Beiträge 43(3): 367–382.

Denys, C., J. Michaux, and Q.B. Hendey. 1987. Les rongeurs *Euryotomys* et *Otomys*: un exemple d'évolution parallèle en Afrique tropicale? Comptes Rendus de l'Académie des Sciences (Paris), ser. 3 (Life Sciences) 305: 1389–1395.

Denys, C., J. Michaux, F. Petter, J.P. Aguilar, and J.J. Jaeger. 1992. Molar morphology as a clue to the phylogenetic relationships of *Acomys* to the Murinae. Israel Journal of Zoology 38: 253–262.

Diamond, M.K. 1992. Homology and evolution of the orbitotemporal venous sinuses of humans. American Journal of Physical Anthropology 88: 211–244.

Ellerman, J.R. 1941. The families and genera of living rodents. Vol. 2. London: British Museum (Natural History).

Emry, R.J. 1981. New material of the Oligocene muroid rodent *Nonomys*, and its bearing on muroid origins. American Museum Novitates 2712: 1–14.

Evans, A.R., G.P. Wilson, M. Fortelius, and J. Jernvall. 2006. High-level similarity of dentitions in carnivorans and rodents. Nature 445: 78–81.

Felsenstein, J. 1978. Cases in which parsimony or compatibility methods will be positively misleading. Systematic Zoology 27: 401–410.

Flannery, T.F. 1995a. Mammals of New Guinea, revised and updated ed. Ithaca, NY: Cornell University Press, 568 pp.

Flannery, T.F. 1995b. Mammals of the South-west Pacific and Moluccan Islands. Ithaca, NY: Cornell University Press, 464 pp.

Flannery, T.F., and S. Wickler. 1990. Quaternary murids (Rodentia: Muridae) from Buka Island, Papua New Guinea, with descriptions of two new species. Australian Mammalogy 13: 127–139.

Flannery, T.F., K. Aplin, C.P. Groves, and M. Adams. 1989. Revision of the New Guinean genus *Mallomys* (Muridae: Rodentia), with descriptions of two new species from subalpine habitats. Records of the Australian Museum 41: 83–105.

Foster, J.B. 1964. Evolution of mammals on islands. Nature 202: 234–235.

Gaunt, W.A. 1961. The development of the molar pattern of the golden hamster (*Mesocricetus auratus* W.) together with a re-assessment of the molar pattern of the mouse (*Mus musculus*). Acta anatomica 45: 219–251.

Geraads, D. 1995. Rongeurs et insectivores (Mammalia) du Pliocene final de Ahl al Oughlam (Casablanca, Maroc). Geobios 28: 99–115.

Geraads, D. 2001. Rongeurs du Miocene Superieur de Chorora, Ethiopie: Murinae, Dendromurinae et conclusions. Palaeovertebrata 30: 89–109.

Gilbert, S.F. 1994. Dobzhansky, Waddington, and Schmalhausen: embryology and the modern synthesis. *In* M. Adams (editor), The evolution of Theodosius Dobzhansky: 143–154. Princeton, NJ: Princeton University Press.

Gilbert, S.F., J.M. Opitz, and R.A. Raff. 1996. Resynthesizing evolutionary and developmental biology. Developmental Biology 173: 357–372.

Glover, I. 1986. Archaeology in Eastern Timor, 1966–67. Terra Australis 11. Canberra: Department of Prehistory, Research School of Pacific Studies, the Australian National University.

Gonzales, P.C., and R.S. Kennedy. 1996. A new species of *Crateromys* (Rodentia: Muridae) from Panay, Philippines. Journal of Mammalogy 77: 25–40.

Goodwin, R.E. 1979. The bats of Timor: systematics and ecology. Bulletin of the American Museum of Natural History 163(2): 73–122.

Greene, E.C. 1968. Anatomy of the rat. New York: Hafner, 370 pp.

Gross, J.B., and J. Hanken. 2008. Review of fate-mapping studies of osteogenic cranial neural crest in vertebrates. Developmental Biology 317: 389–400.

Hall, R. 2002. Cenozoic geological and plate tectonic evolution of SE Asia and the SW Pacific: computer-based reconstructions, model and animations. Journal of Asian Earth Sciences 20: 353–431.

Hamburger, V. 1980. Embryology and the modern synthesis in evolutionary theory. *In* E. Mayr and W. Provine (editors), The evolutionary synthesis: perspectives on the unification of biology: 97–112. New York: Cambridge University Press.

Hanken, J. 1993. Model systems versus outgroups: alternative approaches to the study of head development and evolution. American Zoologist 33: 448–456.

Hanken, J., and B.K. Hall. 1993. The Skull, Vol. 3. Functional and evolutionary mechanisms. Chicago: University of Chicago Press.

Heaney, L.R. 2001. Small mammal diversity along elevational gradients in the Philippines: an assessment of patterns and hypotheses. Global Ecology and Biogeography 10: 15–39.

Heaney, L.R. 2005. Remarkable rats. USA Today January 2005: 44–47.

Heaney, L.R., D.S. Balete, M.L. Dolar, A.C. Alcala, A.T.L. Dans, P.C. Gonzales, N.R. Ingle, M.V. Lepiten, W.L.R. Oliver, P.S. Ong, E.A. Rickart, B.R. Tabaranza, Jr., and R.C.B. Utzurrum. 1998. A synopsis of the mammalian fauna of the Philippine Islands. Fieldiana Zoology New Series 88: 1–61.

Hedges, S.R. 1969. Epigenetic polymorphism in populations of *Apodemus sylvaticus* and *Apodemus flavicollis* (Rodentia, Muridae). Journal of Zoology (London) 159: 425–442.

Helgen, K.M. 2003. A review of the rodent fauna of Seram, Moluccas, with the description of a new subspecies of mosaic-tailed rat, *Melomys rufescens paveli*. Journal of Zoology (London) 261: 165–172.

Helgen, K.M. 2007. A reassessment of taxonomic diversity and geographic patterning in the Melanesian mammal fauna. Unpublished Ph.D. dissertation, University of Adelaide, 446 pp.

Helgen, K.M., R.T. Wells, B.P. Kear, W.L. Gerdtz, and T.F. Flannery. 2006. Ecological and evolutionary significance of sizes of giant extinct kangaroos. Australian Journal of Zoology 54: 293–303.

Hellmayr, C.E. 1914. Die Avifauna von Timor. *In* C.B. Haniel, and A.T. Ergebrisse der unter Leittung von Joh. Zoologie von Timor. Wanner in Jahre 1911: 1–112. Stuttgart: Nagele und Dr. Sproesser.

Hershkovitz, P. 1962. Evolution of Neotropical cricetine rodents (Muridae) with special reference to the phyllotine group. Fieldiana Zoology 46: 1–524.

Hiiemae, K. 1971. The structure and function of the jaw muscles in the rat (*Rattus norvegicus* L.). III. The mechanics of the muscles. Zoological Journal of the Linnaean Society 50: 111–132.

Hiiemae, K., and W.J.B. Houston. 1971. The structure and function of the jaw muscles in the rat (*Rattus norvegicus* L.). I. Their anatomy and internal architecture. Zoological Journal of the Linnaean Society 50: 75–99.

Hooijer, D.A. 1957. Three new giant prehistoric rats from Flores, Lesser Sunda Islands. Zoologische Mededelingen 35: 299–314.

Hooijer, D.A. 1965. Note on *Coryphomys bühleri* Schaub, a gigantic murine rodent from Timor. Israel Journal of Science 14: 128–133.

Hooijer, D.A. 1969a. The stegodon from Timor. Proceedings of the Koninklijk Nederlandsch

Akadamie van Wetenschappen Series B Physical Sciences 72: 203–10.

Hooijer, D.A. 1969b. *Varanus* (Reptilia, Sauria) from the Pleistocene of Timor. Zoologische Mededelingen 47: 445–448.

Hooper, E.T. 1957. Dental patterns in mice of the genus *Peromyscus*. Miscellaneous Publications Museum of Zoology University of Michigan 99: 1–59.

Hori, M. 1993. Frequency-dependent natural selection in the handedness of scale-eating cichlid fish. Science 260: 216–219.

International Commission on Zoological Nomenclature. 2000. International code of zoological nomenclature. 4th ed. London: Natural History Museum, 306 pp.

Jacob, A., and R.A. Chole. 2006. Survey anatomy of the paranasal sinuses in the normal mouse. Laryngoscope 116: 558–563.

Jacob, T., E. Indriati, R.P. Soejono, K. Hsü, D.W. Frayer, R.B. Eckhardt, A.J. Kuperavage, A. Thorne, and M. Henneberg. 2006. Pygmoid Australomelanesian *Homo sapiens* skeletal remains from Liang Bua, Flores: population affinities and pathological abnormalities. Proceedings of the National Academy of Sciences 103: 13421–13426.

Jacobs, L.L. 1977. A new genus of murid rodent from the Miocene of Pakistan and comments on the origin of the Muridae. Paleobios 25: 1–11.

Jacobs, L.L. 1978. Fossil rodents (Rhizomyidae and Muridae) from Neogene Siwalik deposits, Pakistan. Museum of Northern Arizona Bulletin 52: 1–103.

Jacobs, L.L., and L. Chuan-Kluei. 1982. A new genus (*Chardinomys*) of murid rodent (Mammalia, Rodentia) from the Neogene of China, and comments on its biogeography. Geobios 15(2): 255–259.

Jacobs, L.L., and W.R. Downs. 1994. The evolution of murine rodents in Asia. *In* Y. Tomida, C.K. Li, and T. Setogushi (editors), Rodent and Lagomorph families of Asian origins and diversification: 149–156. Tokyo: National Science Museum Monographs.

Jacobs, L.L., L.J. Flynn, and W.R. Downs. 1989. Neogene rodents of southern Asia. *In* C.C. Black and M.R. Dawson (editors), Papers on fossil rodents, in honor of Albert Elmer Wood: 157–177. Los Angeles: Natural History Museum of Los Angeles County, Science Series.

Jacobs, L.L., L.J. Flynn, W.R. Downs, and J.C. Barry. 1990. *Quo vadis, Antemus*? The Siwalik muroid record. *In* E.H. Lindsay, V. Fahlbusch, and P. Mein (editors), European Neogene mammal chronology: 573–586. New York and London: Plenum Press, 658 pp.

Jansa, S.A., F.K. Barker, and L.R. Heaney. 2006. The pattern and timing of diversification of Philippine endemic rodents: evidence from mitochondrial and nuclear gene sequences. Systematic Biology 55: 73–88.

Jansa, S.A., and M. Weksler. 2004. Phylogeny of muroid rodents: relationships within and among major lineages as determined by IRBP gene sequences. Molecular Phylogenetics and Evolution 31: 256–276.

Jenkins, P.D. 1982. A discussion of Malayan and Indonesian shrews of the genus *Crocidura* (Insectivora: Soricidae). Zoologische Mededelingen 56: 267–279.

Jernvall, J., and H.-S. Jung. 2000. Genotype, phenotype, and developmental biology of molar tooth characters. Yearbook of Physical Anthropology 43: 171–190.

Johnson, D.H. 1952. The occurrence and significance of extra molar teeth in rodents. Journal of Mammalogy 33: 70–72.

Kaneko, Y., S. Maruyama, A. Kadarusman, T. Ota, M. Ishikawa, T. Tsujimori, A. Ishikawa, and K. Okamoto. 1987. On-going orogeny in the outer-arc of the Timor–Tanimbar region, eastern Indonesia. Gondwana Research. 11: 218–233.

Kangas, A.T., A.R. Evans, I. Thesleff, and J. Jernvall. 2004. Nonindependence of mammalian dental characters. Nature 423: 211–214.

Kassai, Y., P. Munne, Y. Hotta, E. Penttilä, K. Kavanagh, N. Ohbayahi, S. Tanada, I. Thesleff, J. Jernvall, and N. Itoh. 2005. Regulation of mammalian tooth cusp patterning by ectodin. Science 309: 2067–2070.

Kavanagh, K.D., A.R. Evans, and J. Jernvall. 2007. Predicting evolutionary patterns of mammalian teeth from development. Nature 449: 427–432.

Kemper, C.M., and L.H. Schmitt. 1992. Morphological variation between populations of the brush-tailed tree rat (*Conilurus penicillatus*) in northern Australia and New Guinea. Australian Journal of Zoology 40: 437–452.

Keränen, S.V.E., T. Äberg, P. Kettunen, I. Thesleff, and J. Jernvall. 1998. Association of developmental regulatory genes with the development of different molar tooth shapes in two species of rodents. Development Genes and Evolution 208: 477–486.

Kitchener, D.J., K.P. Aplin, and Boeadi. 1991a. A new species of *Rattus* from Gunung Mutis, South West Timor Island, Indonesia. Records of the Western Australian Museum 15: 445–465.

Kitchener, D.J., and A. Suyanto. 1996. Intraspecific morphological variation among island populations of small mammals in southern Indonesia. *In* D.J. Kitchener and A. Suyanto

(editors), Proceedings of the First International Conference on Eastern Indonesia-Australian Vertebrate Fauna, Manado, Indonesia, November 22–26 1994: 7–13. Perth: Western Australian Museum.

Kitchener, D.J., S. Hisheh, L.H. Schmitt, and A. Suyanto. 1994. Shrews (Soricidae: *Crocidura*) from the Lesser Sunda Islands, and south-east Maluku, eastern Indonesia. Australian Mammalogy 17: 7–17.

Kitchener, D.J., R.A. How, and Maharadatunkamsi. 1991b. *Paulamys* sp. cf. *P. naso* (Musser, 1981) (Rodentia; Muridae) from Flores Island, Nusa Tenggara, Indonesia—description of a modern specimen and a consideration of its phylogenetic affinities. Records of the Western Australian Museum 15: 171–189.

Kitchener, D.J., R.A. How, and Maharadatunkamsi. 1991c. A new species of *Rattus* from the mountains of West Flores, Indonesia. Records of the Western Australian Museum 15: 555–570.

Kitchener, D.J., R.A. How, and Maharadatunkamsi. 1991d. A new species of *Nyctophilus* (Chiroptera: Vespertilionidae) from Lembata Island, Nusa Tenggara, Indonesia. Records of the Western Australian Museum 15: 97–107.

Kitchener, D.J., and I. Maryanto. 1993. Taxonomic appraisal of the *Hipposideros larvatus* species complex (Chiroptera: Hipposideridae) in the Greater and Lesser Sunda Islands, Indonesia. Records of the Western Australian Museum 16: 119–173.

Kitchener, D.J., and I. Maryanto. 1995. Small *Pteropus* (Chiroptera: Pteropodidae) from Timor and surrounding islands, Indonesia. Records of the Western Australian Museum 17: 147–152.

Kitching, I.J., P.L. Forey, C.J. Humphries, and D.M. Williams. 1998. Cladistics. the theory and practice of parsimony analysis. 2nd ed. Oxford: Oxford University Press, 228 pp.

Kock, D. 1974. Eine neue *Suncus*-Art von Flores. Senckenbergiana Biologica 55: 197–203.

Kuratani, S. 2005. Craniofacial development and the evolution of vertebrates: the old problems on a new background. Zoological Science 22: 1–19.

Kurtén, B., and E. Anderson. 1980. Pleistocene mammals of North America. New York: Columbia University Press, 442 pp.

Lavocat, R. 1962. Etudes systématiques sur la dentition des Muridés. Mammalia 26: 107–127.

Lazzari, V., P. Tafforeau, J.-P. Aguilar, and J. Michaux. 2008. Topographic maps applied to comparative molar morphology: the case of murine and cricetine dental plans (Rodentia, Muroidea). Paleobiology 34: 46–64.

Lecompte, E., K. Aplin, C. Denys, F. Catzeflis, M. Chades, and P. Chevret. 2008. Phylogeny and biogeography of African Murinae based on mitochondrial and nuclear gene sequences, with a new tribal classification of the subfamily. BMC Evolutionary Biology 8: 199 (21 pp.).

Lecompte, E., L. Granjon, and C. Denys. 2002b. The phylogeny of the *Praomys* complex (Rodentia: Muridae) and its phylogeographic implications. Journal of Zoological Systematics and Evolutionary Research 40: 8–25.

Lecompte, É., L. Granjon, J.K. Peterhans, and C. Denys. 2002a. Cytochrome b-based phylogeny of the *Praomys* group (Rodentia, Murinae): a new African radiation? Comptes Rendes Biologie 325: 827–840.

Lewis, P.O. 2001. A likelihood approach to estimating phylogeny from discrete morphological character data. Systematic Biology 50: 913–925.

Linthout, K., H. Helmers, and J. Sopaheluwakan. 1997. Late Miocene obduction and microplate migration around the southern Banda Sea and the closure of the Indonesian seaway. Tectonophysics 281: 17–30.

Lister, A.M. 1989. Rapid dwarfing of red deer on Jersey in the last interglacial. Nature 342: 539–542.

Lomolino, M.V. 1985. Body size of mammals on islands: the island rule reexamined. American Naturalist 125: 310–316.

Lomolino, M.V. 2005. Body size evolution in insular vertebrates: generality of the island rule. Journal of Biogeography 32: 1683–1699.

López-Martínez, N., J. Michaux, and R. Hutterer. 1998. The skull of *Stephanomys* and a review of *Malpaisomys* relationships (Rodentia: Muridae): taxonomic incongruence in murids. Journal of Mammalian Evolution 5: 185–215.

MacPhee, R.D.E. 1981. Auditory regions of primates and eutherian insectivores: morphology, ontogeny, and character analysis. Contributions to Primatology 18: 1–282.

Mahirta, K.P. Aplin, D. Bulbeck, W.E. Boles, and P. Bellwood. 2004. Pia Hudale Rockshelter: a terminal Pleistocene occupation site on Roti Island, Nusa Tenggara Timur, Indonesia. *In* S. Keates and J.M. Pasveer (editors), Quaternary research in Indonesia: 361–394. Modern Quaternary research in South East Asia No. 18, Rotterdam: A.A. Balkema.

Majnep, I.S., and R. Bulmer. 2007. Animals the ancestors hunted. An account of the wild mammals of the Kalam Area, Papua New Guinea. Belair, South Australia: Crawford House, 452 pp.

Malmquist, M.G. 1985. Character displacement and biogeography of the pygmy shrew in northern Europe. Ecology 66: 372–377.

Martin, B., and C. Cossalter. 1977. The eucalyptuses of the Sunda Isles (parts 1–4). Wellington: New Zealand Forestry Service.

Martin, B., and C. Cossalter. 1979. The eucalyptuses of the Sunda Isles. Final instalment. Wellington: New Zealand Forestry Service.

Martín Suárez, E., and P. Mein. 1998. Revision of the genera *Parapodemus*, *Apodemus*, *Rhagamys* and *Rhagapodemus* (Rodentia, Mammalia). Geobios 31: 87–97.

Mayr, E. 1944. The birds of Timor and Sumba. Bulletin of the American Museum of Natural History 83(2): 125–194.

Mein, P., E. Martín Suárez, and J. Agustí. 1993. *Progonomys* Schaub, 1938 and *Huerzelerimys* gen. nov. (Rodentia); their evolution in Western Europe. Scripta Geologica 103: 41–64.

Mein, P., E. Moissenet, and R. Adrover. 1983. L'extension et l'âge des formations continentales pliocènes du fossé de Teruel (Espagne). Comptes Rendus de l'Académie des Sciences (Paris), ser. 2 296: 1603–1610.

Menzies, J.I. 1996. A systematic revision of *Melomys* (Rodentia: Muridae) of New Guinea. Australian Journal of Zoology 44: 367–426.

Metzner, J. 1977. Man and environment in Eastern Timor: a geoecological analysis of the Boucau-Viqueque area as a possible basis for regional planning. Canberra: Australian National University Development Studies Centre Monograph 8.

Michaux, J. 1969. Sur l'origine du dessin dentaire "Apodemus"; remarques sur l'évolution des faunes de Muridés du Néogène d'Europe sud-occidentale. Comptes Rendus de l'Académie des Sciences (Paris) 264: 711–714.

Michaux, J. 1971. Données nouvelles sur les *Muridae (Rodentia)* neogènes d'Europe sud-occidentale. Evolution et rapports avec les formes actuelles. Paléobiologie Contributionale 2: 1–67.

Michaux, J., P. Chevret, and S. Renaud. 2007. Morphological diversity of Old World rats and mice (Rodentia, Muridae) mandible in relation with phylogeny and adaptation. Journal of Zoological Systematic and Evolutionary Research 45: 263–279.

Michaux, J.R., A. Reyes, and F. Catzeflis. 2001. Evolutionary history of the most speciose mammals: molecular phylogeny of muroid rodents. Molecular Biology and Evolution 18: 2017–2031.

Middleton, G., S. White, and N. White. 2006. Hydro-electric power proposal for the Iralalaro-Paitchau karst, Timor-Leste. Australasian Cave and Karst Management Association Journal 63, 12 pp. (www.ackma.org/journals/63/).

Miller, G.S., Jr. 1912. Catalogue of the mammals of Western Europe (Europe exclusive of Russia) in the collection of the British Museum. London: British Museum (Natural History), 1019 pp.

Minwer-Barakat, R., A. García-Alix, E. Martín Suárez, and M. Freudenthal. 2005. Muridae (Rodentia) from the Pliocene of Tollo de Chiclana (Granada, Southeastern Spain). Journal of Vertebrate Paleontology 25: 426–441.

Misonne, X. 1969. African and Indo-Australian Muridae. Evolutionary trends. Musée Royal de l'Afrique Centrale Tervuren Belgique Annales, série 8, Sciences Zoologiques 172: 1–219.

Monk, K.A., Y. de Fretes, and G. Reksodiharjo-Lilley. 1997. The ecology of Nusa Tenggara and Maluku. Jakarta: Periplus Editions, 966 pp + xvii pp.

Morwood, M.J., F. Aziz, P. O'Sullivan, Nasruddin, D.R. Hobbs, and A. Raza. 1999. Archaeological and palaeontological research in central Flores, East Indonesia: results of fieldwork 1997–98. Antiquity 73: 273–86.

Morwood, M.J., P. O'Sullivan, F. Aziz, and A. Raza. 1998. Fission track age of stone tools and fossils on the east Indonesian island of Flores. Nature 392: 173–76.

Morwood, M.J., R.P. Soejono, and R.G. Roberts, et al. 2004. Archaeology and age of a new hominin from Flores in Eastern Indonesia. Nature 431: 1087–91.

Musser, G.G. 1969. Results of the Archbold Expeditions. No. 91. A new genus and species of murid rodent from Celebes, with a discussion of its relationships. American Museum Novitates 2384: 1–41.

Musser, G.G. 1972. The species of *Hapalomys* (Rodentia, Muridae). American Museum Novitates 2503: 1–27.

Musser, G.G. 1979. Results of the Archbold Expeditions. No.102. The species of *Chiropodomys*, arboreal mice of Indochina and the Malay Archipelago. Bulletin of the American Museum of Natural History 162(6): 377–445.

Musser, G.G. 1981a. Results of the Archbold Expeditions. No.105. Notes on systematics of Indo-Malayan murid rodents, and descriptions of new genera and species from Ceylon, Sulawesi and the Philippines. Bulletin of the American Museum of Natural History 168(3): 225–334.

Musser, G.G. 1981b. The giant rat of Flores and its relatives east of Borneo and Bali. Bulletin of the American Museum of Natural History 169(2): 67–176.

Musser, G.G. 1982a. Results of the Archbold Expeditions. No.110. *Crunomys* and the small-bodied shrew rats native to the Philippine Islands and Sulawesi. Bulletin of the American Museum of Natural History 174(1): 1–95.

Musser, G.G. 1982b. Results of the Archbold Expeditions. No.108. The definition of *Apomys*, a native rat of the Philippine Islands. American Museum Novitates 2746: 1–43.

Musser, G.G. 1986. Sundaic *Rattus*: definitions of *Rattus baluensis* and *Rattus korinchi*. American Museum Novitates 2862: 1–24.

Musser, G.G. 1987. The occurrence of *Hadromys* (Rodentia: Muridae) in Early Pleistocene Siwalik strata in northern Pakistan and its bearing on biogeographic affinities between Indian and northeastern African murine faunas. American Museum Novitates 2883: 1–36.

Musser, G.G. 1991. Sulawesi rodents: descriptions of new species of *Bunomys* and *Maxomys* (Muridae, Murinae). American Museum Novitates 3001: 1–41.

Musser, G.G., and Boeadi. 1980. A new genus of murid rodent from the Komodo Islands in Nusatenggara, Indonesia. Journal of Mammalogy 61: 395–413.

Musser, G.G., and E.M. Brothers. 1994. Identification of Bandicoot rats from Thailand (*Bandicota*, Muridae, Rodentia). American Museum Novitates 3110: 1–56.

Musser, G.G., and M.D. Carleton. 1993. Family Muridae. *In* D.M. Wilson and D.M. Reeder (editors), Mammal species of the world. 2nd ed.: 50–755. Washington DC: Smithsonian Institution Press.

Musser, G.G., and M.D. Carleton. 2005. Superfamily Muroidea. *In* D.E. Wilson and D.M. Reeder (editors), Mammal species of the world. A taxonomic and geographic reference, vol. 2, 3rd ed.: 894–1531. Baltimore, MD: Johns Hopkins University.

Musser, G.G., M.D. Carleton, E.M. Brothers, and A.L. Gardner. 1998b. Systematic studies of oryzomyine rodents (Muridae, Sigmodontinae): diagnoses and distributions of species formerly assigned to *Oryzomys* "*capito*." Bulletin of the American Museum of Natural History 236: 1–376.

Musser, G.G., and L.A. Durden. 2002. Sulawesi rodents: description of a new genus and species of Murinae (Muridae, Rodentia) and its parasitic new species of sucking louse (Insecta, Anopleura). American Museum Novitates 3368: 1–50.

Musser, G.G., and L.K. Gordon. 1981. A new species of *Crateromys* (Muridae) from the Philippines. Journal of Mammalogy 62: 513–525.

Musser, G.G., and L.R. Heaney. 1985. Philippine *Rattus*: a new species from the Sulu Archipelago. American Museum Novitates 2818: 1–32.

Musser, G.G., and L.R. Heaney. 1992. Philippine rodents: definitions of *Tarsomys* and *Limnomys* plus a preliminary assessment of phylogenetic patterns among native Philippine murines (Murinae, Muridae). Bulletin of the American Museum of Natural History 211: 1–138.

Musser, G.G., L.R. Heaney, and B.R. Tabaranza, Jr. 1998a. Philippine rodents: redefinitions of known species of *Batomys* (Muridae, Murinae) and description of a new species from Dinagat Island. American Museum Novitates 3237: 1–51.

Musser, G.G., K.M. Helgen, and D.P. Lunde. 2008. Systematic review of New Guinea *Leptomys* (Muridae, Murinae) with descriptions of two new species. American Museum Novitates 3624: 1–60.

Musser, G.G., and M.E. Holden. 1991. Sulawesi rodents (Muridae: Murinae): morphological and geographical boundaries of species in the *Rattus hoffmani* Group and a new species from Pulau Peleng. *In* T.A. Griffith and D. Klingener (editors), Contributions to Mammalogy in Honor of Karl F. Koopman. Bulletin of the American Museum of Natural History 206: 322–413.

Musser, G.G., D.P. Lunde, and N. Trong Son. 2006. Description of a new genus and species of rodent (Murinae, Muridae, Rodentia) from the tower karst region of northeastern Vietnam. American Museum Novitates 3517: 1–41.

Musser, G.G., and C. Newcomb. 1983. Malaysian murids and the giant rat of Sumatra. Bulletin of the American Museum of Natural History 174(4): 327–598.

Musser, G.G., J.T. Marshall, Jr, and Boeadi. 1979. Definition and contents of the Sundaic genus *Maxomys* (Rodentia, Muridae). Journal of Mammalogy 60: 592–606.

Musser, G.G., A.L. Smith, M.F. Robinson, and D.P. Lunde. 2005. Description of a new genus and species of rodent (Murinae, Muridae, Rodentia) from the Khammouan Limestone National Biodiversity Conservation Area in Lao PDR. American Museum Novitates 3497: 1–31.

Nagase, T., M. Nagase, M. Machida, and T. Fujita. 2008. Hedgehog signaling in vascular development. Angiogenesis 11: 71–77.

Negus, V. 1958. Comparative anatomy and physiology of the nose and paranasal sinuses. Edinburgh: F. & S. Livingstone, 402 pp.

Obara, N., and H. Lesot. 2007. Asymmetrical growth, differential cell proliferation, and dynamic cell rearrangement underlie epithelial morphogenesis in mouse molar development. Cell and Tissue Research 330: 461–473.

O'Connor, S., and Aplin, K.P. 2007. A matter of balance: an overview of Pleistocene occupation history and the impact of the last glacial phase in East Timor and the Aru Islands, eastern Indonesia. Archaeology in Oceania 42: 82–90.

O'Connor, S., M. Spriggs, and P. Veth. 2002. Excavation at Lene Hara Cave establishes occupation in East Timor at least 30,000–35,000 years ago. Antiquity 76: 45–50.

Oliveira, N.V. 2006. Returning to East Timor: prospects and possibilities from an archaeobotanical project in the new country. *In* E.A. Bacus, I.C. Glover, and V.C. Pigott (editors), Uncovering Southeast Asia's past—selected papers from the Tenth Biennial Conference of the European Association of Southeast Asian Archaeologists, London, 14th–17th September 2004: 88–97. Singapore: National University Press.

Oliver, W.L.R., C.R. Cox, P.C. Gonzales, and L.R. Heaney. 1993. Cloud rats in the Philippines–preliminary report on distribution and status. Oryx 27: 41–48.

Peterkova, R., H. Lesot, and M. Peterka. 2006. Phylogenetic memory of developing mammalian dentition. Journal of Experimental Zoology Part B: Molecular and Developmental Evolution 306: 234–250.

Peterkova, R., H. Lesot, L. Viriot, and M. Peterka. 2005. The supernumerary cheek tooth in tabby/EDA mice—a reminiscence of the premolar in mouse ancestors. Archives of Oral Biology 50: 219–225.

Petter, F. 1959. Evolution du dessin de la surface d'usure des molaires des Gerbillides. Mammalia 23: 304–315.

Petter, F. 1966a. Affinites des genres *Beamys*, *Saccostomus* et *Cricetomys* (Rongeurs, Cricetomyinae). Annales Musée Royal de l'Afrique Centrale Tervuren Belgique, ser. 8 (Sciences Zoologiques) 144: 13–25.

Petter, F. 1966b. L'origine des murides plan cricetin et plans murins. Mammalia 30: 205–225.

Petter, F. 1967. Particularités dentaires des Petromyscinae Roberts 1951 (Rongeurs, Cricetides). Mammalia 31: 217–224.

Petter, F. 1972. Deux rongeurs nouveaux d'Etiophie: *Stenocephalemys griseicauda* sp. nov. et *Lophuromys melanonyx* sp nov. Mammalia 36: 171–181.

Petter, F. 1973. Tendances évolutives dans le genre *Gerbillus* (Rongeurs, Gerbillides). Mammalia 37: 631–636.

Petter, F. 1975. Family Cricetidae: subfamily Nesomyinae, Part 6.2. *In* J. Meester and H.W. Setzer (editors), The mammals of Africa: an identification manual: 1–4. Washington, DC: Smithsonian Institution Press.

Petter, F. 1983. Elements d'une revision des *Acomys* Africains. Un sous-genre nouveau, *Peracomys* Petter et Roche, 1981 (Rongeurs, Murides). Annales Musée Royal de l'Afrique Centrale Tervuren Belgique, ser. 8 (Sciences Zoologiques) 237: 109–119.

Petter, F. 1986. Un rongeur nouveau du Mont Oku (Cameroun) *Lamottemys okuensis*, gen. nov., sp. nov. (Rodentia, Muridae). Cimbebasia, ser. A 8: 97–105.

Petter, F., and F. de Beaufort. 1960. Description d'une forme nouvelle de rongeur d'Angola, *Thallomys damarensis quissamae*. Bulletin du Muséum National d'Histoire Naturelle (Paris), ser. 2 32: 269–271.

Petter, F., and J. Roche. 1981. Remarques préliminaires sur la systematique des *Acomys* (Rongeurs, Muridae *Peracomys*, sous-genre nouveau. Mammalia 45: 381–383.

Petter, F., and M. Tranier. 1975. Contribution à l'étude des *Thamnomys* du groupe *dolichurus* (Rongeurs, Murides). Systématique et caryologie. Mammalia 39: 405–414.

Pfennig, D.W. 1992. Proximate and functional causes of polyphenism in an anuran tadpole. Functional Ecology 6: 167–174.

Price, N.J., and M.G. Audley-Charles. 1987. Tectonic collision processes after plate rupture. Tectonophysics 140: 121–129.

Quay, W.B. 1954. The anatomy of the diastemal palate in microtine rodents. Museum of Zoology University of Michigan Miscellaneous Publications No. 86, 41 pp.

Rabor, D.S. 1955. Notes on mammals and birds of the central Luzon highlands, Philippines. Pt. 1. Notes on mammals. Silliman Journal 2: 193–218.

Reiss, M.J. 1989. The allometry of growth and reproduction. London: Cambridge University Press, 182 pp.

Renaud, S., J. Michaux, P. Mein, J.-P. Aguliar, and J.-C. Auffray. 1999. Patterns of size and shape differentiation during the evolutionary radiation of the European Miocene murine rodents. Lethaia 32: 61–71.

Rice, W.R., and E.E. Hostert. 1993. Laboratory experiments on speciation: what have we learned in 40 years? Evolution 47: 1637–1653.

Rickart, E.A., and L.R. Heaney. 2002. Further studies on the chromosomes of Philippine rodents. Proceedings of the Biological Society of Washington 115: 473–487.

Robson, B.A. 2002. Chromosomal speciation via monobrachial homology in native Australian *Rattus* species. Unpublished Ph.D. dissertation, School of Resource Science and Management, Southern Cross University, Lismore, New South Wales.

Rosevear, D.R. 1969. The rodents of West Africa. London: British Museum (Natural History).

Roughgarden, J. 1972. Evolution of niche width. American Naturalist 106: 683–718.

Rowe, K.C., M.L. Reno, D.M. Richmond, R.M. Adkins, and S.J. Steppan. 2008. Pliocene

colonization and adaptive radiations in Australia and New Guinea (Sahul): multilocus systematics of the old endemic rodents (Muroidea: Murinae). Molecular Phylogenetics and Evolution 47: 84–101.

Salazar, I., and P.S. Quinteiro. 1998. Supporting tissue and vasculature of the mammalian vomeronasal organ: the rat as a model. Microscopy Research and Technique 41: 492–505.

Salazar-Ciudad, I., and J. Jernvall. 2002. A gene network model accounting for development and evolution of mammalian teeth. Proceedings of the National Academy of Science 99: 8116–8120.

Sarasin, F. 1936. Beiträge zur Prähistorie der Inseln Timor und Roti, mit einem einleitenden Grabungs—und Fundbericht von Alfred Bühler. Verhandlungen der Naturforschenden Gesellschaft in Basel 47: 1–59.

Satoh, K. 1997. Comparative functional morphology of mandibular forward movement during mastication of two murid rodents, *Apodemus speciosus* (Murinae) and *Clethrionomys rufocanus* (Arvicolinae). Journal of Morphology 231: 131–142.

Satoh, K. 1999. Mechanical advantage of area of origin for the external pterygoid muscle in two murid rodents, *Apodemus speciosus* and *Clethrionomys rufocanus*. Journal of Morphology 240: 1–14.

Satoh, K., and F. Iwaku. 2004. Internal architecture, origin-insertion site, and mass of jaw muscles in Old World hamsters. Journal of Morphology 260: 101–116.

Satoh, K., and F. Iwaku. 2006. Jaw muscle functional anatomy in northern grasshopper mouse, *Onychomys leucogaster*, a carnivorous murid. Journal of Morphology 267: 987–999.

Satoh, K., and F. Iwaku. 2008. Masticatory muscle architecture in a murine murid, *Rattus rattus*, and its functional significance. Mammal Study 33: 35–42.

Schaub, S. 1937. Ein neuer Muridae von Timor. Verhandlungen der Naturforschenden Gesellschaft in Basel 48: 1–6.

Scheiner, S.M. 1993. Genetics and evolution of phenotypic plasticity. Annual Review of Ecology and Systematics 24: 35–68.

Scotland, R.W., R.G. Olmstead, and J.R. Bennett. 2003. Phylogeny reconstruction: the role of morphology. Systematic Biology 52: 539–548.

Sen, S. 1983. Rongeurs et Lagomorphes du gisement pliocène de Pul-e Charkhi, bassin de Kabul, Afghanistan. Bulletin du Museum d'National Histoire Naturelle (Paris), C (Sciences de la Terre Paléontologie Géologie, Minéralogie) 5: 33–74.

Sen, S., H. Brunet, and É. Heintz. 1979. Découverte de ronguers "africains" dans le Pliocène d'Afghanistan (bassin de Sarobi). Implications paléobiogéographiques et stratigraphiques. Bulletin du Museum National d'Histoire Naturelle (Paris), Series 4 1: 65–75.

Sénégas, F., and D.M. Avery. 1998. New evidence for the murine origins of the Otomyinae (Mammalia, Rodentia) and the age of Bolt's Farm (South Africa). South African Journal of Science 94: 503–507.

Sheppe, W. 1964. Supernumerary teeth in the deer mouse, *Peromyscus*. Zeitschrift für Säugetierkunde 29: 33–36.

Skúlason, S., and T.B. Smith. 1995. Resource polymorphisms in vertebrates. Trends in Ecology and Evolution 10: 366–370.

Slaughter, B.H., and G.T. James. 1979. *Saidomys natrunesis*, an arvicanthine rodent from the Pliocene of Egypt. Journal of Mammalogy 60: 421–425.

Smartt, R.A., and C.A. Lemen. 1980. Intrapopulational morphological variation as a predictor of feeding behaviour in deermice. American Naturalist 116: 891–894.

Smith, T.B. 1987. Bill size polymorphism and interspecific niche utilization in an African finch. Nature 329: 717–719.

Smith, T.B. 1993. Disruptive selection and the genetic basis of bill size polymorphism in the African finch, *Pyrnestes*. Nature 363: 618–620.

Smith, T.B., and S. Skúlason. 1996. Evolutionary significance of resource polymorphisms in fishes, amphibians, and birds. Annual Review of Ecology and Systematics 27: 111–133.

Sody, H.J.V. 1941. On a collection of rats from the Indo-Malayan and Indo-Australian regions (with descriptions of 43 new genera, species and subspecies). Treubia 18: 255–325.

Soltis, P.S., D.E. Soltis, and M.W. Chase. 1999. Angiosperm phylogeny inferred from multiple genes as a tool for comparative biology. Nature 402: 402–404.

Soulé, M., and B.R. Stewart. 1970. The "niche-variation" hypothesis: a test and alternatives. American Naturalist 104: 85–97.

Stehlin, H.G., and S. Schaub. 1951. Die Trigonodontie der simplicidentaten Nager. Basel: Birkhäuser, 385 pp.

Steppan, S.J., R.M. Adkins, and J. Anderson. 2004. Phylogeny and divergence-date estimates of rapid radiations in muroid rodents based on multiple nuclear genes. Systematic Biology 53: 533–553.

Steppan, S.J., R.M. Adkins, P.Q. Spinks, and C. Hale. 2005. Multigene phylogeny of the Old World mice, Murinae, reveals distinct geographic lineages and the declining utility of mitochondrial genes compared to nuclear genes.

Molecular Phylogenetics and Evolution 37: 370–388.

Steppan, S.J., C. Zawadzki, and L.R. Heaney. 2003. Phylogeny of the endemic Philippine rodent *Apomys* (Muridae) and the dynamics of diversification in an oceanic archipelago. Biological Journal of the Linnean Society 80: 699–715.

Storch, G. 1987. The Neogene mammalian faunas of Ertemte and Harr Obo in Inner Mongolia (Nei Mongol), China. 7. Muridae (Rodentia). Senckenbergiana Lethaea 67: 401–431.

Storch, G., and T. Dahlmann. 1995. The vertebrate locality Maramena (Macedonia, Greece) at the Turolian-Ruscinian Boundary (Neogene). 10. Murinae (Rodentia, Mammalia). Münchner Geowissenschaftliche Abhandlungen (A) 28: 121–132.

Storch, G., and X. Ni. 2002. New Late Miocene murids from China (Mammalia, Rodentia). Geobios 35: 515–521.

Tate, G.H.H. 1951. Results of the Archbold Expeditions. No. 65. The rodents of Australia and New Guinea. Bulletin of the American Museum of Natural History 97(4): 183–430.

Taylor, E.H. 1934. Philippine land mammals. Monograph of the Bureau of Science (Manila) 30: 1–548.

Taylor, P.J., C. Denys, and M. Mukerjee. 2004. Phylogeny of the African murid tribe Otomyini (Rodentia), based on morphological and allozyme evidence. Zoologica Scripta 33: 389–402.

Thaler, L. 1966. Les rongeurs fossiles du Bas-Languedoc dans leurs rapports avec l'histoire des faunes et la stratigraphie du Tertiaire d'Europe. Mémoires du Museum National d'Histoire Naturelle (Paris) série C (Sciences de la Terre) 17: 1–296.

Thomas, O. 1898. On the mammals collected by Mr. John Whitehead during his recent expedition to the Philippines with field notes by the collector. Transactions of the Zoological Society of London 14: 377–414.

Thomas, O. 1906. On the generic arrangement of the Australian rats hitherto referred to *Conilurus*, with remarks on the structure and evolution of their molar cusps. Annals and Magazine of Natural History (series 7) 17: 81–85.

Thomas, O. 1919. The method of taking the incisive index in rodents. Annals and Magazine of Natural History (series 9) 4: 289–290.

Uraih, L.C., and R.R. Maronpot. 1990. Normal histology of the nasal cavity and application of special techniques. Environmental Health Perspectives 85: 187–208.

Vaccarezza, O.L., L.N. Sepich, and J.H. Tramezzani. 1981. The vomeronasal organ of the rat. Journal of Anatomy 132: 167–185.

Vandebroek, G. 1961. The comparative anatomy of the teeth of lower and non specialized mammals. International Colloquium on the Evolution of Lower and Non Specialized Mammals 1: 215–320; 2: 1–181. Brussels: Paleis der Academiën.

Van Valen, L. 1965. Morphological variation and the width of the ecological niche. American Naturalist 99: 377–390.

Van Valen, L. 1973. A new evolutionary law. Evolutionary Theory 1: 1–30.

Van Valen, L. 1982. Homology and causes. Journal of Morphology 173: 305–312.

Vartanyan, S.L., V.E. Garutt, and A.V. Sher. 1993. Holocene dwarf mammoths from Wrangel Island in the Siberian Arctic. Nature 362: 337–340.

Verhoeven, T. 1959. Der Klingenkultur der Insel Timor. Anthropos 54: 970–972.

Verhoeven, T. 1964. Stegodon-fossilien auf der insel Timor. Anthropos 59: 634 pp.

Veth, P., M. Spriggs, and S. O'Connor. 2005. Continuity in tropical cave use: examples from East Timor and the Aru Islands, Maluku. Asian Perspectives 44: 180–192.

Vidic, B. 1971. The prenatal morphogenesis of the lateral nasal wall in the rat (*Mus rattus*). Journal of Morphology 133: 303–318.

Vidic, B., and H.G. Greditzer. 1971. The histochemical and microscopical differentiation of the respiratory glands around the maxillary sinus of the rat. American Journal of Anatomy 132: 491–514.

Voss, R.S. 1988. Systematics and ecology of ichthyomyine rodents (Muroidea): patterns of morphological evolution in a small adaptive radiation. Bulletin of the American Museum of Natural History 188(2): 259–493.

Wahlert, J.H. 1974. The cranial foramina of protrogomorphous rodents: an anatomical and phylogenetic study. Bulletin of the Museum of Comparative Zoology 146: 363–410.

Wahlert, J.H. 1985. Cranial foramina of rodents. *In* W.P. Luckett and J.L. Hartenberger (editors), Evolutionary relationships among rodents, a multidisciplinary analysis: 311–332. New York: Plenum Press.

Watts, C.H.S. 1976. *Leggadina lakedownensis*, a new species of murid rodent from North Queensland. Transactions of the Royal Society of South Australia 100: 105–108.

WCMC. 1995. Conservation status listing of plants: Bali, Lesser Sundan Islands, Moluccas and East Timor WCMC database. Cambridge: World Conservation Monitoring Centre.

Weckerly, F.W. 1998. Sexual-size dimorphism: influence of mass and mating systems in the

most dimorphic mammals. Journal of Mammalogy 79: 33–52.

Weerd, A. van de. 1976. Rodent faunas of the Mio-Pliocene continental sediments of the Teruel-Alfambra region, Spain. Utrecht Micropalaeontological Bulletins Special Publication 2: 1–217.

Weijs, W.A., and B. Dantuma. 1975. Electromyography and mechanics of mastication in the albino rat. Journal of Morphology 146: 1–34.

Weksler, M. 2006. Phylogenetic realtionships of oryzomine rodents (Muroidea: Sigmodontinae): separate and combined analyses of morphological and molecular data. Bulletin of the American Museum of Natural History 296: 1–149.

Wenyu, W., and L.J. Flynn. 1992. New murid rodents from the Late Cenozoic of Yushe Basin, Shanxi. Vertebrata Palasiatica 30: 17–38.

Wessels, W., H. de Bruijn, S.T. Hussain, and J.J.M. Leinders. 1982. Fossil rodents from the Chinj Formation, Banda Daud Shah, Kohat, Pakistan. Proceedings of the Koninklijke Nederlandse Akademie van Wetenschappen (Amsterdam) B Physical Sciences 85: 337–364.

West-Eberhard, M.J. 1998. Evolution in the light of development and cell biology, and vice versa. Proceedings of the National Academy of Science of the United States of America 95: 8417–8419.

Whitmore, T.C., I.G.M. Tantra, and U. Sutisna (editors). 1989. Tree flora of Indonesia: check list for Bali, Nusa Tenggara and Timor. Bogor: Forest Research and Development Centre.

Wible, J.R. 1987. The eutherian stapedial artery: character analysis and implications for superordinal relationships. Zoological Journal of the Linnean Society 91: 107–135.

Wible, J.R. 1990. Petrosals of Late Cretaceous marsupials from North America, and a cladistic analysis of the petrosal in therian mammals. Journal of Vertebrate Paleontology 10: 183–205.

Wible, J.R., and J.A. Hopson. 1995. Homologies of the prootic canal in mammals and nonmammalian cynodonts. Journal of Vertebrate Paleontology 15: 331–356.

Wible, J.R., G.W. Rougier, M.J. Novacek, and M.C. McKenna. 2001. Earliest eutherian ear region: a petrosal referred to *Prokennalestes* from the Early Cretaceous of Mongolia. American Museum Novitates 3322: 1–44.

Wimberger, P.H. 1994. Trophic polymorphisms, plasticity, and speciation in vertebrates: 19–43. *In* D.J. Stouder, K.L. Fresh, and R.J. Feller (editors), Theory and Application in Fish Feeding Ecology. Columbia, SC: University of South Carolina Press.

Wood, A.E., and R.W. Wilson. 1936. A suggested nomenclature for the cusps of the cheek teeth of rodents. Journal of Paleontology 10: 388–391.